JCTC Journal of Chemical Theory and Computation

pubs.acs.org/JCTC Article

Reference Energies for Valence Ionizations and Satellite Transitions

Antoine Marie* and Pierre-François Loos*

Cite This: J. Chem. Theory Comput. 2024, 20, 4751−4777 Read Online

ACCESS | Metrics & More | Article Recommendations | Supporting Information

ABSTRACT: Upon ionization of an atom or a molecule, another electron (or more) can be simultaneously excited. These concurrently generated states are called "satellites" (or shakeup transitions) as they appear in ionization spectra as higher-energy peaks with weaker intensity and larger width than the main peaks associated with single-particle ionizations. Satellites, which correspond to electronically excited states of the cationic species, are notoriously challenging to model using conventional single-reference methods due to their high excitation degree compared to the neutral reference state. This work reports 42 satellite transition energies and 58 valence ionization potentials (IPs) of full configuration interaction quality computed in small molecular systems. Following the protocol developed for the QUEST database [Véril, M.; Scemama, A.; Caffarel, M.; Lipparini, F.; Boggio-Pasqua, M.; Jacquemin, D.; and Loos, P.-F. Wiley Interdiscip. Rev.: Comput. Mol. Sci. **2021**, *11*, e1517], these reference energies are computed using the configuration interaction using a perturbative selection made iteratively (CIPSI) method. In addition, the accuracy of the well-known coupled-cluster (CC) hierarchy (CC2, CCSD, CC3, CCSDT, CC4, and CCSDTQ) is gauged against these new accurate references. The performances of various approximations based on many-body Green's functions (*GW*, GF2, and *T*-matrix) for IPs are also analyzed. Their limitations in correctly modeling satellite transitions are discussed.

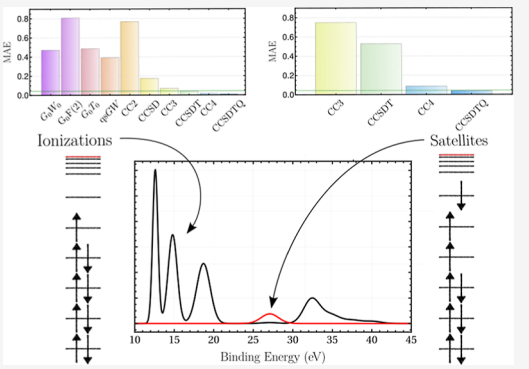

1. INTRODUCTION

Ionization spectra, probed through techniques like UV−vis, X-ray, synchrotron radiation, or electron impact spectroscopy, are invaluable tools in experimental chemistry for unraveling the structural intricacies of atoms, molecules, clusters, or solids.[1−3] Through the positions and intensities of their peaks, these spectra offer key information about the sampled system. For example, these measurements can be realized in various phases (gas, liquid, or solid) and, hence, analyzed to understand changes in electronic structure in these different phases.[4−7]

Typically, within the energy range from 10 to 40 eV, valence-shell ionization occurs, while the core−shell is probed at significantly higher energies.[8] This higher-energy region is not considered in the present study but the concepts that we discuss below in the context of valence-shell spectra are also encountered in the case of core electron spectroscopy. Particularly, between 10 and 20 eV, ionization spectra of small molecules usually exhibit well-defined peaks. These sharp and intense ionization peaks are essentially single-particle processes, i.e., an electron is ejected from the molecule and measured by the detector. These first peaks are associated with outer-valence orbitals. At slightly higher energies, typically several eV, the situation is more complex as, in addition to inner-valence single-particle ionization peaks, additional broader and less intense peaks appear. These are referred to as satellites or shakeup transitions.

In molecules, satellites represent ionization events coupled with the simultaneous excitation of one or more electrons. They are thus intrinsically many-body phenomena, as one must describe at least two electrons and one hole. Satellite transitions can be seen as the equivalent of double excitations in the realm of neutral excitations. Because one must describe processes involving two electrons and two holes, double excitations pose significant challenges for theoretical methods,[9−11] and the same holds true for satellite transitions. Consequently, such states can hardly be described by mean-field formalisms, such as Hartree−Fock (HF) theory. Thus, properly accounting for correlation effects is crucial to describe satellite transitions.[12] In particular, a recent study has emphasized the dynamic nature of this correlation.[13] In the following, the term "ionization" is employed to refer to single-particle processes, also called Koopmans' states.

Theoretical benchmarks play a pivotal role in evaluating the accuracy of approximation methods.[14−23] Concerning principal ionization potentials (IPs), which correspond to an electron detachment from the highest-occupied molecular orbital, two prominent benchmark sets are widely recognized: the extensively used *GW*100 test set[24−26] and a set comprising 24 organic acceptor molecules.[27−30] Both sets rely on reference

Received: February 21, 2024
Revised: April 10, 2024
Accepted: April 11, 2024
Published: May 22, 2024

https://doi.org/10.1021/acs.jctc.4c00216
J. Chem. Theory Comput. 2024, 20, 4751−4777

values obtained from coupled-cluster (CC) with singles, doubles, and perturbative triples [CCSD(T)] calculations[31−33] and determined by the energy difference between the neutral and cationic ground-state energies.[34] Recently, Ranasinghe et al. created a comprehensive benchmark set including not only principal IPs but also outer- and inner-valence IPs of organic molecules.[35] Reference values for this set were computed using the IP version of the equation-of-motion (IP-EOM) formalism[36−40] of CC theory with up to quadruple excitations (IP-EOM-CCSDTQ) for the smallest molecules.[35] Note that these benchmarks and the present work deal with vertical IPs, and we shall not address their adiabatic counterparts here.

To demonstrate its predictive capability for valence ionization spectra, an electronic structure method must precisely locate the positions of both outer- and inner-valence IPs, along with valence satellites. However, to the best of our knowledge, no established theoretical benchmarks exist for satellite energies in molecules. Consequently, the primary goal of this manuscript is to establish such a set of values. Finally, it is important to mention that to be fully predictive, a method should be able to predict the intensities associated with of these transitions. However, benchmarking intensities is beyond the scope of this work and will be considered in a future study.

Nowadays, a plethora of methods exist to compute IPs in molecular systems. The most straightforward among them is HF where occupied orbital energies serve as approximations of the IPs (up to a minus sign) by virtue of Koopmans' theorem.[41] Similarly, within density-functional theory (DFT), the Kohn−Sham (KS) orbital energies can be used as approximate ionization energies.[42−44] The accurate computation of IPs within KS-DFT is still an ongoing research field with, for example, long-range corrected functionals,[45] KS potential adjustors,[46,47] double-hybrids functionals,[48] or even functionals directly optimized for IPs.[35,49−51] An alternative way to compute electron detachment energies at the HF or KS-DFT levels is through the state-specific self-consistent-field (ΔSCF) formalism, where one optimizes both the neutral ground state and the cationic state of interest, the IPs being computed as the difference between these two total energies. This strategy has been mainly used to compute core binding energies and is known to perform better than Koopmans' theorem thanks to orbital relaxation.[52−58]

Mean-field methods, such as HF and KS-DFT, provide a first approximation to IPs but greater accuracy is often required. The well-known configuration interaction (CI) and CC formalisms provide two systematically improvable paths toward the exact IPs.[38−40,59] Within both frameworks, IPs can be obtained through a diagonalization of a given Hamiltonian matrix in the $(N-1)$-electron sector of the Fock space or through a state-specific formalism similar to ΔSCF. Ranasinghe et al. have shown that the mean absolute error (MAE) of IP-EOM-CCSDT with respect to CCSDTQ is only 0.03 eV for a set containing 42 IPs of small molecules.[35] Considering the same set, the cheaper IP-EOM-CCSD method has a MAE of 0.2 eV. Recently, the unitary CC formalism has also been employed within the IP-EOM formalism to compute IPs.[60] As mentioned above, the ΔSCF strategy can be extended to correlated methods which leads to the ΔCC method as an alternative to obtain IPs.[61] Once again, it has been mainly used to compute core IPs but it is also possible to determine valence IPs.[62−64] Selected CI (SCI)[65−68] provides yet another systematically improvable formalism for IPs. Indeed, by increasing progressively the number of determinants included in the variational space, one can in principle reach any desired accuracy, up to the full CI (FCI) limit.[69−75] Recently, the adaptative sampling CI algorithm[72,76−78] has been used to compute accurate valence ionization spectra of small molecules.[13]

In contrast to the wave function methods previously mentioned, one can also compute IPs via a more natural way based on electron propagators (or Green's functions), such as the *GW* approximation[79−81] or the algebraic diagrammatic construction (ADC).[82,83] The *GW* methodology has a myriad of variants. Its one-shot G_0W_0 version,[84−90] which was first popularized in condensed matter physics, is now routinely employed to compute IPs of molecular systems and can be applied to systems with thousands of correlated electrons.[91−103] Other flavors of *GW* such as eigenvalue-only self-consistent *GW* (ev*GW*)[104−108] and quasi-particle self-consistent *GW* (qs*GW*)[108−113] have also been benchmarked for IPs. Although the *GW* method is by far the most popular approach nowadays, there exist some alternatives, such as the second Born [also known as second-order Green's function (GF2) in the quantum chemistry community][41,114−129] or the *T*-matrix[130−147] approximations. However, none of them has enjoyed the popularity and performances reached by *GW*.[148−150] On the darker side, one of the main flaws of the *GW* approximation is its lack of systematic improvability, especially compared to the wave function methods mentioned above. Various beyond-*GW* schemes have been designed and gauged, but none of them seem to offer, at a reasonable cost, a systematic route toward exact IPs.[131,132,137,151−168]

The prediction of satellite peaks in molecules garnered attention in the late 20th century. In the 70s, Schirmer and co-workers applied extensively the 2ph-TDA [and the closely related ADC(3)] formalism to study the inner-valence region of small molecules.[12,169−181] CI methods were also employed by other groups to study this energetic region.[182−193] In both formalisms, the satellite energies are easily accessible as they correspond to higher-energy roots of the ADC and CI matrices. After relative successes for outer-valence ionizations, it was quickly realized that the inner-valence shell is much more difficult to describe due to the overlap between the inner-valence ionization and the outer-valence satellite peaks.[173] As mentioned above, the satellites present in this energy range cannot be described without taking into account electron correlation at a high level of theory. Even more troublesome, in some cases, the orbital picture (or quasiparticle approximation) completely breaks down. In other words, it becomes meaningless to assign the character of ionization or satellite to a given transition.[169,173] In the following decades, the symmetry-adapted-cluster (SAC) CI was extensively used to study the inner-valence ionization spectra of small organic molecules.[194−205] SAC-CI was shown to be able to compute satellite energies in quantitative agreement with experiments while methods based on Green's functions have been in qualitative agreement, at best.

Satellites, sometimes called sidebands, have been extensively studied in the context of materials.[79] These additional peaks, which can have different natures, are observed in photoemission spectra of metals, semiconductors, and insulators.[206−215] In "simple" metals, such as bulk sodium[206,213] or its paradigmatic version, the uniform electron gas,[25,214,216−221] satellites are usually created by the strong coupling between electrons and plasmon excitations. It is widely recognized that *GW* does not properly describe satellite structures in solids, and it is required to include vertex corrections to describe these many-body

https://doi.org/10.1021/acs.jctc.4c00216
J. Chem. Theory Comput. 2024, 20, 4751−4777

effects. One of the most common schemes to study satellites in solids is the cumulant expansion,[210,219,222−224] which is formally linked to electron-boson Hamiltonians.[156,225−227]

Nowadays, computational and theoretical progress allows us to systematically converge to exact neutral excitation energies of small molecules,[10,73,228−231] and this holds as well for charged excitations like IPs. For example, Olsen et al. computed the exact first three IPs of water using FCI,[59] while Kamiya and Hirata went up to IP-EOM-CCSDTQ to compute highly accurate satellite energies for CO and N_2.[39] As mentioned previously, a set of 42 IPs of CCSDTQ quality is also available now.[35] Finally, Chatterjee and Sokolov recently computed 27 valence IPs using the semistochastic heatbath SCI method[73,232,233] in order to benchmark their multireference implementation of ADC.[234,235] They also report FCI-quality energies for the four lowest satellite states of the carbon dimer. The present manuscript contributes to this line of research by providing 42 satellite energies of FCI quality. Additionally, 58 valence IPs are reported as well, among which 37 were not present in Ranasinghe's CCSDTQ nor Chatterjee's FCI benchmark set.[35,234] This study is part of a larger database of highly accurate vertical neutral excitation energies named QUEST which now includes more than 900 excitation energies.[10,23,230,231,236−242] Our hope is that these new data will serve as a valuable resource for encouraging the development of novel approximate methods dedicated to computing satellite energies, building on the success of benchmarks with highly accurate reference energies and properties.

2. COMPUTATIONAL DETAILS

The geometries of the molecular systems considered here have been optimized using CFOUR[243] following QUEST's protocol,[23,237] i.e., at the CC3/aug-cc-pVTZ level[244,245] without frozen-core approximation. The corresponding Cartesian coordinates can be found in the Supporting Information. Throughout the paper, the basis sets considered are Pople's 6-31+G*[246−252] and Dunning's aug-cc-pVXZ (where X = D, T, and Q).[253−256]

2.1. Selected CI Calculations. All SCI calculations have been performed using the configuration interaction using a perturbative selection made iteratively (CIPSI) algorithm[67,228,257−260] as implemented in QUANTUM PACKAGE.[261] The multistate CIPSI calculations are performed by converging several eigenvalues (using the iterative Davidson diagonalization procedure) at each iteration and then selecting determinants for these eigenvectors in a state-averaged way.[262] For more details about the CIPSI method and its implementation, see ref 261. The frozen-core approximation has been enforced in all calculations using the conventions of GAUSSIAN16[263] and CFOUR,[243] except for Li and Be where the 1s orbital was not frozen.

We followed a two-step procedure to obtain the ionization and satellite energies, I_ν^N, at the SCI level. First, two single-state calculations are performed for the N- and $(N-1)$-electron ground states. This yields the principal IP of the system, $I_0^N = E_0^{N-1} - E_0^N$, where E_0^{N-1} and E_0^N are the ground-state energies of the N- and $(N-1)$-electron systems, respectively. Then, a third, multistate calculation is performed to compute the neutral excitation energies of the $(N-1)$-electron system, $\Delta E_\nu^{N-1} = E_\nu^{N-1} - E_0^{N-1}$, where E_ν^{N-1} is the energy of the νth excited states associated with the $(N-1)$-electron system. Combining these three calculations, one gets

$$I_\nu^N = E_0^{N-1} - E_0^N + \Delta E_\nu^{N-1} \quad (1)$$

Because single-state calculations converge faster than their multistate counterparts, the limiting factor associated with the present CIPSI calculations are the convergence of the excitation energies ΔE_ν^{N-1}, and this is what determines ultimately the overall accuracy of I_ν^N.

For each system and state, the SCI variational energy has been extrapolated as a function of the second-order perturbative correction using a linear weighted fit using the last 3 to 6 CIPSI iterations.[73,74,264,265] The weights have been taken as the square of the inverse of the perturbative correction. The estimated FCI energy is then chosen among these extrapolated values obtained with a variable number of points such that the standard error associated with the extrapolated energy is minimal. Below, we report error bars associated with these extrapolated FCI values. However, it is worth remembering that these do not correspond to genuine statistical errors. The fitting procedure has been performed with MATHEMATICA using default settings.[266]

The SCI values and their corresponding error bars are reported with three decimal places to enable fair and reliable comparisons between methods, ensuring a precision well below the chemical accuracy threshold (i.e., 0.043 eV). One should keep in mind that only the first decimal might be experimentally meaningful (i.e., measured without uncertainty). Finally, note that comparing theoretical and experimental IPs is a complex task, requiring consideration of vibrational effects (see for example ref 267) and possibly relativistic effects for inner-valence IP and/or molecules containing third-row atoms.

2.2. CC Calculations. The EOM-CC calculations have been done using CFOUR with the default convergence thresholds.[243] Again, the frozen-core approximation was enforced systematically. IP-EOM-CC calculations, i.e., diagonalization of the CC effective Hamiltonian in the $(N-1)$-electron sector of the Fock space,[36−40] have been performed for CCSD,[32,36,268−271] CCSDT,[37,272−274] and CCSDTQ.[275−279] At the CCSD level, the EOM space includes the one-hole (1h) and the two-hole-one-particle (2h1p) configurations, while the three-hole-two-particle (3h2p) and four-hole-three-particle (4h3p) configurations are further added at the CCSDT and CCSDTQ, respectively. Note that, within the CC formalism, we assume that the IP and electron affinity (EA) sectors are decoupled.[280−283] For CC2,[284,285] CC3,[244,245,286−288] and CC4,[239,289−291] diagonalization in the $(N-1)$-electron sector of the Fock space is not available yet. Hence, it has been carried out in the N-electron sector of the Fock space[36,37,292−296] with an additional very diffuse (or bath) orbital with zero energy to obtain ionization and satellite energies. Therefore, at the CC2 level, the EOM space includes the one-hole-one-particle (1h1p) and the two-hole-two-particle (2h2p) configurations, while the three-hole-three-particle (3h3p) and four-hole-four-particle (4h4p) configurations are further added at the CC3 and CC4 levels, respectively. These two schemes produce identical IPs and satellite energies but, for a given level of theory, the diagonalization in the N-electron sector is more computationally demanding due to the larger size of the EOM space (see ref 297 for more details). In each scheme, the desired states have been obtained thanks to the root-following Davidson algorithm implemented in CFOUR. The initial vectors were built using the dominant configurations of the SCI vectors.

The ΔCCSD(T) calculations have been performed with GAUSSIAN16.[263] These calculations are based on a closed-shell

https://doi.org/10.1021/acs.jctc.4c00216
J. Chem. Theory Comput. 2024, 20, 4751−4777

restricted HF reference and an open-shell unrestricted HF reference for the neutral and cationic species, respectively.[149]

2.3. Green's Function Calculations. Many-body Green's function calculations have been carried out with the open-source software QUACK.[298] In the following, we use the acronyms G_0W_0, $G_0F(2)$, and G_0T_0 to refer to the one-shot schemes where one relies on the *GW*, second-Born, and *T*-matrix self-energies, respectively. Each approximated scheme considered in this work (G_0W_0, qs*GW*, $G_0F(2)$, and G_0T_0) relies on HF quantities as starting point. We refer the reader to refs 81 and 150 for additional details about the theory and implementation of these methods. The infinitesimal broadening parameter η is set to 0.001 E_h for all calculations. It is worth mentioning that we do not linearize the quasiparticle equation to obtain the quasiparticle energies. The qs*GW* calculations are performed with the regularized scheme based on the similarity renormalization group approach, as described in ref 113. A flow parameter of $s = 500$ is employed. All (occupied and virtual) orbitals are corrected. The spectral weight of each quasiparticle solution is reported in Supporting Information. Compared to the EOM-CC formalism discussed in Section 2.2, it is important to mention that, in the Green's function framework, the IP and EA sectors [i.e., the 1h and one-particle (1p) configurations] are actually coupled,[150,282,299] effectively creating higher-order diagrams.[82,299]

3. RESULTS AND DISCUSSION

The present section is partitioned into subsections, each dedicated to a distinct group of related molecules. Within these subsections, we focus our attention mainly on the satellite states, while IPs are addressed in Section 3.7.

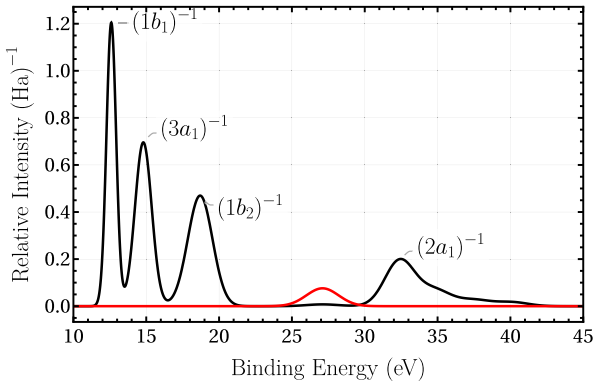

Figure 1. Gaussian fit of the experimental ionization spectrum of water in the gas phase measured by Ning and co-workers. The fitting parameters can be found in ref 204. The red peak at 27.1 eV has been magnified by a factor 10.

Each state considered in this work is reported alongside its symmetry label, e.g., 1 $^2B_1$ for the principal IP of water. Furthermore, the main orbitals involved in the ionization process are specified. For example, the *N*-electron ground state of water has the following dominant configuration $(1a_1)^2(2a_1)^2(1b_2)^2(3a_1)^2(1b_1)^2$, while the configuration of the $(N-1)$-electron ground state is $(1a_1)^2(2a_1)^2(1b_2)^2(3a_1)^2(1b_1)^1$. Hence, we denote the principal IP as $(1b_1)^{-1}$ to indicate that an electron has been ionized from the $1b_1$ orbital. The lowest satellite of water, i.e., the 2 $^2B_1$ state of configuration $(1a_1)^2(2a_1)^2(1b_2)^2(3a_1)^1(1b_1)^1(4a_1)^1$, is labeled as $(3a_1)^{-1}(1b_1)^{-1}(4a_1)^1$ to signify that one electron was detached from the orbital $1b_1$ and $3a_1$, one of them being subsequently promoted to the virtual orbital $4a_1$ and the other ionized. In some cases, additional valence complete-active-space CI calculations have been performed using MOLPRO to determine the symmetry of the FCI states.[300]

3.1. 10-Electron Molecules: Ne, HF, H_2O, NH_3, and CH_4. The water molecule has been extensively studied experimentally using photoionization and electron impact spectroscopy.[204,306,307] For example, a high-resolution spectrum of liquid water is crucial as a first step for understanding the photoelectron spectra of aqueous phases.[5,6] On the other hand, its gas-phase ionization spectrum is now well understood. The experimental ionization spectrum of water is plotted in Figure 1, serving as a representative example to illustrate the following discussion. The first three sharp peaks at 12.6, 14.8, and 18.7 eV are associated with electron detachments from the three outer-valence orbitals, $1b_1$, $3a_1$, and $1b_2$, respectively.[204] Then, a broader yet intense peak corresponding to the fourth ionization, $(2a_1)^{-1}$, is found at 32.4 eV surrounded by several close-lying satellite peaks. Additionally, there is a smaller broad satellite peak at 27.1 eV (magnified red peak in Figure 1).

Table 1 gathers the FCI reference values corresponding to the three lowest satellites identified in our study. The first two, which are of $^2B_1$ and $^2A_1$ symmetries, lie close to each other around 27.1 eV. The third satellite is of $^2B_1$ symmetry and is found at slightly higher energy, approximately 29 eV. The ordering and the absolute energies of the three satellites align well with previous SAC-CI results reported by Ning et al.[204] In addition, they showed that, at the ADC(3) level, the energy of the 2 $^2A_1$ state is overestimated by approximately 2.7 eV, while the 2 $^2B_1$ and 3 $^2B_1$ states are missing. It is also worth noting that early CI and Green's function studies had qualitatively predicted the 2 $^2A_1$ satellite.[12,187] Finally, we do not consider the broad peak at 32.4 eV here because it is technically out of reach for our current SCI implementation. However, it has been studied by Mejuto-Zaera and co-workers who have shown that vertex corrections are required to correctly describe this complex part of the spectrum where strong many-body effects are at play.[13]

For the three satellites of water, CCSDTQ is in near-perfect agreement with FCI in all basis sets with errors inferior to 0.03 eV. CC4 is slightly worse than CCSDTQ but is still an excellent approximation given its lower computational cost and its approximate treatment of quadruples. The CCSDT satellite energies are overestimated by approximately 0.5 eV, while CC3 appears to struggle for this system. Indeed, the CC3 energies are badly underestimated with errors up to 1.5 eV, and the ordering of the first two satellites is wrongly predicted.[308] Finally, CCSD and CC2 are not considered for satellites as their poor performance (wrong by several eV) makes the assignment of these states extremely challenging.

The remainder of this section is concerned with four molecules isoelectronic to water, namely CH_4, NH_3, HF, and Ne. For each of these molecules, Table 1 provides FCI reference values for the IPs corresponding to the two outermost valence orbitals. In addition, two satellite energies are reported for hydrogen fluoride and ammonia, while one satellite is presented for methane and neon. Experimental values for the IPs of these four molecules have been measured multiple times and are reported in Table 1.[4,7,189,191,192,301,303,309−311]

Yencha and co-workers measured the inner-valence photoelectron spectrum of HF. It displays a well-defined peak around

https://doi.org/10.1021/acs.jctc.4c00216
J. Chem. Theory Comput. 2024, 20, 4751−4777

Table 1. Valence Ionizations and Satellite Transition Energies (in eV) of the 10-Electron Series for Various Methods and Basis Sets[a]

	basis				basis				basis			
methods	6-31+G*	AVDZ	AVTZ	AVQZ	6-31+G*	AVDZ	AVTZ	AVQZ	6-31+G*	AVDZ	AVTZ	AVQZ
mol.	water (H_2O)											
state/conf.	$1\,^2B_1/(1b_1)^{-1}$				$1\,^2A_1/(3a_1)^{-1}$				$1\,^2B_2/(1b_2)^{-1}$			
exp.	12.6[204]				14.8[204]				18.7[204]			
CC2	11.159	11.345	11.541	11.620	13.513	13.645	13.791	13.863	18.035	18.039	18.145	18.211
CCSD	12.170	12.386	12.594	12.675	14.502	14.677	14.825	14.895	18.861	18.888	18.972	19.032
CC3	12.287	12.519	12.661	12.722	14.621	14.811	14.899	14.949	18.950	18.993	19.023	19.065
CCSDT	12.276	12.491	12.629	12.689	14.601	14.776	14.861	14.910	18.919	18.951	18.981	19.022
CC4	12.307	12.543	12.683	12.741	14.635	14.832	14.920	14.968	18.952	18.999	19.030	19.070
CCSDTQ	12.304	12.534	12.673	×	14.631	14.822	14.907	×	18.947	18.990	19.018	×
FCI	12.309	12.540	12.679	12.737	14.636	14.829	14.915	14.962	18.950	18.995	19.024	19.063
G_0W_0	12.312	12.485	12.884	13.080	14.625	14.781	15.106	15.285	18.818	18.865	19.129	19.290
qsGW	12.379	12.640	12.879	12.982	14.696	14.932	15.107	15.197	18.965	19.069	19.188	19.271
G_0F(2)	11.110	11.279	11.555	11.675	13.507	13.626	13.837	13.945	17.983	17.978	18.141	18.236
G_0T_0	11.967	12.095	12.357	×	14.240	14.336	14.532	×	18.459	18.429	18.572	×
mol.	ammonia (NH_3)											
state/conf.	$1\,^2A_1/(3a_1)^{-1}$				$1\,^2E/(1e_g)^{-1}$				$3\,^2A_1/(2a_1)^{-1}$			
exp.	10.93[301]				16.6[301]							
CC2	9.779	9.986	10.168	10.234	15.794	15.828	15.960	16.019	27.646	27.381	27.365	×
CCSD	10.434	10.677	10.862	10.923	16.403	16.473	16.588	16.639	27.745	27.696	27.855	27.915
CC3	10.447	10.746	10.888	10.935	16.407	16.520	16.592	16.629	27.252	27.114	27.191	×
CCSDT	10.449	10.734	10.876	10.922	16.399	16.500	16.573	16.609	26.773	26.724	26.899	×
CC4	10.461	10.761	10.901	×	16.417	16.533	16.603	×	26.669	26.621	26.746	×
CCSDTQ	10.461	10.760	10.899	×	16.415	16.529	16.598	×	26.698	26.645	26.768	×
FCI	10.463	10.762	10.901	10.945	16.418	16.534	16.603	16.640	26.683	26.659	26.779	26.833(1)
G_0W_0	10.675	10.837	11.201	11.362	16.527	16.578	16.867	17.007	28.241	28.117	28.427	28.463
qsGW	10.520	10.870	11.094	11.176	16.468	16.655	16.805	16.878	28.029	27.962	27.980	28.151
G_0F(2)	9.841	9.994	10.244	10.345	15.817	15.814	16.002	16.088	27.589	27.638	27.729	×
G_0T_0	10.399	10.497	10.716	×	16.217	16.170	16.330	×	28.860	28.738	28.860	×
mol.	methane (CH_4)								hydrogen fluoride (HF)			
state/conf.	$1\,^2T_2/(1t_2)^{-1}$				$1\,^2A_1/(2a_1)^{-1}$				$1\,^2\Pi/(1\pi)^{-1}$			
exp.	14.5[302]				23.0[302]				16.19[303]			
CC2	13.787	13.888	14.028	14.079	23.289	23.227	23.311	23.352	14.431	14.559	14.725	14.813
CCSD	14.102	14.258	14.387	14.428	23.238	23.247	23.383	23.426	15.688	15.837	16.021	16.117
CC3	14.060	14.270	14.365	14.395	23.034	23.035	23.138	23.173	15.917	16.036	16.126	16.194
CCSDT	14.068	14.269	14.365	14.395	23.040	23.035	23.135	23.171	15.885	15.992	16.077	16.145
CC4	14.072	14.284	14.376	×	23.039	23.050	23.142	×	15.947	16.068	16.161	16.227
CCSDTQ	14.073	14.284	14.376	×	23.042	23.052	23.143	×	15.935	16.051	16.140	16.205
FCI	14.073	14.285	14.377	14.407	23.043	23.056	23.146	23.148(10)	15.941	16.059	16.149	16.214
G_0W_0	14.338	14.466	14.753	14.872	23.647	23.626	23.875	23.988	15.679	15.868	16.237	16.453
qsGW	14.142	14.446	14.621	14.686	23.248	23.426	23.550	23.605	16.001	16.144	16.349	16.469
G_0F(2)	13.861	13.913	14.102	14.176	23.377	23.257	23.385	23.447	14.280	14.437	14.685	14.815
G_0T_0	14.117	14.117	14.275	×	24.107	24.051	24.163	×	15.334	15.466	15.721	×
mol.	hydrogen fluoride (HF)								neon (Ne)			
state/conf.	$1\,^2\Sigma^+/(3\sigma)^{-1}$				$1\,^2P/(2p)^{-1}$				$1\,^2S/(2s)^{-1}$			
exp.	19.90[303]				21.57[304]				48.46[304]			
CC2	18.740	18.814	18.908	18.982	19.874	20.017	20.144	20.236	47.483	47.265	47.187	47.207
CCSD	19.777	19.861	19.946	20.021	21.030	21.168	21.326	21.432	48.735	48.363	48.426	48.494
CC3	19.980	20.040	20.050	20.100	21.353	21.417	21.449	21.522	48.652	48.263	48.145	48.168
CCSDT	19.933	19.989	19.995	20.045	21.304	21.367	21.398	21.473	48.725	48.330	48.229	48.270
CC4	19.986	20.051	20.065	20.114	21.375	21.434	21.473	21.546	48.829	48.424	48.316	48.349
CCSDTQ	19.974	20.036	20.046	20.094	21.362	21.421	21.455	21.527	48.811	48.406	48.293	48.326
FCI	19.979	20.043	20.054	20.102	21.365	21.426	21.461	21.533	48.822	48.417	48.306	48.340
G_0W_0	19.662	19.812	20.074	20.259	20.859	21.104	21.432	21.655	47.851	47.785	47.950	48.085
qsGW	19.984	20.084	20.203	20.304	21.361	21.435	21.592	21.729	47.844	47.652	47.560	47.566
G_0F(2)	18.644	18.744	18.899	19.007	19.642	19.851	20.066	20.202	47.246	47.082	47.055	47.096
G_0T_0	19.312	19.402	19.551	×	20.671	20.847	21.085	×	48.966	48.851	48.886	×

https://doi.org/10.1021/acs.jctc.4c00216
J. Chem. Theory Comput. 2024, 20, 4751−4777

Table 1. continued

	basis				basis				basis			
methods	6-31+G*	AVDZ	AVTZ	AVQZ	6-31+G*	AVDZ	AVTZ	AVQZ	6-31+G*	AVDZ	AVTZ	AVQZ
mol.	water (H_2O)											
state/conf.	$2\,^2B_1/(3a_1)^{-1}(1b_1)^{-1}(4a_1)^1$				$2\,^2A_1/(1b_1)^{-2}(4a_1)^1$				$3\,^2B_1/(3a_1)^{-1}(1b_1)^{-1}(4a_1)^1$			
exp.	27.1[204]				27.1[204]							
CC3	26.152	25.797	26.075	26.174	25.949	25.763	26.038	26.130	27.654	27.425	27.661	27.747
CCSDT	27.566	27.694	28.103	28.246	27.324	27.476	27.831	27.954	29.005	29.129	29.442	29.559
CC4	26.894	26.844	27.090	27.195	26.943	26.965	27.159	27.239	28.588	28.580	28.737	28.813
CCSDTQ	27.051	27.049	27.297	×	27.065	27.104	27.294	×	28.714	28.729	28.882	×
FCI	27.062	27.065	27.300	27.389	27.084	27.131	27.312	27.404	28.731	28.754	28.899	28.973
mol.	ammonia (NH_3)								methane (CH_4)			
state/conf.	$2\,^2A_1/(3a_1)^{-2}(4a_1)^1$				$2\,^2E/(3a_1)^{-2}(3e)^1$				$2\,^2T_2/(1t_2)^{-2}(3a_1)^1$			
exp.									29.2[302]			
CC3	23.112	23.126	23.367	23.440	25.489	25.220	25.418	25.471	28.102	28.188	28.388	28.445
CCSDT	23.866	24.101	24.408	24.503	25.881	25.882	26.113	26.189	28.210	28.415	28.643	28.713
CC4	23.579	23.764	23.952	×	25.666	25.618	25.743	×	27.922	28.111	28.271	×
CCSDTQ	23.631	23.818	24.003	×	25.688	25.648	25.773	×	27.931	28.123	28.282	×
FCI	23.630	23.829	24.004	24.061	25.685	25.655	25.771	25.815	27.859	28.108	28.238	28.277(5)
mol.	hydrogen fluoride (HF)								Neon (Ne)			
state/conf.	$2\,^2\Sigma^+/(1\pi)^{-2}(4\sigma)^1$				$1\,^2\Delta/(1\pi)^{-2}(4\sigma)^1$				$2\,^2P/(2p)^{-2}(3s)^1$			
exp.									49.16[305]			
CC3	31.076	30.636	30.916	31.039	32.872	32.516	32.749	32.852	46.502	46.690	46.436	46.343
CCSDT	32.849	32.917	33.356	33.531	34.845	34.885	35.218	35.365	49.774	49.917	50.197	50.322
CC4	32.110	31.981	32.210	×	34.309	34.181	34.304	34.399	48.932	48.980	48.920	48.962
CCSDTQ	32.312	32.228	32.466	32.603	34.503	34.403	34.528	34.631	49.258	49.283	49.313	49.394
FCI	32.347	32.257	32.474	32.605	34.547	34.445	34.554	34.648	49.339	49.349	49.343	49.414

[a]AVXZ stands for aug-cc-pVXZ (where X = D, T, and Q). Selected experimental values are also reported.

Table 2. Satellite Tansition Energies of Ammonia and Water Computed with Green's Function Methods in the aug-cc-pVDZ Basis Set[a]

molecule	state	method	diag. element	eigenvalue	FCI
		$G_0F(2)$	24.324	24.328	
NH_3	$2\,^2A_1$	G_0W_0	24.408	24.410	23.829
		G_0T_0	40.441	40.444	
		$G_0F(2)$	24.977	24.977	
NH_3	$2\,^2E$	G_0W_0	24.997	24.997	25.655
		G_0T_0	41.094	41.094	
		$G_0F(2)$	30.759	30.759	
H_2O	$2\,^2B_1$	G_0W_0	30.846	30.846	27.065
		G_0T_0	×	×	
		$G_0F(2)$	28.683	28.683	
H_2O	$2\,^2A_1$	G_0W_0	28.770	28.770	27.131
		G_0T_0	×	×	
		$G_0F(2)$	30.759	30.781	
H_2O	$3\,^2B_1$	G_0W_0	30.863	30.867	28.754
		G_0T_0	×	×	

[a]The FCI values are reported for comparison purposes.

33 eV which appears in close agreement with the FCI energies for the $2\,^2\Sigma^+$ state.[311] In addition, a doubly degenerate satellite of $^2\Delta$ symmetry has also been computed. In the various NH_3 ionization spectra reported in the literature, there is no satellite peak around 24 eV which may correspond to the $2\,^2A_1$ and $2\,^2E$ FCI states.[189,201,301] Nevertheless, the FCI energies align well with the SAC-CI energies of Ishida and co-workers who predicted that these two satellite states have very low intensity.[201] The first satellite observed in the inner-valence region of the photoionization spectrum of CH_4 is a very weak and broad peak at 29.2 eV.[302] This peak is also measured at 28.56 eV using electron momentum spectroscopy experiments.[192] The energy of the first satellite calculated at the FCI level, and associated with the $(2t_2)^{-2}(3a_1)^1$ process, compares well with the experimental data. Finally, the lowest-energy satellite state of neon is also reported along with the corresponding experimental value measured by Joshi and co-workers.[305] It is worth noting that CC3 behaves similarly in Ne, HF, and H_2O, yet it appears to be a much better approximation for the satellite states of NH_3 and CH_4.

Among the 12 IPs computed for this series of molecules, 11 of them have a weight larger than 0.85 on the 1h dominant configuration (in the aug-cc-pVDZ basis set). Only the $3\,^2A_1$ state of ammonia has a quite smaller weight (0.58) on the corresponding 1h determinant. This exemplifies the breakdown of the orbital picture in the inner-valence ionization spectrum,[12,169−181] which signature is a significant weight on both 1h and 2h1p configurations, hence preventing us from assigning the solution as a clear IP or satellite. The performance of the various approximations for IPs will be statistically gauged in Section 3.7.

3.2. Satellite in Green's Functions Methods. Thus, far, we have exclusively assessed the performance of different rungs of the CC hierarchy. Although shakeup transition energies can also be computed within the Green's function framework, the task is notably more challenging, especially when compared to the more straightforward nature of IP-EOM-CC. This complexity arises from the fact that satellites, existing as nonlinear solutions of the quasiparticle equation,[79] prove much more difficult to converge using Newton−Raphson algorithms than the quasiparticle solutions, which are representative of typical

https://doi.org/10.1021/acs.jctc.4c00216
J. Chem. Theory Comput. 2024, 20, 4751−4777

Table 3. Valence (in eV) of the 14-Electron Series for Various Methods and Basis Sets[a]

	basis				basis				basis			
methods	6-31 +G*	AVDZ	AVTZ	AVQZ		AVDZ	AVTZ	AVQZ	6-31 +G*	AVDZ	AVTZ	AVQZ
mol.					boron fluoride (BF)							
state/conf.			$1\,^2\Sigma^+/(5\sigma)^{-1}$				$2\,^2\Pi/(1\pi)^{-1}$				$2\,^2\Sigma^+/(4\sigma)^{-1}$	
exp.			11.06[325]									
CC2	10.751	10.824	10.944	10.987	17.136	17.274	17.385	17.467	19.767	19.957	19.962	20.041
CCSD	11.080	11.154	11.250	11.279	17.920	18.028	18.172	18.246	21.017	21.208	21.253	21.342
CC3	10.914	11.004	11.100	11.127	18.606	18.722	18.743	18.794	20.745	20.910	20.918	20.984
CCSDT	10.969	11.057	11.157	11.185	18.474	18.584	18.622	18.677	20.708	20.866	20.875	20.946
CC4	10.965	11.053	11.148	11.175	18.475	18.593	18.626	18.679	20.770	20.920	20.917	20.981
CCSDTQ	10.967	11.054	11.150	×	18.453	18.569	18.599	×	20.734	20.882	20.874	×
FCI	10.966	11.054	11.149	11.175	18.466	18.581	18.612	18.664	20.765	20.913	20.906	20.970(1)
G_0W_0	11.053	11.117	11.325	11.420	18.237	18.456	18.743	18.949	21.142	21.402	21.567	21.778
qsGW	10.862	10.989	11.167	11.240	18.513	18.662	18.784	18.899	21.389	21.583	21.585	21.701
$G_0F(2)$	10.859	10.915	11.052	11.114	16.958	17.132	17.328	17.454	19.654	19.878	19.955	20.079
G_0T_0	10.821	10.856	10.955	×	17.947	18.105	18.304	×	20.739	20.955	21.041	×
mol.					carbon monoxide (CO)							
state/conf.			$1\,^2\Sigma^+/(5\sigma)^{-1}$				$1\,^2\Pi/(1\pi)^{-1}$				$2\,^2\Sigma^+/(4\sigma)^{-1}$	
exp.			14.01[326]				17.0[326]				19.7[326]	
CC2	13.550	13.584	13.748	13.809	16.289	16.349	16.505	16.581	18.175	18.316	18.400	18.464
CCSD	13.948	13.998	14.190	14.246	16.793	16.865	17.024	17.095	19.501	19.657	19.790	19.867
CC3	13.614	13.697	13.863	13.912	16.826	16.902	17.018	17.075	19.512	19.664	19.744	19.807
CCSDT	13.693	13.770	13.952	14.005	16.762	16.838	16.960	17.016	19.347	19.498	19.583	19.647
CC4	13.678	13.760	13.933	13.984	16.751	16.835	16.955	17.009	19.410	19.566	19.653	19.715
CCSDTQ	13.679	13.761	13.935	×	16.755	16.837	16.958	×	19.376	19.532	19.616	×
FCI	13.670	13.752	13.925	13.975	16.762	16.845	16.966	17.017(2)	19.393	19.550	19.637	19.699(1)
G_0W_0	14.461	14.467	14.777	14.915	16.677	16.762	17.083	17.264	19.869	20.045	20.300	20.485
qsGW	13.980	14.080	14.318	14.416	16.836	16.932	17.124	17.231	19.899	20.071	20.191	20.298
$G_0F(2)$	13.856	13.857	14.067	14.154	16.134	16.204	16.422	16.534	18.165	18.317	18.460	18.564
G_0T_0	14.163	14.143	14.324	×	16.422	16.470	16.666	×	19.333	19.481	19.613	×
mol.					dinitrogen (N_2)							
state/conf.			$1\,^2\Sigma_u^+/(3\sigma_g)^{-1}$				$1\,^2\Pi_u/(1\pi_u)^{-1}$				$1\,^2\Sigma_u^+/(2\sigma_u)^{-1}$	
exp.			15.580[327]				16.926[327]				18.751[327]	
CC2	14.613	14.649	14.814	14.877	16.932	16.943	17.104	17.178	17.803	17.862	17.991	18.037
CCSD	15.382	15.424	15.641	15.709	17.065	17.087	17.228	17.287	18.654	18.721	18.931	18.991
CC3	15.282	15.349	15.519	15.574	16.669	16.719	16.837	16.885	18.598	18.680	18.849	18.899
CCSDT	15.270	15.333	15.517	15.574	16.765	16.812	16.950	17.001	18.502	18.585	18.763	18.816
CC4	15.220	15.293	15.471	15.526	16.770	16.821	16.940	16.987	18.403	18.493	18.669	18.720
CCSDTQ	15.237	15.309	15.487	×	16.764	16.815	16.936	×	18.429	18.519	18.696	×
FCI	15.235	15.308	15.486	15.541	16.759	16.811	16.933	16.981	18.427	18.516	18.692	18.742
G_0W_0	15.959	15.984	16.350	16.519	16.781	16.790	17.093	17.259	19.515	19.558	19.862	20.000
qsGW	15.575	15.663	15.914	16.020	16.640	16.706	16.903	17.006	19.125	19.221	19.425	19.513
$G_0F(2)$	14.824	14.845	15.080	15.181	16.956	16.952	17.158	17.261	17.974	18.020	18.201	18.274
G_0T_0	15.494	15.502	15.722	×	16.673	16.653	16.820	×	18.993	19.021	19.190	×
mol.			boron fluoride (BF)									
state/conf.			$1\,^2\Pi/(5\sigma)^{-2}(2\pi)^1$									
exp.												
CC3	17.494	17.541	17.607	17.637								
CCSDT	17.410	17.462	17.532	17.567								
CC4	17.293	17.345	17.393	17.419								
CCSDTQ	17.303	17.355	17.405	×								
FCI	17.297	17.346	17.392	17.417								
mol.					carbon monoxide (CO)							
state/conf.			$2\,^2\Pi/(5\sigma)^{-2}(2\pi)^1$				$2\,^2\Sigma^+/(1\pi)^{-1}(5\sigma)^{-1}(2\pi)^1$				$1\,^2\Delta/(1\pi)^{-1}(5\sigma)^{-1}(2\pi)^1$	
exp.			22.7[326]				23.7[326]					
CC3	23.406	23.507	23.597	23.640	23.640	23.729	23.839	23.881	23.730	23.814	23.926	23.968
CCSDT	23.205	23.313	23.441	23.507	23.381	23.472	23.602	23.669	23.417	23.503	23.647	23.713
CC4	22.862	22.957	22.997	23.040	23.102	23.166	23.193	23.236	23.143	23.206	23.251	23.293×
CCSDTQ	22.841	22.937	22.995	×	23.101	23.167	23.209	×	23.141	23.205	23.264	×
FCI	22.791	22.889	22.908(1)	22.962(3)	23.074(1)	23.140(2)	23.194(1)	23.232(1)	23.114	23.181	23.233	23.271(1)

https://doi.org/10.1021/acs.jctc.4c00216
J. Chem. Theory Comput. 2024, 20, 4751−4777

Table 3. continued

	basis				basis				basis			
methods	6-31 +G*	AVDZ	AVTZ	AVQZ		AVDZ	AVTZ	AVQZ	6-31 +G*	AVDZ	AVTZ	AVQZ
mol.						dinitrogen (N_2)						
state/conf.		$1\,^2\Pi_g/(3\sigma_g)^{-2}(4\pi_g)^1$				$1\,^2\Sigma_u^+/(3\sigma_g)^{-1}(3\pi_u)^{-1}(4\pi_g)^1$				$1\,^2\Sigma_u^-/(3\sigma_g)^{-1}(3\pi_u)^{-1}(4\pi_g)^1$		
exp.		24.788[327]				25.514[327]						
CC3	25.280	25.331	25.495	25.535	25.656	25.699	25.856	25.908	26.584	26.599	26.686	26.723
CCSDT	24.945	25.008	25.232	25.304	25.405	25.453	25.643	25.721	26.209	26.250	26.362	26.427
CC4	24.394	24.458	24.575	24.621	25.099	25.142	25.235	25.288	25.990	26.012	26.022	26.058
CCSDTQ	24.363	24.431	24.574	×	25.088	25.134	25.238	×	25.721	25.756	25.762	×
FCI	24.277	24.348	24.470(1)	24.519(1)	25.054	25.103	25.199	×	25.658	25.695	25.689	×

[a]AVXZ stands for aug-cc-pVXZ (where X = D, T, and Q). Selected experimental values are also reported.

IPs. Fortunately, an alternative and equivalent pathway exists where one solves a larger linear eigenvalue problem instead of solving the nonlinear quasiparticle equation.[82,125,150,283,312−316] In such a case, satellites are obtained as higher-energy roots via diagonalization of the so-called "upfolded" matrix built in the basis of the 2h1p and two-particle-one-hole (2p1h) configurations in addition to the 1h and 1p configurations.

The satellite energies of H_2O and NH_3 computed with G_0W_0, $G_0F(2)$, and G_0T_0 are presented in Table 2. qsGW is not considered here as its static approximation naturally discards all the satellite solutions. The third column shows the diagonal elements of the upfolded matrix associated with the 2h1p configurations, while the fourth column displays the associated eigenvalues. One can immediately observe that the eigenvalues do not improve upon the diagonal elements. This is due to the lack of higher-order (such as 3h2p) configurations that are essential to correlate satellites. This parallels the description of double excitations which require at least triple excitations (i.e., 3h3p configurations) in addition to the 2h2p configurations to correlate doubly excited states.[9−11] Regarding the two satellites of ammonia, the T-matrix zeroth-order elements are utterly inaccurate. This discrepancy arises because, at the T-matrix level, satellite energies are described as the sum of a Koopmans' electron attachment energy (1p configuration) and a double electron detachment energy [two-hole (2h) configuration] stemming from the particle−particle random-phase approximation.[150,317−320] On the other hand, G_0W_0 and $G_0F(2)$ offer decent estimates of these satellite energies. The difference in performance of G_0T_0 and G_0W_0 can be understood in terms of the scattering channels that are accounted for in each of these approximations. We refer the interested reader to ref 147 and references therein.

The remaining three rows of Table 2 contain the energies corresponding to the three satellites of water discussed previously. The 2 $^2A_1$ state is the easiest to identify as its 2h1p dominant configuration clearly corresponds to the $(1b_1)^{-2}(4a_1)^1$ process. The eigenvectors associated with the 2 $^2B_1$ and 3 $^2B_1$ states, which correspond to the $(3a_1)^{-1}(1b_1)^{-1}(4a_1)^1$ and $(1b_1)^{-1}(3a_1)^{-1}(4a_1)^1$ processes respectively, are nearly degenerate and highly entangled. This is thus harder, if not impossible, to assign these states.

Because of these assignment problems, the G_0W_0, $G_0F(2)$, and G_0T_0 satellite energies have not been computed for the other molecules considered in this study. To alleviate this issue, there is a notable appeal for a self-energy approximation including vertex corrections capable of effectively addressing satellite states. As mentioned previously, Green's-function-based methods such as the 2ph-TDA[171] and ADC(3)[180,321,322] (first named extended 2ph-TDA[179]) have shown success in qualitatively modeling the inner-valence region of experimental spectra.[12,169−179,181,323] Sokolov's recent multireference ADC(2) scheme[324] is also a promising avenue. In particular, it has shown potential in describing the satellites of the carbon dimer (see below).[234,235] While a detailed quantitative analysis of these approaches on the present benchmark set would be interesting, it lies beyond the scope of this study.

3.3. 14-Electron Molecules: N_2, CO, and BF. The nitrogen and carbon monoxide molecules have been extensively studied both experimentally[326−332] and theoretically.[39,169,180,182,183,185,197,333−335] Their ionization spectra are similar as they exhibit three sharp and intense peaks, corresponding to Koopmans' states, below 20 eV. Their respective fourth IP, corresponding to electron detachment from the orbital $2\sigma_g$ for N_2 and 3σ for CO, lies above 30 eV. Several peaks can be found below these ionizations, i.e., between 20 and 30 eV.[326,329,330] These correspond to satellite states associated with the three outer-valence orbitals. Note that Schirmer et al. have shown (using the 2ph-TDA method[171]) that the quasiparticle approximation breaks down in the region of the fourth ionizations of CO and N_2.[169,180] However, as shown below, the peaks between 20 and 30 eV have a well-defined satellite character.

Baltzer et al. produced, using He(II) photoelectron spectroscopy, accurate experimental values for the outer-valence IPs (see Table 3) and the first satellite peaks of N_2.[327] In particular, they reported a value of 25.514 eV for an intense satellite peak, as well as 24.788 eV for a very weak peak. These peaks were assigned $^2\Sigma_u^+$ and $^2\Pi_g$ symmetry, respectively, based on CI calculations. Note that the $^2\Pi_g$ satellite peak is more intense when measured by resonance Auger spectroscopy.[326] We report FCI values for both satellites as well as a slightly higher third one with $^2\Sigma_u^-$ symmetry. This latter state is not observed experimentally but plays an important role nonetheless as it is involved in the dissociation pathways between the $^2\Sigma_u^+$ and $^4\Pi_u$ states.[333]

Similar to its isoelectronic N_2 molecule, CO exhibits shakeup peaks between the $(4\sigma)^{-1}$ and $(3\sigma)^{-1}$ ionizations. Using monochromatized X-ray excited photoelectron spectroscopy, Svensson et al. observed an intense $^2\Sigma^+$ satellite peak with energy 23.7 eV as well as a weak $^2\Pi$ satellite at 22.7 eV.[326] This is in agreement with older He(II) photoelectron spectroscopy experiments done by Åsbrink and co-workers.[330] FCI values for both satellites, as well as for the higher-energy 1 $^2\Delta$state, are reported in Table 2.

https://doi.org/10.1021/acs.jctc.4c00216
J. Chem. Theory Comput. 2024, 20, 4751−4777

Table 4. Valence Ionizations and Satellite Transition Energies (in eV) of the 12-Electron Series for Various Methods and Basis Sets[a]

	basis				basis				basis			
methods	6-31+G*	AVDZ	AVTZ	AVQZ	6-31+G*	AVDZ	AVTZ	AVQZ	6-31+G*	AVDZ	AVTZ	AVQZ
mol.	lithium fluoride (LiF)								beryllium oxide (BeO)			
state/conf.	$1\,^2\Pi/(1\pi)^{-1}$				$1\,^2\Sigma^+/(4\sigma)^{-1}$				$1\,^2\Pi/(1\pi)^{-1}$			
exp.	11.50,11.67[336]				11.94[336]							
CC2	9.481	9.588	9.804	9.895	9.801	9.923	10.109	10.209	9.615	9.712	9.818	9.894
CCSD	11.078	11.193	11.398	11.493	11.566	11.701	11.874	11.979	9.708	9.808	9.875	9.941
CC3	11.142	11.222	11.375	11.449	11.588	11.682	11.802	11.883	9.976	10.096	10.243	10.320
CCSDT	11.165	11.247	11.379	11.452	11.641	11.738	11.834	11.914	9.750	9.849	9.916	
CC4	11.270	11.351	11.496	11.567	11.764	11.863	11.971	12.049	9.749	9.850	9.867	9.922
CCSDTQ	11.234	11.315	11.453	×	11.719	11.816	11.917	×	9.831	9.930	9.939	×
FCI	11.246	11.328	11.468	11.538	11.735	11.833	11.933	12.018(2)	9.863	9.962	9.972	10.018
G_0W_0	10.797	10.979	11.384	11.594	11.339	11.549	11.915	12.139	9.356	9.489	9.727	9.907
qsGW	11.249	11.330	11.575	11.699	11.809	11.926	12.119	12.255	9.991	10.079	10.168	10.251
$G_0F(2)$	9.294	9.445	9.729	9.857	9.644	9.812	10.063	10.200	7.957	8.072	8.195	8.302
G_0T_0	10.512	10.644	10.923	×	10.968	11.120	11.366	×	8.885	8.975	9.108	×
mol.	beryllium oxide (BeO)				boron nitride (BN)							
state/conf.	$1\,^2\Sigma^+/(4\sigma)^{-1}$				$1\,^2\Pi/(1\pi)^{-1}$				$1\,^2\Sigma^+/(4\sigma)^{-1}$			
exp.												
CC2	10.523	10.620	10.667	10.735	10.734	10.792	10.927	10.991	12.842	12.870	12.979	13.018
CCSD	10.861	10.987	11.006	11.082	11.776	11.850	11.971	12.018	13.571	13.624	13.697	13.720
CC3	11.128	11.269	11.370	11.454	11.825	11.941	12.057	12.101	13.641	13.718	13.806	13.828
CCSDT	10.830	10.962	10.916	10.975	11.778	11.871	11.980	12.019	13.642	13.716	13.790	13.808
CC4	10.825	10.959	10.915	10.977	11.681	11.797	11.902	11.940	13.534	13.626	13.700	13.718
CCSDTQ	10.923	11.056	11.007	×	11.754	11.860	11.966	×	13.580	13.667	13.745	×
FCI	10.970	11.103	11.056	11.115(2)	11.767	11.875	11.980	12.019	13.571	13.660	13.729(11)	13.710(70)
G_0W_0	10.628	10.798	10.996	11.200	11.423	11.447	11.752	11.907	13.154	13.171	13.447	13.590
qsGW	11.083	11.199	11.241	11.341	11.597	11.711	11.898	11.987	13.376	13.490	13.621	13.693
$G_0F(2)$	8.499	8.648	8.720	8.837	10.817	10.857	11.031	11.122	12.207	12.195	12.382	12.454
G_0T_0	9.930	10.064	10.155	×	10.988	10.996	11.159	×	12.499	12.512	12.657	×
mol.	carbon dimer (C_2)											
state/conf.	$1\,^2\Pi_u/(2\pi_u)^{-1}$											
exp.												
CC2	12.742	12.779	12.951	13.023								
CCSD	12.770	12.830	12.978	13.030								
CC3	11.930	12.058	12.177	12.215								
CCSDT	12.289	12.391	12.540	12.585								
CC4	12.231	12.347	12.472	12.511								
CCSDTQ	12.225	12.340	12.471	×								
FCI	12.205	12.323	12.463	12.497								
G_0W_0	12.621	12.613	12.928	13.082								
qsGW	12.202	12.344	12.561	12.656								
$G_0F(2)$	12.882	12.870	13.078	13.175								
G_0T_0	12.482	12.454	12.625	×								
mol.					carbon dimer (C_2)							
state/conf.	$1\,^2\Delta_g/(2\pi_u)^{-2}(3\sigma_g)^1$				$1\,^2\Sigma_g^-/(2\pi_u)^{-2}(3\sigma_g)^1$				$1\,^2\Sigma_g^+/(2\pi_u)^{-2}(3\sigma_g)^1$			
exp.												
CC3	14.644	14.713	14.815	14.850	14.846	14.957	15.087	15.123	15.360	15.353	15.435	15.460
CCSDT	14.494	14.568	14.680	14.729	14.721	14.833	14.998	15.051	15.086	15.072	15.194	15.246
CC4	13.920	14.007	14.052	14.076	14.196	14.308	14.359	14.388	14.304	14.331	14.413	14.439
CCSDTQ	13.879	13.969	14.041	×	14.182	14.200	14.310	×	14.209	14.316	14.423	×
FCI	13.798	13.889	13.944	13.963	14.084	14.099	14.167	14.193	14.108	14.244	14.337	14.359(1)
mol.	lithium fluoride (LiF)								beryllium oxide (BeO)			
state/conf.	$1\,^2\Sigma^-/(1\pi)^{-2}(5\sigma)^1$				$2\,^2\Pi/(4\sigma)^{-1}(1\pi)^{-1}(5\sigma)^1$				$1\,^2\Sigma^-/(1\pi)^{-2}(5\sigma)^1$			
exp.												
CC3	×	×	×	×	×	×	×	×	×	×	×	×
CCSDT	26.917	27.177	27.738	27.945	27.545	27.810	28.345	28.559	15.515	15.699	16.062	16.206
CC4	24.868	25.062	25.341	×	25.125	25.295	25.565	×	13.215	13.376	×	×
CCSDTQ	25.937	26.105	26.401	×	26.464	26.632	26.900	×	14.198	14.349	14.517	×
FCI	25.958	26.118	26.381	×	26.471	26.627	26.856	27.016(1)	14.095	14.244	14.380	×

https://doi.org/10.1021/acs.jctc.4c00216
J. Chem. Theory Comput. 2024, 20, 4751−4777

Table 4. continued

	basis				basis				basis			
methods	6-31+G*	AVDZ	AVTZ	AVQZ	6-31+G*	AVDZ	AVTZ	AVQZ	6-31+G*	AVDZ	AVTZ	AVQZ
mol.	beryllium oxide (BeO)				boron nitride (BN)							
state/conf.	$2\ ^2\Pi/(4\sigma)^{-1}(1\pi)^{-1}(5\sigma)^1$				$1\ ^2\Sigma^-/(1\pi)^{-2}(5\sigma)^1$				$1\ ^2\Delta/(1\pi)^{-2}(5\sigma)^1$			
exp.												
CC3	×	×	×	×	13.120	13.132	13.270	13.289	13.299	13.331	13.489	13.517
CCSDT	17.306	17.501	17.826	17.984	13.432	13.515	13.795	13.870	13.942	14.024	14.252	14.315
CC4	13.361	13.558	×	×	12.569	12.627	12.758	12.790	13.221	13.289	13.383	13.402
CCSDTQ	15.677	15.840	15.954	×	12.510	12.582	12.739	×	13.244	13.324	13.431	×
FCI	15.455	15.616	15.683	15.805	12.393	12.463	12.600	×	13.185	13.263	13.351	13.357(21)

[a]AVXZ stands for aug-cc-pVXZ (where X = D, T, and Q). Selected experimental values are also reported.

The performance of CC schemes for these six satellites is similar to what we have observed for the 10-electron series. Yet, it is interesting to note that CCSDTQ seems to struggle slightly more with the $2\ ^2\Pi$ satellite of CO and the $1\ ^2\Pi_g$ and $1\ ^2\Sigma_u^-$ states of N_2.

The boron fluoride molecule is isoelectronic to CO and N_2 but its ionization spectrum is much harder to obtain experimentally because BF is a quite nonvolatile compound, meaning that the measurements have to be done at high temperatures.[325] Yet, Hildenbrand and co-workers managed to measure its principal IP using electron impact spectroscopic and they reported a value of 11.06 eV. The $1\ ^2\Sigma^+$ FCI state is in good agreement with this value. Table 2 also displays two additional IPs and one satellite. The order of the $^2\Pi$ states in BF is reversed with respect to its isoelectronic species: the $(5\sigma)^{-2}(2\pi)^1$ satellite state has a lower energy than the $(1\pi)^{-1}$ ionization. In this case, CCSDTQ accurately describes the satellite of Π symmetry.

3.4. 12-Electron Molecules: LiF, BeO, BN, and C_2. We now direct our attention toward the 12-electron isoelectronic molecules: LiF, BeO, BN, and C_2. These four molecules are quite challenging for theoretical methods as, except for LiF, their ground states have a strong multireference character.[337−344] For example, BN and BeO are among the eight molecules of the *GW*100 set having multiple solution issues at the *GW* level.[24,25] (C_2 is not considered in the *GW*100 set but would certainly fall in the same category.) Another noteworthy observation about these molecules is that their lowest unoccupied molecular orbital has a negative energy, which means that their respective anions are stable.

LiF is a relatively nonvolatile molecule, and as a result, experimental data became accessible during the second phase of the development of ultraviolet photoelectron spectroscopy.[336] In addition, lithium fluoride vapor is not solely composed of monomers but also includes dimers, trimers, or even tetramers, posing challenges for more precise measurements of the Koopmans' states of LiF. Berkowitz et al. measured the first two IPs using He(I) photoelectron spectroscopy: 11.50, 11.67, and 11.94 eV for the $1\ ^2\Pi_{3/2,3/2}$, $1\ ^2\Pi_{3/2,1/2}$, and $1\ ^2\Sigma^+$ states, respectively. In our study, the spin−orbit coupling is not accounted for. Therefore, we report a single value for the $1\ ^2\Pi$ state, while experimentally two distinct ionization energies are measured.

To the best of our knowledge, no gas phase experimental values are available for the three remaining species (see ref 345 for a study in solid phase). Nonetheless, they are an interesting playground for theoretical methods due to their multireference character. We start by discussing BeO as it has the less pronounced multireference character out of these three molecules. Table 4 displays the excitation energies of the two lowest Koopmans' states and the first two satellites. These four states have the same dominant configurations and ordering as the ones of lithium fluoride. However, the satellite states of BeO are much lower in energy than those of LiF. The $2\ ^2\Pi$ state of BeO is interesting as it exhibits the largest error of this benchmark set at the CCSDTQ level. At the CC4 level, the $2\ ^2\Pi$ and $1\ ^2\Sigma^-$ states are drastically underestimated. This is also the case for the two satellite states of LiF, these four states having, by far, the largest CC4 errors of this benchmark set. They are also hugely underestimated at the CC3 level and, as for CC2 and CCSD, we have not reported these energies as they are not meaningful. Unfortunately, at this stage, we have no clear explanation for the failure of CC3 and CC4 in LiF and BeO.

BN and C_2 have the strongest multireference character among these four molecules.[344] The ordering of their state differs from the one of LiF and BeO as their lowest satellite states are below their second IP. Furthermore, the ordering of the satellites is also different than the two previous molecules. The first satellite of boron nitride has the same dominant configuration as in the latter two molecules, but the second satellite is of $1\ ^2\Delta$ symmetry with a $(1\pi)^{-2}(5\sigma)^1$ dominant process. This satellite is also found in C_2 but even lower in the energy spectrum as the $1\ ^2\Delta_g$ state is the lowest-energy satellite of the carbon dimer. Table 4 reports two additional FCI satellite transition energies of C_2. Note that the satellite transition energies of BeO, BN, and C_2 are the lowest of the present set. The three satellite states of the carbon dimer have already been studied by Chatterjee and Sokolov.[234,235] In particular, they have shown that ADC(3) performs poorly and does not even predict enough satellite states. On the other hand, their extension of ADC(2) using a multideterminantal reference[324] can predict each state and be in quantitative agreement with FCI.[234,235]

3.5. Third-Row Molecules: CS, Ar, HCl, H_2S, PH_3, SiH_4, and LiCl. The molecules examined in this subsection have been obtained by substituting a second-row atom with its third-row analogue in some of the molecules discussed above. These molecules with more diffuse density have their ionization shifted toward zero with respect to their second-row counterparts (see V, VI, and VII). Consequently, the breakdown of the orbital picture occurs at lower energy,[172] which has been of interest historically as it allowed measuring spectra featuring such intricate structures more easily.

The first molecule considered in this subsection is carbon sulfide. In 1972, two independent studies measured its photoelectron spectrum up to 20 eV.[348,349] One can clearly distinguish four well-defined peaks in this energy range. While the assignment of the two lowest peaks is straightforward, i.e., IPs associated with the two outermost orbitals, the interpretation of the other two remained elusive for several years. Thanks

https://doi.org/10.1021/acs.jctc.4c00216
J. Chem. Theory Comput. 2024, 20, 4751−4777

Table 5. Valence Ionizations and Satellite Transition Energies (in eV) of the Third-Row Molecules for Various Methods and Basis Sets[a]

	basis				basis				basis			
methods	6-31 +G*	AVDZ	AVTZ	AVQZ	6-31 +G*	AVDZ	AVTZ	AVQZ		AVDZ	AVTZ	AVQZ
mol.	carbon sulfide (CS)											
state/conf.	$1\,^2\Sigma^+/(7\sigma)^{-1}$				$1\,^2\Pi/(2\pi)^{-1}$				$^2\Sigma^+/(6\sigma)^{-1}$			
exp.												
CC2	10.627	10.745	10.847	10.900	12.791	12.897	13.014	13.083	16.698	16.817	16.945	17.005
CCSD	11.245	11.402	11.553	11.609	12.726	12.883	13.000	13.059	16.854	16.997	17.220	17.288
CC3	10.949	11.186	11.325	11.377	12.553	12.766	12.880	12.937	18.201	18.290	18.389	18.422
CCSDT	10.966	11.190	11.346	11.404	12.596	12.799	12.918	12.974	17.915	18.023	18.134	18.179
CC4	10.914	11.161	11.310	11.368	12.542	12.764	12.878	12.934	17.764	17.881	17.959	17.994
CCSDTQ	10.920	11.166	11.316	×	12.548	12.768	12.885	×	17.749	17.865	17.947	×
FCI	10.899	11.151	11.300	11.355	12.545	12.768	12.882(1)	12.936	17.723	17.844	17.920	17.958(2)
G_0W_0	12.092	12.119	12.378	12.523	12.602	12.679	12.907	13.063	17.666	17.713	17.976	18.119
qsGW	11.369	11.589	11.775	11.880	12.498	12.705	12.852	12.958	17.323	17.505	17.688	17.788
G_0F(2)	11.109	11.152	11.292	11.371	12.696	12.774	12.923	13.018	16.704	16.779	16.942	17.026
G_0T_0	11.595	11.594	11.713	×	12.479	12.505	12.609	×	17.422	17.455	17.591	×
mol.	carbon sulfide (CS)											
state/conf.	$2\,^2\Sigma^+/(2\pi)^{-1}(7\sigma)^{-1}(3\pi)^1$				$3\,^2\Sigma^+/(2\pi)^{-1}(7\sigma)^{-1}(3\pi)^1$				$1\,^2\Delta/(2\pi)^{-1}(7\sigma)^{-1}(3\pi)^1$			
exp.												
CC3	16.183	16.329	16.500	16.560	17.358	17.491	17.558	17.584	17.448	17.558	17.635	17.662
CCSDT	15.921	16.089	16.278	16.352	16.986	17.145	17.208	17.264	17.039	17.178	17.266	17.319
CC4	15.677	15.863	15.997	16.059	16.628	16.799	16.773	16.807	16.701	16.861	16.871	16.902
CCSDTQ	15.646	15.838	15.982	×	16.600	16.772	16.754	×	16.678	16.840	16.858	×
FCI	15.604	15.803	15.935	15.996(1)	16.551	16.727	16.691	16.728(2)	16.632	16.800	16.802	16.837(2)
mol.	lithium chloride (LiCl)											
state/conf.	$1\,^2\Pi/(2\pi)^{-1}$				$1\,^2\Sigma^+/(6\sigma)^{-1}$							
exp.	9.98, 10.06[346]				10.77[346]							
CC2	9.215	9.396	9.535	9.639	9.902	10.109	10.189	10.299				
CCSD	9.604	9.830	9.956	10.067	10.327	10.566	10.637	10.757				
CC3	9.529	9.788	9.880	9.992	10.235	10.518	10.552	10.671				
CCSDT	9.533	9.787	9.883	9.993	10.241	10.517	10.554	10.673				
CC4	9.556	9.811	9.898	×	10.265	10.544	10.573	×				
CCSDTQ	9.552	9.808	9.896	×	10.261	10.540	10.570	×				
FCI	9.555	9.810	9.897	10.007	10.267	10.545	10.577	10.696				
G_0W_0	9.611	9.734	9.984	10.180	10.357	10.500	10.690	10.897				
qsGW	9.574	9.808	9.947	10.086	10.307	10.569	10.642	10.789				
G_0F(2)	9.222	9.365	9.551	9.676	9.916	10.083	10.210	10.341				
G_0T_0	9.567	9.619	9.761	×	10.274	10.360	10.448	×				
mol.	lithium chloride (LiCl)								fluorine (F_2)			
state/conf.	$2\,^2\Sigma^+/(2\pi)^{-2}(7\sigma)^1$				$2\,^2\Pi/(6\sigma)^{-1}(2\pi)^{-1}(7\sigma)^1$				$2\,^2\Sigma_g^-/(1\pi_u)^{-1}(1\pi_g)^{-1}(3\sigma_u)^1$			
exp.												
CC3	18.447	18.788	19.156	19.328	19.055	19.402	19.717	19.897	22.465	22.584	22.866	22.934
CCSDT	19.582	20.043	20.508	20.729	20.304	20.745	21.168	21.397	22.293	22.387	22.663	22.758
CC4	18.837	19.326	19.639	×	19.477	19.959	20.224	×	22.050	22.064	22.177	22.234
CCSDTQ	18.963	19.468	19.788	×	19.645	20.141	20.413	×	22.025	22.038	22.174	×
FCI	18.942	19.446	19.741	19.955	19.617	20.115	20.357	20.577	22.024(2)	22.039(1)	22.165(1)	22.224(4)
mol.	fluorine (F_2)											
state/conf.	$1\,^2\Pi_g/(1\pi_g)^{-1}$				$1\,^2\Pi_u/(1\pi_u)^{-1}$				$1\,^2\Sigma_g^-/(3\sigma_g)^{-1}$			
exp.	15.8[347]				18.9[347]				20.9[347]			
CC2	13.903	14.001	14.145	14.233	17.050	17.122	17.224	17.297	20.325	20.458	20.522	20.604
CCSD	15.279	15.405	15.616	15.722	18.633	18.753	18.946	19.047	21.068	21.155	21.174	21.241
CC3	15.574	15.646	15.746	15.825	18.786	18.847	18.924	18.994	21.091	21.155	21.130	21.182
CCSDT	15.529	15.594	15.688	15.767	18.745	18.797	18.865	18.936	21.048	21.109	21.094	21.148
CC4	15.555	15.621	15.701	15.804	18.746	18.797	18.864	18.941	21.086	21.142	21.146	21.171
CCSDTQ	15.559	15.623	15.725	×	18.754	18.803	18.874	×	21.077	21.132	21.106	×
FCI	15.564	15.628	15.729	15.808	18.758	18.807	18.874	18.943(1)	21.077	21.132	21.100(2)	21.149
G_0W_0	15.763	15.964	16.334	16.559	19.423	19.589	19.902	20.104	20.434	20.625	20.836	21.029
qsGW	15.927	16.016	16.229	16.368	19.524	19.585	19.752	19.875	20.855	20.934	21.000	21.114
G_0F(2)	13.809	13.960	14.194	14.328	16.965	17.087	17.275	17.389	20.137	20.308	20.420	20.534

https://doi.org/10.1021/acs.jctc.4c00216
J. Chem. Theory Comput. 2024, 20, 4751−4777

Table 5. continued

	basis				basis				basis			
methods	6-31 +G*	AVDZ	AVTZ	AVQZ	6-31 +G*	AVDZ	AVTZ	AVQZ		AVDZ	AVTZ	AVQZ
G_0T_0	15.026	15.157	15.401	×	18.615	18.724	18.928	×	19.934	20.083	20.190	×

[a]AVXZ stands for aug-cc-pVXZ (where X = D, T, and Q). Selected experimental values are also reported.

Table 6. MAE, Mean Signed Error (MSE), Root Mean Square Error (RMSE), Standard Deviation Error (SDE), and Minimum and Maximum Errors (in eV) with Respect to FCI of the Various Methods Considered in This Work[a]

methods	MAE	MSE	RMSE	SDE	min	max
CC2	0.769	−0.594	0.940	0.735	−2.207	1.565
CCSD	0.175	0.097	0.280	0.265	−0.700	1.075
CC3	0.070	0.001	0.125	0.126	−0.395	0.469
CCSDT	0.041	−0.010	0.057	0.057	−0.140	0.214
CC4	0.015	0.005	0.027	0.027	−0.078	0.118
CCSDTQ	0.010	−0.005	0.013	0.012	−0.049	0.027
G_0W_0	0.470	0.399	0.664	0.535	−0.504	2.053
qsGW	0.391	0.268	0.559	0.494	−1.348	1.747
$G_0F(2)$	0.807	−0.550	0.987	0.827	−2.336	1.623
G_0T_0	0.485	0.007	0.752	0.758	−1.169	2.959
ΔCCSD(T)	0.021	0.016	0.037	0.035	−0.020	0.120

[a]These descriptors are computed for the 58 IPs of this set in the aug-cc-pVTZ basis set. The ΔCCSD(T) statistical descriptors correspond only to the 23 principal IPs.

Table 7. MAE, MSE, RMSE, SDE, and Minimum and Maximum Errors (in eV) with Respect to FCI of the Various Methods Considered in This Work[a]

methods	MAE	MSE	RMSE	SDE	min	max
CC3	0.787	0.143	0.936	0.937	−2.907	1.098
CCSDT	0.537	0.537	0.590	0.248	0.104	1.195
CC4	0.093	−0.001	0.134	0.136	−0.423	0.333
CCSDTQ	0.039	0.034	0.054	0.043	−0.030	0.143

[a]These descriptors are computed for the 36 satellites of this set in the aug-cc-pVTZ basis set. The satellites of LiF and BeO have been excluded (see main text).

to theoretical studies performed several years later, it became clear that the third peak is due to a multiparticle process while the fourth one is associated with an electron detachment from the orbital 6σ.[172,234,235,308] Note that, as explained by Schirmer et al.,[172] one has to be particularly careful when labeling the third peak as a satellite because its FCI vector has a coefficient of 0.49 on the 1h configuration $(6\sigma)^{-1}$ and of 0.40 on the 2h1p configuration $(2\pi)^{-1}(7\sigma)^{-1}(3\pi)^{1}$ (in 6-31+G* basis set). This is yet another example of a strong configuration mixing.

Despite this, the 2 $^2\Sigma^+$ state is classified as a satellite in Table 5. Indeed, higher in energy, there is another FCI solution of $^2\Sigma^+$ symmetry with an even larger weight, 0.63, on the 1h determinant $(6\sigma)^{-1}$ and coefficients smaller than 0.31 on the 2h1p determinants. In addition, the third peak has a pronounced vibrational structure, while the fourth peak is sharp like the $(7\sigma)^{-1}$ one.[349] This is why the higher $^2\Sigma^+$ state is classified as the third single ionization in Table 5. Two other satellite states, 3 $^2\Sigma^+$ and 1 $^2\Delta$, that are not visible on the experimental spectrum, are reported in Table 5.

Next, we consider lithium chloride and compare it with its second-row analogue, lithium fluoride. The experimental challenges outlined earlier for LiF are similar for LiCl. Experimental values have first been reported independently by two groups in 1979,[336,350] and revised values, measured by He(I) spectroscopy, have been published recently,[346] and are reported in Table 5. The FCI results predict two close-lying satellites around 20 eV. Unfortunately, the experimental studies mentioned above do not probe this energy range. The ADC(3) calculations of Tomasello and von Niessen also predict two satellite lines around 21.5 eV (Table 6).[351]

Finally, we examine the 18-electron isoelectronic hydrides as analogues to the 10-electron series discussed in Sub Section 3.1. Historically, it was quickly realized that the satellite structure of H_2S is significantly more complex than the one of H_2O.[174] This intricate structure can be observed in the electron momentum spectrum of French et al.[352] They recorded a first very weak satellite at 19.63 eV which is in agreement with earlier measurements[353] as well as photoelectron spectrum measured using synchrotron radiation.[354] Several years later, extensive SAC−CI results have been reported and show qualitative agreement with experiments.[200] (See also earlier calculations from refs 193 and 195). However, the FCI results (see Table 7) exhibit some significant difference with the SAC−CI results of Ehara et al. because the 2 $^2A_1$ satellite has a lower energy than the 2 $^2B_2$ state. In addition, the FCI transition energy associated with the 2 $^2B_1$ state is 2 eV lower than the one computed in ref 200. The 2 $^2A_1$ state is known to be the one observed at 19.63 eV in ref 352 and is sometimes referred to as a shake-down state as it "borrows" intensity from the higher-lying $(4a_1)^{-1}$ ionization.[200,354,355] Our FCI estimate for this state is 18.745 eV, while the SAC−CI energy of Ehara and collaborators is 20.00 eV.[200] In this specific scenario, calculating the adiabatic transition energy related to this state would undoubtedly provide a more faithful comparison with the experimental result.

For PH_3, there is one satellite of symmetry E that is analogue to the two 2 ^2E state of NH_3. However, in the case of phosphine, there is no analogue for the 2 $^2A_1$ satellite of ammonia. This is in agreement with the SAC−CI results of Ishida et al., who also found a single satellite below the $(4a_1)^{-1}$ ionization threshold.[201]

Two FCI states, with symmetry $^2\Sigma^+$ and $^2\Delta$, are reported for HCl. These states are analogue to the HF satellites reported in Table 1 although they have significantly lower energies in HCl. The satellite structure between 20 eV and the $(4\sigma)^{-1}$ ionization around 26 eV is notably intricate.[356] Additionally, this structure is characterized by weak signals and some of its features were even not observed in previous studies performed at a lower level of theory.[357−359] The assignment of the various peaks in this energy range is beyond the scope of this work. Yet, one can mention that the first FCI satellite is in qualitative agreement with the first satellite peak measured by synchrotron radiation spectroscopy at 21.57 eV.[356]

The lowest-energy satellite of argon, which is the analogue of the 2 ^2P satellite state of neon, is also reported. This satellite has been observed experimentally by Kikas et al. and is also reported in Table 7.[360] The agreement of the FCI value with the experimental one is definitely not as good as for neon. On the other hand, CC3 provides an excellent approximation of the 2 ^2P

https://doi.org/10.1021/acs.jctc.4c00216
J. Chem. Theory Comput. 2024, 20, 4751−4777

Table 8. Valence Ionizations and Satellite Transition Energies (in eV) of the 18-Electron Series for Various Methods and Basis Sets[a]

	basis				basis				basis			
methods	6-31+G*	AVDZ	AVTZ	AVQZ	6-31+G*	AVDZ	AVTZ	AVQZ	6-31+G*	AVDZ	AVTZ	AVQZ
mol.							(H_2S)					
state/conf.			$1\,^2B_1/(2b_1)^{-1}$				$1\,^2A_1/(5a_1)^{-1}$				$1\,^2B_2/(2b_2)^{-1}$	
exp.			10.5[352]				13.1[352]				15.6[352]	
CC2	9.699	9.953	10.156	10.228	12.833	13.004	13.155	13.220	15.393	15.368	15.464	15.521
CCSD	9.908	10.208	10.421	10.490	13.057	13.280	13.440	13.497	15.540	15.591	15.684	15.734
CC3	9.846	10.189	10.388	10.454	12.985	13.259	13.407	13.459	15.475	15.567	15.635	15.680
CCSDT	9.853	10.190	10.390	10.455	12.985	13.253	13.399	13.450	15.460	15.552	15.619	15.664
CC4	9.855	10.199	10.394	10.458	12.990	13.265	13.407	13.456	15.458	15.560	15.624	15.668
CCSDTQ	9.855	10.199	10.393	×	12.990	13.265	13.406	×	15.457	15.558	15.622	×
FCI	9.855	10.199	10.393	10.456	12.992	13.268	13.411	13.460	15.459	15.562	15.627	15.672
G_0W_0	10.034	10.172	10.500	10.660	13.212	13.339	13.614	13.758	15.684	15.698	15.928	16.058
qsGW	9.890	10.201	10.445	10.549	13.048	13.337	13.530	13.619	15.524	15.651	15.785	15.868
$G_0F(2)$	9.747	9.940	10.180	10.282	12.887	13.005	13.188	13.278	15.420	15.364	15.494	15.569
G_0T_0	9.927	10.011	10.188	×	13.068	13.112	13.250	×	15.588	15.477	15.582	×
mol.							(PH_3)					
state/conf.			$1\,^2A_1/(5a_1)^{-1}$				$1\,^2E/(2e_g)^{-1}$				$2\,^2A_1/(4a_1)^{-1}$	
exp.			10.85[201]				16.4[201]				27.6[201]	
CC2	10.030	10.219	10.392	10.444	13.463	13.493	13.638	13.689	21.308	21.046	21.079	21.106
CCSD	10.198	10.448	10.623	10.662	13.521	13.637	13.784	13.825	20.144	20.221	20.361	20.396
CC3	10.130	10.431	10.599	10.634	13.464	13.615	13.744	13.779	19.528	19.643	19.739	19.763
CCSDT	10.129	10.431	10.599	10.634	13.454	13.606	13.734	13.769	19.317	19.487	19.583	19.610
CC4	10.127	10.436	10.600	×	13.452	13.611	13.737	×	19.263	19.446	19.520	×
CCSDTQ	10.127	10.437	10.600	×	13.451	13.611	13.737	×	19.259	19.442	19.511	×
FCI	10.126	10.436	10.596	10.628	13.456	13.615	13.745	13.784	19.261	19.445	19.514	19.537
G_0W_0	10.365	10.497	10.787	10.911	13.717	13.831	14.099	14.214	21.505	21.378	21.567	21.673
qsGW	10.190	10.506	10.725	10.802	13.545	13.761	13.954	14.027	21.128	21.155	21.261	21.322
$G_0F(2)$	10.095	10.223	10.428	10.508	13.495	13.503	13.675	13.741	21.354	21.067	21.137	21.184
G_0T_0	10.186	10.236	10.387	×	13.665	13.619	13.759	×	22.142	21.976	22.040	×
mol.							(SiH_4)				(HCl)	
state/conf.			$1\,^2T_2/(2t_2)^{-1}$				$1\,^2A_1/(3a_1)^{-1}$				$1\,^2\Pi/(1\pi)^{-1}$	
exp.			12.8[375]				18.2[375]				12.745/12.830[356]	
CC2	12.515	12.653	12.802	12.848	18.704	18.759	18.823	18.846	11.990	12.230	12.401	12.491
CCSD	12.477	12.701	12.844	12.877	18.266	18.379	18.483	18.505	12.250	12.538	12.712	12.812
CC3	12.417	12.681	12.806	12.832	18.109	18.236	18.316	18.331	12.186	12.529	12.672	12.771
CCSDT	12.407	12.673	12.794	12.820	18.046	18.172	18.247	18.262	12.190	12.524	12.667	12.764
CC4	12.404	12.676	12.795	×	18.033	18.171	18.241	×	12.199	12.539	12.678	12.773
CCSDTQ	12.404	12.677	12.795	×	18.030	18.170	18.238	×	12.199	12.538	12.676	×
FCI	12.403	12.676	12.793	12.818	18.031	18.173	18.240	18.258(2)	12.199	12.539	12.676	12.770
G_0W_0	12.716	12.960	13.214	13.312	18.701	18.824	19.007	19.097	12.343	12.488	12.778	12.967
qsGW	12.541	12.906	13.107	13.170	18.422	18.700	18.828	18.879	12.224	12.539	12.723	12.855
$G_0F(2)$	12.550	12.662	12.830	12.886	18.742	18.768	18.855	18.899	12.022	12.200	12.415	12.535
G_0T_0	12.712	12.762	12.891	×	19.119	19.156	19.204	×	12.273	12.347	12.507	×
mol.			(HCl)					argon (Ar)				
state/conf.			$1\,^2\Sigma^+/(5\sigma)^{-1}$				$1\,^2P/(3p)^{-1}$				$1\,^2S/(3s)^{-1}$	
exp.			16.270[356]				15.8[304]				29.24[304]	
CC2	16.245	16.329	16.438	16.512	15.055	15.236	15.379	15.486	31.123	30.459	30.439	30.437
CCSD	16.467	16.599	16.708	16.782	15.308	15.534	15.672	15.802	30.353	29.838	29.881	29.907
CC3	16.395	16.577	16.658	16.730	15.230	15.525	15.614	15.745	30.255	29.437	29.238	29.227
CCSDT	16.388	16.564	16.644	16.715	15.228	15.514	15.606	15.735	30.261	29.445	29.214	29.216
CC4	16.394	16.577	16.653	16.723	15.238	15.531	15.616	15.743	30.263	29.442	29.186	29.179
CCSDTQ	16.393	16.576	16.651	×	15.237	15.529	15.614	15.740	30.261	29.442	29.182	29.175
FCI	16.396	16.579	16.657	16.728	15.237	15.529	15.613	15.739	30.265	29.449	29.188	29.182
G_0W_0	16.574	16.635	16.872	17.031	15.333	15.458	15.711	15.926	31.226	30.759	31.089	31.224
qsGW	16.417	16.619	16.752	16.861	15.232	15.507	15.633	15.794	30.858	30.576	30.681	30.751
$G_0F(2)$	16.286	16.325	16.469	16.564	15.072	15.196	15.387	15.523	31.130	30.399	30.426	30.427
G_0T_0	16.461	16.436	16.548	×	15.326	15.368	15.511	×	32.255	32.007	32.147	×

https://doi.org/10.1021/acs.jctc.4c00216
J. Chem. Theory Comput. 2024, 20, 4751−4777

Table 8. continued

	basis				basis				basis			
methods	6-31+G*	AVDZ	AVTZ	AVQZ	6-31+G*	AVDZ	AVTZ	AVQZ	6-31+G*	AVDZ	AVTZ	AVQZ
mol.						(H_2S)						
state/conf.		$2\,^2A_1/(2b_1)^{-2}(6a_1)^1$				$2\,^2B_2/(2b_1)^{-2}(3b_2)^1$				$2\,^2B_1/(5a_1)^{-1}(2b_1)^{-1}(6a_1)^1$		
exp.		19.63[352]										
CC3	19.182	19.350	19.377	×	19.973	20.137	20.317	20.355	20.456	20.620	20.702	×
CCSDT	18.761	19.018	19.043	×	19.675	19.961	20.136	20.190	19.948	20.185	20.269	×
CC4	18.607	18.848	18.801	×	19.485	19.777	19.892	×	19.775	19.995	20.019	×
CCSDTQ	18.582	18.827	18.772	×	19.467	19.765	19.868	×	19.744	19.969	19.986	×
FCI	18.575	18.819	18.755	18.745	19.462	19.759	19.853	19.889	19.741	19.965	19.974	×
mol.		PH_3						HCl				
state/conf.		$2\,^2E/(5a_1)^{-2}(4e_g)^1$				$2\,^2E^+/(2\pi)^{-2}(6\sigma)^1$				$1\,^2\Delta/(2\pi)^{-2}(6\sigma)^1$		
exp.												
CC3	19.513	19.613	19.630	19.606	22.798	22.997	23.197	23.262	23.556	23.732	23.795	23.829
CCSDT	19.072	19.217	19.255	19.245	22.277	22.676	22.885	22.982	23.188	23.532	23.532	23.590
CC4	18.940	19.084	19.080	×	21.932	22.328	22.439	×	22.918	23.273	23.185	×
CCSDTQ	18.907	19.055	19.046	×	21.889	22.303	22.400	×	22.885	23.257	23.155	×
FCI	18.897	19.047	19.025	18.997	21.878	22.293	22.377	22.463	22.881	23.254	23.142	23.185
mol.		Ar										
state/conf.		$2\,^2P/(3p)^{-2}(4s)^1$										
exp.		34.21[360]										
CC3	31.956	32.384	32.638	32.719								
CCSDT	32.381	32.811	33.220	33.423								
CC4	31.913	32.397	32.650	32.833								
CCSDTQ	31.933	32.420	32.678	32.869								
FCI	31.924	32.420	32.657	32.855								

[a]AVXZ stands for aug-cc-pVXZ (where X = D, T, and Q). Selected experimental values are also reported.

satellite state of argon which is not the case for neon (see Table 1).

3.6. Miscellaneous Molecules: F_2, CO_2, CH_2O, and BH_3. In this last subset, a few miscellaneous molecules are considered. First, the F_2 molecule is of interest as it is isoelectronic to SiH_4, PH_3, H_2S, HCl, and Ar. Due to the absence of third-row atoms in F_2, Cederbaum et al. observed that there is no breakdown of the orbital picture, as observed in the 18-electron hydride series.[170] Three IPs and one satellite transition energy of fluorine are reported in Table 5. As documented in ref 170, these four states have a clear dominant configuration in their corresponding FCI vectors. The $2\,^2\Sigma_g^+$ satellite is not observed in photoionization[303,361] or in electron impact spectra.[347] However, a satellite state with the same symmetry and similar energy has been computed using ADC(4) and multireference CI.[347]

Carbon dioxide and formaldehyde are two small organic molecules that have been widely studied both experimentally and theoretically. Experimental studies have shown that CO_2 first measurable satellite peak is around 22 eV,[188,205,328,362] while four ionization peaks are observed below 20 eV. Tian's experimental values for these IPs, measured by electron momentum spectroscopy, are reported alongside our FCI estimates in Table 8.[205] These IPs have already been computed at various levels of theory such as CI,[188] ADC,[234,235,362] SAC−CI,[194,205] CC,[35] and even FCI.[234,235]

The spectrum of formaldehyde is slightly harder to interpret. The electron momentum spectrum displays a shark peak at 10.9 eV as well as a broad band between 12 and 18 eV.[190] On the other hand, one can observe four different peaks below 17 eV in the corresponding photoionization spectra.[177,363] These peaks clearly correspond to ionizations from the four outermost orbitals (see Table 8) and have already been computed using both wave function and Green's function methods.[35,38,177,234,235,334] Hochlaf and Eland also mention a very weak band around 18 eV assigned as a satellite of $^2B_2$ symmetry,[363] which can also be observed in ref 177. This is in nice agreement with the $3\,^2B_2$ FCI satellite state. There is an additional $2\,^2B_1$ satellite state with slightly lower energy than the previous one.

Finally, a small boron hydride is considered as we have seen above that boron-containing molecules such as BN are quite challenging. To the best of our knowledge, experimental results on BH_3 are quite scarce but the principal IP has been measured using mass spectroscopy in the 60s.[364,365] These two research groups reported quite different values of 12.32[364] and 11.4 eV.[365] The FCI values, presented in Table 9, is closer to the first one, corroborating the findings of Tian, who computed similar values using propagator-based methods as well as CCSD(T).[366] Finally, two FCI satellite transition energies of BH_3 are reported in Table 9.

3.7. Global Statistics. Finally, after discussing each molecule individually, the statistics over the whole set are reported and discussed in this subsection. Figure 2 displays the mean sign error (MSE) and MAE of the various methods considered in this study with respect to the new FCI references. These statistical errors have been computed for the 58 IPs in the aug-cc-pVTZ basis set. Several other statistical descriptors are also reported in Table 6.

The CC hierarchy (CCSD, CCSDT, and CCSDTQ) behaves as expected, i.e., being more and more accurate as the rank of the excitation is increased. Chemical accuracy (i.e., error below 0.043 eV as represented by the horizontal green line in the lower panel Figure 2) is reached at the CCSDT level. The least expensive CC2 method does not perform well for IPs as already

https://doi.org/10.1021/acs.jctc.4c00216
J. Chem. Theory Comput. 2024, 20, 4751−4777

Table 9. Valence Ionizations and Satellite Transition Energies (in eV) of the Remaining Molecules for Various Methods and Basis Sets[a]

	basis				basis				basis			
methods	6-31+G*	AVDZ	AVTZ	AVQZ	6-31+G*	AVDZ	AVTZ	AVQZ	6-31+G*	AVDZ	AVTZ	AVQZ
mol.						carbon dioxide (CO_2)						
state/conf.		$1\,^2\Pi_g/(1\pi_g)^{-1}$				$1\,^2\Pi_u/(1\pi_u)^{-1}$				$1\,^2\Sigma_g^+/(3\sigma_u)^{-1}$		
exp.		13.8[205]				17.6[205]				18.1[205]		
CC2	12.747	12.812	13.015	13.103	16.508	16.630	16.751	16.829	16.866	16.889	17.034	17.107
CCSD	13.490	13.561	13.787	13.879	17.767	17.809	17.996	18.080	17.885	18.006	18.171	18.259
CC3	13.456	13.528	13.696	13.773	17.275	17.335	17.463	17.531	17.708	17.829	17.928	17.999
CCSDT	13.474	13.539	13.716	13.794	17.351	17.406	17.553	17.628	17.708	17.821	17.930	18.005
CC4	13.488	13.562	13.733	×	17.339	17.396	17.521	×	17.783	17.904	18.009	×
CCSDTQ	13.491	13.563	13.734	×	17.341	17.396	17.522	×	17.750	17.869	17.972	×
FCI	13.496	13.567	13.733	13.823	17.337	17.391	17.513(7)	17.618(6)	17.766(1)	17.889(1)	17.996(2)	×
G_0W_0	13.743	13.837	14.221	14.425	18.184	18.209	18.519	18.697	18.335	18.474	18.791	18.994
qsGW	13.712	13.806	14.054	14.182	17.950	18.008	18.200	18.315	18.120	18.264	18.442	18.566
G_0F(2)	12.783	12.854	13.129	13.254	16.993	17.012	17.224	17.332	16.714	16.840	17.035	17.153
G_0T_0	13.284	13.334	13.586	×	17.700	17.696	17.890	×	17.693	17.816	17.995	×
mol.		carbon dioxide (CO_2)										
state/conf.		$1\,^2\Sigma_g^+/(4\sigma_g)^{-1}$										
exp.		19.4[205]										
CC2	17.746	17.864	17.980	18.048								
CCSD	19.237	19.351	19.523	19.605								
CC3	18.959	19.073	19.184	19.250								
CCSDT	18.968	19.075	19.198	19.268								
CC4	19.047	19.158	19.274	×								
CCSDTQ	19.008	19.119	19.232	×								
FCI	19.024(1)	19.137(2)	19.254(3)	×								
G_0W_0	19.730	19.856	20.150	20.334								
qsGW	19.474	19.604	19.776	19.888								
G_0F(2)	17.949	18.069	18.245	18.348								
G_0T_0	19.083	19.193	19.353	×								
mol.						formaldehyde (CH_2O)						
state/conf.		$1\,^2B_2/(2b_2)^{-1}$				$1\,^2B_1/(1b_1)^{-1}$				$1\,^2A_1/(5a_1)^{-1}$		
exp.		10.9[177]				14.5[177]				16.1[177]		
CC2	9.444	9.553	9.753	9.828	13.854	13.903	14.053	14.127	14.596	14.705	14.820	14.893
CCSD	10.486	10.625	10.848	10.924	14.410	14.480	14.606	14.667	15.833	15.964	16.105	16.181
CC3	10.555	10.710	10.873	10.932	14.377	14.482	14.562	14.609	15.832	15.985	16.063	16.119
CCSDT	10.533	10.680	10.840	10.898	14.381	14.478	14.562	14.609	15.811	15.953	16.030	16.086
CC4	10.578	10.736	10.897	×	14.395	14.504	14.578	×	15.879	16.039	16.114	×
CCSDTQ	10.574	10.729	10.887	×	14.391	14.498	14.572	×	15.864	16.018	16.090	×
FCI	10.582	10.739	10.899	10.954	14.395	14.502	14.578(1)	14.618(9)	15.876	16.032	16.106(1)	16.161(4)
G_0W_0	10.835	10.996	11.380	11.556	14.232	14.283	14.587	14.759	16.170	16.292	16.602	16.794
qsGW	10.780	10.990	11.241	11.342	14.395	14.543	14.693	14.780	16.118	16.313	16.459	16.557

https://doi.org/10.1021/acs.jctc.4c00216
J. Chem. Theory Comput. 2024, 20, 4751−4777

Table 9. continued

	basis				basis				basis			
methods	6-31+G*	AVDZ	AVTZ	AVQZ	6-31+G*	AVDZ	AVTZ	AVQZ	6-31+G*	AVDZ	AVTZ	AVQZ
$G_0F(2)$	9.605	9.712	9.981	10.088	13.740	13.772	13.985	14.093	14.747	14.856	15.040	15.153
G_0T_0	10.345	10.407	10.655	×	13.879	13.896	14.082	×	15.625	15.716	15.888	×
mol.	formaldehyde (CH_2O)								borane (BH_3)			
state/conf.	$2\ ^2B_2/(1b_2)^{-1}$				$1\ ^2E'/(1e')^{-1}$				$1\ ^2A_1'/(2a_1')^{-1}$			
exp.	17.0[177]											
CC2	16.704	16.738	16.866	16.921	12.942	13.081	13.231	13.276	18.210	18.337	18.427	18.465
CCSD	17.256	17.338	17.494	17.553	12.995	13.204	13.342	13.375	18.100	18.300	18.398	18.428
CC3	16.898	16.992	17.102	17.148	12.941	13.191	13.309	13.334	18.018	18.249	18.326	18.349
CCSDT	16.938	17.036	17.156	17.207	12.938	13.189	13.304	13.330	18.002	18.232	18.307	18.331
CC4	16.905	17.005	17.107	×	12.938	13.193	13.306	13.331	18.001	18.236	18.308	18.331
CCSDTQ	16.906	17.005	17.108	×	12.938	13.193	13.307	×	18.001	18.237	18.309	×
FCI	16.901	17.002	17.107	17.156(5)	12.938	13.194	13.307	13.332	18.001	18.238	18.310	18.332
G_0W_0	17.651	17.714	18.015	18.162	13.202	13.395	13.678	13.780	18.320	18.470	18.685	18.780
qsGW	17.463	17.635	17.821	17.909	13.047	13.371	13.584	13.651	18.111	18.410	18.544	18.601
$G_0F(2)$	16.460	16.463	16.656	16.742	12.989	13.093	13.278	13.341	18.255	18.342	18.459	18.515
G_0T_0	17.317	17.298	17.473	×	13.130	13.179	13.327	×	18.536	18.598	18.683	×
mol.	formaldehyde (CH_2O)											
state/conf.	$2\ ^2B_1/(2b_2)^{-1}(2b_1)^1$				$3\ ^2B_2/(1b_1)^{-1}(2b_2)^{-1}(2b_1)^1$							
exp.												
CC3	16.564	16.632	16.800	16.847	18.826	18.991	19.154	19.208				
CCSDT	16.684	16.786	17.004	17.083	18.761	18.956	19.153	19.233				
CC4	16.348	16.407	16.495	×	18.503	18.663	18.751	×				
CCSDTQ	16.363	16.425	16.522	×	18.515	18.679	18.772	×				
FCI	16.345	16.409	16.498(1)	×	18.512	18.678	18.763(1)	×				
mol.	borane (BH_3)											
state/conf.	$1\ ^2B_1'/(1e')^{-2}(1b_1)^1$				$2\ ^2E'/(1e')^{-2}(1b_1)^1$							
exp.												
CC3	19.485	19.803	19.889	19.894	20.026	20.212	20.324	20.346				
CCSDT	18.896	19.228	19.331	19.355	19.482	19.669	19.789	19.824				
CC4	18.790	19.130	19.209	19.226	19.403	19.602	19.704	19.732				
CCSDTQ	18.756	19.100	19.178	×	19.379	19.584	19.684	×				
FCI	18.754	19.099	19.176	19.194	19.377	19.583	19.685	19.714				

[a]AVXZ stands for aug-cc-pVXZ (where X = D, T, and Q). Selected experimental values are also reported.

https://doi.org/10.1021/acs.jctc.4c00216
J. Chem. Theory Comput. 2024, 20, 4751−4777

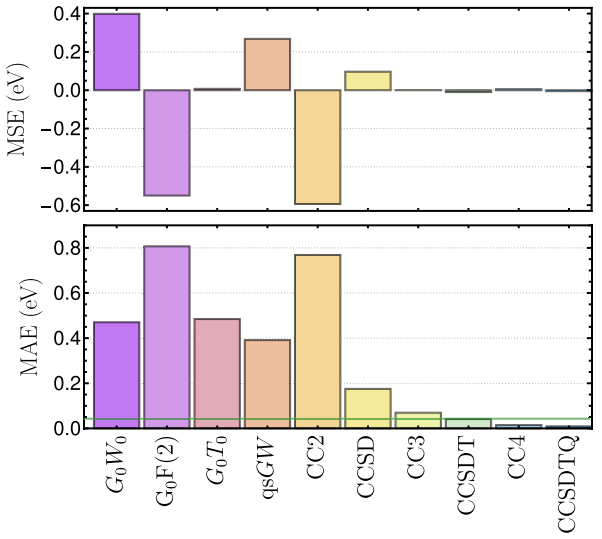

Figure 2. MSE [upper panel] and MAE [lower panel] with respect to FCI of the various methods considered in this work. These errors are computed for the 58 IPs of this set in the aug-cc-pVTZ basis set.

observed previously.[367−369] This has been attributed to the same underlying issue observed in CC2 for Rydberg[370] and charge-transfer excited states.[371]

Figure 2 also shows that CC3 and CC4 are good approximations, for IPs, of their respective parents, CCSDT and CCSDTQ. This could have been expected for CC3 as it is known to be a good approximation of CCSDT for Rydberg excited states.[370] In addition, these four methods have very small MSEs and do not, on average, underestimate (as CC2) or overestimate (as CCSD) the IPs. Therefore, implementations of IP-EOM-CC3 and IP-EOM-CC4 would be valuable to lower the cost of the present implementation based on EE-EOM. CC3 and CC4 could be certainly employed as reference methods for larger molecular systems.[239,291,372]

For the sake of completeness, we also report in Table 6 the statistical descriptors for the propagator methods. However, their trends are now well-known.[113,142,149,150] The G_0T_0 MAE is very close to the G_0W_0 one, whereas the second-Born approximation exhibits significantly poorer performance.[142,149,150] The self-consistent qsGW slightly mitigates the error compared to the one-shot GW version. It is also interesting to note that GF2 results are very close to those of CC2. This could have been expected as GF2 is equivalent to ADC(2),[82,124,150] and the latter is closely related to the CC2 approximation.[373]

Finally, the principal IP of the 23 molecules considered so far has been computed at the ΔCCSD(T) in the aug-cc-pVTZ basis set (see Supporting Information). This method has been used as the reference for the GW100 data set, and it is interesting to benchmark it now that we have access to FCI references.[25,61,149,374] The last line of Table 6 reports the corresponding statistical descriptor. In particular, its MAE and MSE of 0.021 and 0.016 eV, respectively, show that the state-specific ΔCCSD(T) method can indeed be employed as a reference.

Figure 3 shows the distribution of the errors associated with the satellite transitions computed with CC methods including at least triple excitations, namely, CC3, CCSDT, CC4, and CCSDTQ. The corresponding statistical descriptors are reported in Table 7. The MAE of CCSDTQ is 0.039 eV, i.e., just below chemical accuracy, while CC4 and its approximate treatment of quadruples achieve a 0.093 eV MAE. Interestingly, while CC4 absolute errors are, on average, larger than CCSDTQ, its MSE is closer to zero. CC3 and CCSDT have MAEs of 0.787 and 0.537 eV, respectively, and once again CC3 has a lower MSE than its parent method (0.143 and 0.537 eV). Hence, methods accounting for triple excitations, even fully, should be used with care for satellites. It is also interesting to note that these MAEs align very well with those computed for double excitations, as reported in ref 10.

4. CONCLUSIONS

We have reported 42 FCI satellite transition energies computed in 23 small molecules. These energies have been calculated with increasingly large basis sets ranging from Pople's 6-31+G* to Dunning's aug-cc-pVXZ (where X = D, T, and Q). In addition, 58 FCI reference values for outer- and inner-valence IPs of the same molecular set have been presented. This work is the tenth layer of reference values of the QUEST database[23,237] and the first one to include charged excitations.

Various CC methods have been employed to compute IPs (CC2, CCSD, CC3, CCSDT, CC4, and CCSDTQ) and satellite transition energies (CC3, CCSDT, CC4, and CCSDTQ), and their performances have been assessed using the FCI reference values. It has been shown that CC3 and CC4 are faithful approximations of CCSDT and CCSDTQ for IPs, respectively, while the CC2 approximate treatment of double excitations induces large errors with respect to CCSD. For the satellites, our study reveals that chemical accuracy is reached only at the CCSDTQ level, highlighting the intricate and complex correlation effects involved in such states and their overall challenging nature for computational methods.

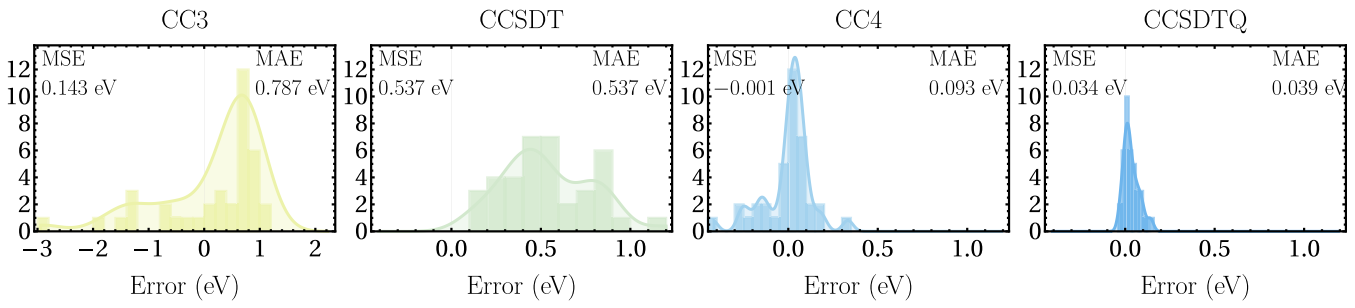

Figure 3. Distribution of the errors with respect to FCI of the various methods considered in this work. These errors are computed for the 36 satellites of this set in the aug-cc-pVTZ basis set. The satellites of LiF and BeO have been excluded (see main text). Note the different scale of the horizontal axis in the leftmost plot.

https://doi.org/10.1021/acs.jctc.4c00216
J. Chem. Theory Comput. 2024, 20, 4751−4777

The performance of various propagator methods (G_0W_0, $G_0F(2)$, G_0T_0, and qsGW) have also been gauged. The poor performance of these methods for satellite transition energies has been discussed in detail. These results call for the development of new methods capable of describing such states. For example, considering explicitly the three-body Green's function in order to describe IPs and satellites on an equal footing could offer significant advantages.[376,377] Studying the convergence of the ADC hierarchy using these new benchmark values is another possible outlook. Finally, assessing methods designed in the condensed matter community, such as the cumulant Green's function, on these small molecular systems would certainly be interesting. Work along this line is presently underway.[378]

One obvious perspective that needs to be addressed is the extension to transition intensities, which are of crucial importance for direct comparisons with experimental spectra. An approximate electronic structure method should not only aim to accurately describe the excited-state energy but also the transition intensities associated with it. Within the present SCI formalism, computing intensities is not straightforward but this is feasible, as demonstrated in refs 13, 379, and, 380 and is planned for future investigation.

■ ASSOCIATED CONTENT

Supporting Information

The Supporting Information is available free of charge at https://pubs.acs.org/doi/10.1021/acs.jctc.4c00216.

Geometry of the 23 molecules considered in this study as well as a json file for each molecule; and IPs and satellite transition energies of a given molecule as well as the FCI incertitudes and the spectral weight associated with the G_0W_0, $G_0F(2)$, and G_0T_0 quasiparticle energies (ZIP)

■ AUTHOR INFORMATION

Corresponding Authors

Antoine Marie − *Laboratoire de Chimie et Physique Quantiques (UMR 5626), Université de Toulouse, CNRS, UPS, Toulouse 31062, France;* orcid.org/0000-0003-3605-0176; Email: amarie@irsamc.ups-tlse.fr

Pierre-François Loos − *Laboratoire de Chimie et Physique Quantiques (UMR 5626), Université de Toulouse, CNRS, UPS, Toulouse 31062, France;* orcid.org/0000-0003-0598-7425; Email: loos@irsamc.ups-tlse.fr

Complete contact information is available at: https://pubs.acs.org/10.1021/acs.jctc.4c00216

Notes

The authors declare no competing financial interest.

■ ACKNOWLEDGMENTS

This project has received funding from the European Research Council (ERC) under the European Union's Horizon 2020 research and innovation programme (Grant agreement no. 863481). This work used the HPC resources from CALMIP (Toulouse) under allocations 2023-18005 and 2024-18005. The authors thank Abdallah Ammar, Fábris Kossoski, Yann Damour, Alexander Sokolov, Devin Matthews, Anthony Scemama, and Denis Jacquemin for helpful comments and/or insightful discussions.

■ REFERENCES

(1) Carlson, T. A. Photoelectron Spectroscopy. *Annu. Rev. Phys. Chem.* **1975**, *26*, 211−234.

(2) Hüfner, S.; Schmidt, S.; Reinert, F. Photoelectron Spectroscopy—An Overview. *Nucl. Instrum. Methods Phys. Res., Sect. A* **2005**, *547*, 8−23.

(3) Fadley, C. S. X-Ray Photoelectron Spectroscopy: Progress and Perspectives. *J. Electron Spectrosc. Relat. Phenom.* **2010**, *178*−*179*, 2−32.

(4) Campbell, M. J.; Liesegang, J.; Riley, J. D.; Jenkin, J. G. Ultraviolet Photoelectron Spectroscopy of the Valence Bands of Solid NH3, H2O, CO2, SO2 and N2O4. *J. Phys. C: Solid State Phys.* **1982**, *15*, 2549−2558.

(5) Winter, B.; Weber, R.; Widdra, W.; Dittmar, M.; Faubel, M.; Hertel, I. V. Full Valence Band Photoemission from Liquid Water Using EUV Synchrotron Radiation. *J. Phys. Chem. A* **2004**, *108*, 2625−2632.

(6) Seidel, R.; Winter, B.; Bradforth, S. E. Valence Electronic Structure of Aqueous Solutions: Insights from Photoelectron Spectroscopy. *Annu. Rev. Phys. Chem.* **2016**, *67*, 283−305.

(7) Buttersack, T.; Mason, P. E.; McMullen, R. S.; Martinek, T.; Brezina, K.; Hein, D.; Ali, H.; Kolbeck, C.; Schewe, C.; Malerz, S.; Winter, B.; Seidel, R.; Marsalek, O.; Jungwirth, P.; Bradforth, S. E. Valence and Core-Level X-ray Photoelectron Spectroscopy of a Liquid Ammonia Microjet. *J. Am. Chem. Soc.* **2019**, *141*, 1838−1841.

(8) Norman, P.; Dreuw, A. Simulating X-ray Spectroscopies and Calculating Core-Excited States of Molecules. *Chem. Rev.* **2018**, *118*, 7208−7248.

(9) Starcke, J. H.; Wormit, M.; Schirmer, J.; Dreuw, A. How Much Double Excitation Character Do the Lowest Excited States of Linear Polyenes Have? *Chem. Phys.* **2006**, *329*, 39−49.

(10) Loos, P.-F.; Boggio-Pasqua, M.; Scemama, A.; Caffarel, M.; Jacquemin, D. Reference Energies for Double Excitations. *J. Chem. Theory Comput.* **2019**, *15*, 1939−1956.

(11) do Casal, M. T.; Toldo, J. M.; Barbatti, M.; Plasser, F. Classification of doubly excited molecular electronic states. *Chem. Sci.* **2023**, *14*, 4012−4026.

(12) Cederbaum, L. Application of Green's Functions to Excitations Accompanying Photoionization in Atoms and Molecules. *Mol. Phys.* **1974**, *28*, 479−493.

(13) Mejuto-Zaera, C.; Weng, G.; Romanova, M.; Cotton, S. J.; Whaley, K. B.; Tubman, N. M.; Vlček, V. Are Multi-Quasiparticle Interactions Important in Molecular Ionization? *J. Chem. Phys.* **2021**, *154*, 121101.

(14) Pople, J. A.; Head-Gordon, M.; Fox, D. J.; Raghavachari, K.; Curtiss, L. A. Gaussian-1 Theory: A General Procedure for Prediction of Molecular Energies. *J. Chem. Phys.* **1989**, *90*, 5622−5629.

(15) Curtiss, L. A.; Raghavachari, K.; Trucks, G. W.; Pople, J. A. Gaussian-2 Theory for Molecular Energies of First- and Second-row Compounds. *J. Chem. Phys.* **1991**, *94*, 7221−7230.

(16) Curtiss, L. A.; Raghavachari, K.; Redfern, P. C.; Rassolov, V.; Pople, J. A. Gaussian-3 (G3) Theory for Molecules Containing First and Second-Row Atoms. *J. Chem. Phys.* **1998**, *109*, 7764−7776.

(17) Tajti, A.; Szalay, P. G.; Császár, A. G.; Kállay, M.; Gauss, J.; Valeev, E. F.; Flowers, B. A.; Vázquez, J.; Stanton, J. F. HEAT: High accuracy extrapolated ab initio thermochemistry. *J. Chem. Phys.* **2004**, *121*, 11599−11613.

(18) Jurečka, P.; Šponer, J.; Černý, J.; Hobza, P. Benchmark database of accurate (MP2 and CCSD(T) complete basis set limit) interaction energies of small model complexes, DNA base pairs, and amino acid pairs. *Phys. Chem. Chem. Phys.* **2006**, *8*, 1985−1993.

(19) Zhao, Y.; Truhlar, D. G. Comparative assessment of density functional methods for 3d transition-metal chemistry. *J. Chem. Phys.* **2006**, *124*, 224105.

(20) Schreiber, M.; Silva-Junior, M. R.; Sauer, S. P. A.; Thiel, W. Benchmarks for Electronically Excited States: CASPT2, CC2, CCSD and CC3. *J. Chem. Phys.* **2008**, *128*, 134110.

(21) Goerigk, L.; Grimme, S. A General Database for Main Group Thermochemistry, Kinetics, and Noncovalent Interactions − Assessment of Common and Reparameterized (meta-)GGA Density Functionals. *J. Chem. Theory Comput.* **2010**, *6*, 107−126.

(22) Mardirossian, N.; Head-Gordon, M. Thirty years of density functional theory in computational chemistry: an overview and extensive assessment of 200 density functionals. *Mol. Phys.* **2017**, *115*, 2315−2372.
(23) Loos, P.-F.; Scemama, A.; Jacquemin, D. The Quest for Highly Accurate Excitation Energies: A Computational Perspective. *J. Phys. Chem. Lett.* **2020**, *11*, 2374−2383.
(24) van Setten, M. J.; Caruso, F.; Sharifzadeh, S.; Ren, X.; Scheffler, M.; Liu, F.; Lischner, J.; Lin, L.; Deslippe, J. R.; Louie, S. G.; Yang, C.; Weigend, F.; Neaton, J. B.; Evers, F.; Rinke, P. GW 100: Benchmarking G_0W_0 for Molecular Systems. *J. Chem. Theory Comput.* **2015**, *11*, 5665−5687.
(25) Caruso, F.; Dauth, M.; van Setten, M. J.; Rinke, P. Benchmark of GW Approaches for the GW100 Test Set. *J. Chem. Theory Comput.* **2016**, *12*, 5076−5087.
(26) Krause, K.; Klopper, W. Implementation of the Bethe-Salpeter equation in the TURBOMOLE program. *J. Comput. Chem.* **2017**, *38*, 383−388.
(27) Gallandi, L.; Marom, N.; Rinke, P.; Körzdörfer, T. Accurate Ionization Potentials and Electron Affinities of Acceptor Molecules II: Non-Empirically Tuned Long-Range Corrected Hybrid Functionals. *J. Chem. Theory Comput.* **2016**, *12*, 605−614.
(28) Richard, R. M.; Marshall, M. S.; Dolgounitcheva, O.; Ortiz, J. V.; Brédas, J. L.; Marom, N.; Sherrill, C. D. Accurate Ionization Potentials and Electron Affinities of Acceptor Molecules I. Reference Data at the CCSD(T) Complete Basis Set Limit. *J. Chem. Theory Comput.* **2016**, *12*, 595−604.
(29) Knight, J. W.; Wang, X.; Gallandi, L.; Dolgounitcheva, O.; Ren, X.; Ortiz, J. V.; Rinke, P.; Körzdörfer, T.; Marom, N. Accurate Ionization Potentials and Electron Affinities of Acceptor Molecules III: A Benchmark of GW Methods. *J. Chem. Theory Comput.* **2016**, *12*, 615−626.
(30) Dolgounitcheva, O.; Díaz-Tinoco, M.; Zakrzewski, V. G.; Richard, R. M.; Marom, N.; Sherrill, C. D.; Ortiz, J. V. Accurate Ionization Potentials and Electron Affinities of Acceptor Molecules IV: Electron-Propagator Methods. *J. Chem. Theory Comput.* **2016**, *12*, 627−637.
(31) Čížek, J. On the Correlation Problem in Atomic and Molecular Systems. Calculation of Wavefunction Components in Ursell-Type Expansion Using Quantum-Field Theoretical Methods. *J. Chem. Phys.* **1966**, *45*, 4256−4266.
(32) Purvis, G. D.; Bartlett, R. J. A Full Coupled-Cluster Singles and Doubles Model: The Inclusion of Disconnected Triples. *J. Chem. Phys.* **1982**, *76*, 1910−1918.
(33) Raghavachari, K.; Trucks, G. W.; Pople, J. A.; Head-Gordon, M. A. A fifth-order perturbation comparison of electron correlation theories. *Chem. Phys. Lett.* **1989**, *157*, 479−483.
(34) Shavitt, I.; Bartlett, R. J. *Many-body Methods in Chemistry and Physics: MBPT and Coupled-Cluster Theory; Cambridge Molecular Science*; Cambridge University Press: Cambridge, 2009.
(35) Ranasinghe, D. S.; Margraf, J. T.; Perera, A.; Bartlett, R. J. Vertical Valence Ionization Potential Benchmarks from Equation-of-Motion Coupled Cluster Theory and QTP Functionals. *J. Chem. Phys.* **2019**, *150*, 074108.
(36) Stanton, J. F.; Bartlett, R. J. The equation of motion coupled-cluster method. A systematic biorthogonal approach to molecular excitation energies, transition probabilities, and excited state properties. *J. Chem. Phys.* **1993**, *98*, 7029−7039.
(37) Watts, J. D.; Bartlett, R. J. The inclusion of connected triple excitations in the equation-of-motion coupled-cluster method. *J. Chem. Phys.* **1994**, *101*, 3073−3078.
(38) Musiał, M.; Kucharski, S. A.; Bartlett, R. J. Equation-of-motion coupled cluster method with full inclusion of the connected triple excitations for ionized states: IP-EOM-CCSDT. *J. Chem. Phys.* **2003**, *118*, 1128−1136.
(39) Kamiya, M.; Hirata, S. Higher-Order Equation-of-Motion Coupled-Cluster Methods for Ionization Processes. *J. Chem. Phys.* **2006**, *125*, 074111.
(40) Gour, J. R.; Piecuch, P. Efficient formulation and computer implementation of the active-space electron-attached and ionized equation-of-motion coupled-cluster methods. *J. Chem. Phys.* **2006**, *125*, 234107.
(41) Szabo, A.; Ostlund, N. S. *Modern Quantum Chemistry*; McGraw-Hill: New York, 1989.
(42) Perdew, J. P.; Norman, M. R. Electron Removal Energies in Kohn-Sham Density-Functional Theory. *Phys. Rev. B: Condens. Matter Mater. Phys.* **1982**, *26*, 5445−5450.
(43) Ivanov, S.; Hirata, S.; Bartlett, R. J. Exact Exchange Treatment for Molecules in Finite-Basis-Set Kohn-Sham Theory. *Phys. Rev. Lett.* **1999**, *83*, 5455−5458.
(44) Chong, D. P.; Gritsenko, O. V.; Baerends, E. J. Interpretation of the Kohn−Sham Orbital Energies as Approximate Vertical Ionization Potentials. *J. Chem. Phys.* **2002**, *116*, 1760−1772.
(45) Hirao, K.; Bae, H.-S.; Song, J.-W.; Chan, B. Vertical Ionization Potential Benchmarks from Koopmans Prediction of Kohn−Sham Theory with Long-Range Corrected (LC) Functional. *J. Phys.: Cond. Mater.* **2022**, *34*, 194001.
(46) Görling, A. Exchange-Correlation Potentials with Proper Discontinuities for Physically Meaningful Kohn-Sham Eigenvalues and Band Structures. *Phys. Rev. B: Condens. Matter Mater. Phys.* **2015**, *91*, 245120.
(47) Thierbach, A.; Neiss, C.; Gallandi, L.; Marom, N.; Körzdörfer, T.; Görling, A. Accurate Valence Ionization Energies from Kohn−Sham Eigenvalues with the Help of Potential Adjustors. *J. Chem. Theory Comput.* **2017**, *13*, 4726−4740.
(48) Mester, D.; Kállay, M. Vertical Ionization Potentials and Electron Affinities at the Double-Hybrid Density Functional Level. *J. Chem. Theory Comput.* **2023**, *19*, 3982−3995.
(49) Verma, P.; Bartlett, R. J. Increasing the Applicability of Density Functional Theory. IV. Consequences of Ionization-Potential Improved Exchange-Correlation Potentials. *J. Chem. Phys.* **2014**, *140*, 18A534.
(50) Jin, Y.; Bartlett, R. J. The QTP Family of Consistent Functionals and Potentials in Kohn-Sham Density Functional Theory. *J. Chem. Phys.* **2016**, *145*, 034107.
(51) Jin, Y.; Bartlett, R. J. Accurate Computation of X-ray Absorption Spectra with Ionization Potential Optimized Global Hybrid Functional. *J. Chem. Phys.* **2018**, *149*, 064111.
(52) Bagus, P. S. Self-Consistent-Field Wave Functions for Hole States of Some Ne-Like and Ar-Like Ions. *Phys. Rev.* **1965**, *139*, A619−A634.
(53) Guest, M.; Saunders, V. The Calculation of Valence Shell Ionization Potentials by the ΔSCF Method. *Mol. Phys.* **1975**, *29*, 873−884.
(54) Besley, N. A.; Gilbert, A. T. B.; Gill, P. M. W. Self-Consistent-Field Calculations of Core Excited States. *J. Chem. Phys.* **2009**, *130*, 124308.
(55) Pueyo Bellafont, N.; Álvarez Saiz, G.; Viñes, F.; Illas, F. Performance of Minnesota Functionals on Predicting Core-Level Binding Energies of Molecules Containing Main-Group Elements. *Theor. Chem. Acc.* **2016**, *135*, 35.
(56) Jorstad, J. V.; Xie, T.; Morales, C. M. Δ-SCF Calculations of Core Electron Binding Energies in First-Row Transition Metal Atoms. *Int. J. Quantum Chem.* **2022**, *122*, No. e26881.
(57) Kahk, J. M.; Lischner, J. Combining the Δ-Self-Consistent-Field and GW Methods for Predicting Core Electron Binding Energies in Periodic Solids. *J. Chem. Theory Comput.* **2023**, *19*, 3276−3283.
(58) Hirao, K.; Nakajima, T.; Chan, B. Core-Level 2s and 2p Binding Energies of Third-Period Elements (P, S, and Cl) Calculated by Hartree−Fock and Kohn−Sham ΔSCF Theory. *J. Phys. Chem. A* **2023**, *127*, 7954−7963.
(59) Olsen, J.; Jo/rgensen, P.; Koch, H.; Balkova, A.; Bartlett, R. J. Full Configuration−Interaction and State of the Art Correlation Calculations on Water in a Valence Double-zeta Basis with Polarization Functions. *J. Chem. Phys.* **1996**, *104*, 8007−8015.
(60) Dempwolff, A. L.; Hodecker, M.; Dreuw, A. Vertical Ionization Potential Benchmark for Unitary Coupled-Cluster and Algebraic-

https://doi.org/10.1021/acs.jctc.4c00216
J. Chem. Theory Comput. 2024, 20, 4751−4777

Diagrammatic Construction Methods. *J. Chem. Phys.* **2022**, *156*, 054114.
(61) Krause, K.; Harding, M. E.; Klopper, W. Coupled-Cluster Reference Values For The Gw27 And Gw100 Test Sets For The Assessment Of Gw Methods. *Mol. Phys.* **2015**, *113*, 1952−1960.
(62) Zheng, X.; Cheng, L. Performance of Delta-Coupled-Cluster Methods for Calculations of Core-Ionization Energies of First-Row Elements. *J. Chem. Theory Comput.* **2019**, *15*, 4945−4955.
(63) Lee, J.; Small, D. W.; Head-Gordon, M. Excited States via Coupled Cluster Theory without Equation-of-Motion Methods: Seeking Higher Roots with Application to Doubly Excited States and Double Core Hole States. *J. Chem. Phys.* **2019**, *151*, 214103.
(64) Zheng, X.; Zhang, C.; Jin, Z.; Southworth, S. H.; Cheng, L. Benchmark Relativistic Delta-Coupled-Cluster Calculations of K-edge Core-Ionization Energies of Third-Row Elements. *Phys. Chem. Chem. Phys.* **2022**, *24*, 13587−13596.
(65) Bender, C. F.; Davidson, E. R. Studies in Configuration Interaction: The First-Row Diatomic Hydrides. *Phys. Rev.* **1969**, *183*, 23−30.
(66) Whitten, J. L.; Hackmeyer, M. Configuration Interaction Studies of Ground and Excited States of Polyatomic Molecules. I. The CI Formulation and Studies of Formaldehyde. *J. Chem. Phys.* **1969**, *51*, 5584−5596.
(67) Huron, B.; Malrieu, J. P.; Rancurel, P. Iterative perturbation calculations of ground and excited state energies from multiconfigurational zeroth-order wavefunctions. *J. Chem. Phys.* **1973**, *58*, 5745−5759.
(68) Buenker, R. J.; Peyerimhoff, S. D. Individualized configuration selection in CI calculations with subsequent energy extrapolation. *Theor. Chim. Acta* **1974**, *35*, 33−58.
(69) Eriksen, J. J.; Anderson, T. A.; Deustua, J. E.; Ghanem, K.; Hait, D.; Hoffmann, M. R.; Lee, S.; Levine, D. S.; Magoulas, I.; Shen, J.; et al. The Ground State Electronic Energy of Benzene. *J. Phys. Chem. Lett.* **2020**, *11*, 8922−8929.
(70) Eriksen, J. J. The Shape of Full Configuration Interaction to Come. *J. Phys. Chem. Lett.* **2021**, *12*, 418−432.
(71) Caffarel, M.; Applencourt, T.; Giner, E.; Scemama, A. Communication: Toward an improved control of the fixed-node error in quantum Monte Carlo: The case of the water molecule. *J. Chem. Phys.* **2016**, *144*, 151103.
(72) Schriber, J. B.; Evangelista, F. A. Communication: An adaptive configuration interaction approach for strongly correlated electrons with tunable accuracy. *J. Chem. Phys.* **2016**, *144*, 161106.
(73) Holmes, A. A.; Umrigar, C. J.; Sharma, S. Excited states using semistochastic heat-bath configuration interaction. *J. Chem. Phys.* **2017**, *147*, 164111.
(74) Damour, Y.; Véril, M.; Kossoski, F.; Caffarel, M.; Jacquemin, D.; Scemama, A.; Loos, P.-F. Accurate full configuration interaction correlation energy estimates for five- and six-membered rings. *J. Chem. Phys.* **2021**, *155*, 134104.
(75) Larsson, H. R.; Zhai, H.; Umrigar, C. J.; Chan, G. K.-L. The Chromium Dimer: Closing a Chapter of Quantum Chemistry. *J. Am. Chem. Soc.* **2022**, *144*, 15932−15937.
(76) Tubman, N. M.; Lee, J.; Takeshita, T. Y.; Head-Gordon, M.; Whaley, K. B. A deterministic alternative to the full configuration interaction quantum Monte Carlo method. *J. Chem. Phys.* **2016**, *145*, 044112.
(77) Tubman, N. M.; Levine, D. S.; Hait, D.; Head-Gordon, M.; Whaley, K. B. An efficient deterministic perturbation theory for selected configuration interaction methods. **2018**, arXiv preprint arXiv:1808.02049
(78) Tubman, N. M.; Freeman, C. D.; Levine, D. S.; Hait, D.; Head-Gordon, M.; Whaley, K. B. Modern Approaches to Exact Diagonalization and Selected Configuration Interaction with the Adaptive Sampling CI Method. *J. Chem. Theory Comput.* **2020**, *16*, 2139−2159.
(79) Martin, R. M.; Reining, L.; Ceperley, D. M. *Interacting Electrons: Theory and Computational Approaches*; Cambridge University Press, 2016.
(80) Golze, D.; Dvorak, M.; Rinke, P. The GW Compendium: A Practical Guide to Theoretical Photoemission Spectroscopy. *Front. Chem.* **2019**, *7*, 377.
(81) Marie, A.; Ammar, A.; Loos, P.-F. The GW Approximation: A Quantum Chemistry Perspective. **2023**, arXiv preprint arXiv:2311.05351.
(82) Schirmer, J. *Many-body Methods for Atoms, Molecules and Clusters*; Springer, 2018.
(83) Banerjee, S.; Sokolov, A. Y. Algebraic Diagrammatic Construction Theory for Simulating Charged Excited States and Photoelectron Spectra. *J. Chem. Theory Comput.* **2023**, *19*, 3037−3053.
(84) Strinati, G.; Mattausch, H. J.; Hanke, W. Dynamical Correlation Effects on the Quasiparticle Bloch States of a Covalent Crystal. *Phys. Rev. Lett.* **1980**, *45*, 290−294.
(85) Hybertsen, M. S.; Louie, S. G. First-Principles Theory of Quasiparticles: Calculation of Band Gaps in Semiconductors and Insulators. *Phys. Rev. Lett.* **1985**, *55*, 1418−1421.
(86) Godby, R. W.; Schlüter, M.; Sham, L. J. Self-Energy Operators and Exchange-Correlation Potentials in Semiconductors. *Phys. Rev. B: Condens. Matter Mater. Phys.* **1988**, *37*, 10159−10175.
(87) von der Linden, W.; Horsch, P. Precise Quasiparticle Energies and Hartree-Fock Bands of Semiconductors and Insulators. *Phys. Rev. B: Condens. Matter Mater. Phys.* **1988**, *37*, 8351−8362.
(88) Northrup, J. E.; Hybertsen, M. S.; Louie, S. G. Many-body calculation of the surface-state energies for Si(111)2×1. *Phys. Rev. Lett.* **1991**, *66*, 500−503.
(89) Blase, X.; Zhu, X.; Louie, S. G. Self-energy effects on the surface-state energies of H-Si(111)1×1. *Phys. Rev. B: Condens. Matter Mater. Phys.* **1994**, *49*, 4973−4980.
(90) Rohlfing, M.; Krüger, P.; Pollmann, J. Efficient scheme forGWquasiparticle band-structure calculations with applications to bulk Si and to the Si(001)-(2×1) surface. *Phys. Rev. B: Condens. Matter Mater. Phys.* **1995**, *52*, 1905−1917.
(91) Neuhauser, D.; Rabani, E.; Baer, R. Expeditious Stochastic Calculation of Random-Phase Approximation Energies for Thousands of Electrons in Three Dimensions. *J. Phys. Chem. Lett.* **2013**, *4*, 1172−1176.
(92) Neuhauser, D.; Gao, Y.; Arntsen, C.; Karshenas, C.; Rabani, E.; Baer, R. Breaking the Theoretical Scaling Limit for Predicting Quasiparticle Energies: The Stochastic G W Approach. *Phys. Rev. Lett.* **2014**, *113*, 076402.
(93) Govoni, M.; Galli, G. Large Scale GW Calculations. *J. Chem. Theory Comput.* **2015**, *11*, 2680−2696.
(94) Vlček, V.; Rabani, E.; Neuhauser, D.; Baer, R. Stochastic GW Calculations for Molecules. *J. Chem. Theory Comput.* **2017**, *13*, 4997−5003.
(95) Wilhelm, J.; Golze, D.; Talirz, L.; Hutter, J.; Pignedoli, C. A. Toward GW Calculations on Thousands of Atoms. *J. Phys. Chem. Lett.* **2018**, *9*, 306−312.
(96) Duchemin, I.; Blase, X. Separable resolution-of-the-identity with all-electron Gaussian bases: Application to cubic-scaling RPA. *J. Chem. Phys.* **2019**, *150*, 174120.
(97) Del Ben, M.; da Jornada, F. H.; Canning, A.; Wichmann, N.; Raman, K.; Sasanka, R.; Yang, C.; Louie, S. G.; Deslippe, J. Large-scale GW calculations on pre-exascale HPC systems. *Comput. Phys. Commun.* **2019**, *235*, 187−195.
(98) Förster, A.; Visscher, L. Low-Order Scaling G0W0 by Pair Atomic Density Fitting. *J. Chem. Theory Comput.* **2020**, *16*, 7381−7399.
(99) Förster, A.; Visscher, L. Low-Order Scaling Quasiparticle Self-Consistent GW for Molecules. *Front. Chem.* **2021**, *9*, 736591.
(100) Duchemin, I.; Blase, X. Robust Analytic-Continuation Approach to Many-Body GW Calculations. *J. Chem. Theory Comput.* **2020**, *16*, 1742−1756.
(101) Duchemin, I.; Blase, X. Cubic-Scaling All-Electron GW Calculations with a Separable Density-Fitting Space−Time Approach. *J. Chem. Theory Comput.* **2021**, *17*, 2383−2393.
(102) Förster, A.; Visscher, L. Quasiparticle Self-Consistent GW-Bethe−Salpeter Equation Calculations for Large Chromophoric Systems. *J. Chem. Theory Comput.* **2022**, *18*, 6779−6793.

https://doi.org/10.1021/acs.jctc.4c00216
J. Chem. Theory Comput. 2024, 20, 4751−4777

(103) Panadés-Barrueta, R. L.; Golze, D. Accelerating Core-Level GW Calculations by Combining the Contour Deformation Approach with the Analytic Continuation of W. *J. Chem. Theory Comput.* **2023**, *19*, 5450−5464.
(104) Shishkin, M.; Kresse, G. Self-Consistent GW Calculations for Semiconductors and Insulators. *Phys. Rev. B: Condens. Matter Mater. Phys.* **2007**, *75*, 235102.
(105) Blase, X.; Attaccalite, C.; Olevano, V. First-Principles $ \mathit{GW}$ Calculations for Fullerenes, Porphyrins, Phtalocyanine, and Other Molecules of Interest for Organic Photovoltaic Applications. *Phys. Rev. B: Condens. Matter Mater. Phys.* **2011**, *83*, 115103.
(106) Marom, N.; Caruso, F.; Ren, X.; Hofmann, O. T.; Körzdörfer, T.; Chelikowsky, J. R.; Rubio, A.; Scheffler, M.; Rinke, P. Benchmark of GW Methods for Azabenzenes. *Phys. Rev. B: Condens. Matter Mater. Phys.* **2012**, *86*, 245127.
(107) Wilhelm, J.; Del Ben, M.; Hutter, J. GW in the Gaussian and Plane Waves Scheme with Application to Linear Acenes. *J. Chem. Theory Comput.* **2016**, *12*, 3623−3635.
(108) Kaplan, F.; Harding, M. E.; Seiler, C.; Weigend, F.; Evers, F.; van Setten, M. J. Quasi-Particle Self-Consistent GW for Molecules. *J. Chem. Theory Comput.* **2016**, *12*, 2528−2541.
(109) Faleev, S. V.; van Schilfgaarde, M.; Kotani, T. All-Electron Self-Consistent G W Approximation: Application to Si, MnO, and NiO. *Phys. Rev. Lett.* **2004**, *93*, 126406.
(110) van Schilfgaarde, M.; Kotani, T.; Faleev, S. Quasiparticle Self-Consistent G W Theory. *Phys. Rev. Lett.* **2006**, *96*, 226402.
(111) Kotani, T.; van Schilfgaarde, M.; Faleev, S. V. Quasiparticle Self-Consistent G W Method: A Basis for the Independent-Particle Approximation. *Phys. Rev. B: Condens. Matter Mater. Phys.* **2007**, *76*, 165106.
(112) Ke, S.-H. All-Electron G W Methods Implemented in Molecular Orbital Space: Ionization Energy and Electron Affinity of Conjugated Molecules. *Phys. Rev. B: Condens. Matter Mater. Phys.* **2011**, *84*, 205415.
(113) Marie, A.; Loos, P.-F. A Similarity Renormalization Group Approach to Green's Function Methods. *J. Chem. Theory Comput.* **2023**, *19*, 3943−3957.
(114) Casida, M. E.; Chong, D. P. Physical Interpretation and Assessment of the Coulomb-Hole and Screened-Exchange Approximation for Molecules. *Phys. Rev. A* **1989**, *40*, 4837−4848.
(115) Casida, M. E.; Chong, D. P. Simplified Green-Function Approximations: Further Assessment of a Polarization Model for Second-Order Calculation of Outer-Valence Ionization Potentials in Molecules. *Phys. Rev. A* **1991**, *44*, 5773−5783.
(116) Stefanucci, G.; van Leeuwen, R. *Nonequilibrium Many-Body Theory of Quantum Systems: A Modern Introduction*; Cambridge University Press: Cambridge, 2013.
(117) Ortiz, J. V. Electron propagator theory: an approach to prediction and interpretation in quantum chemistry. *Wiley Interdiscip. Rev. Comput. Mol. Sci.* **2013**, *3*, 123−142.
(118) Phillips, J. J.; Zgid, D. C. Communication: The description of strong correlation within self-consistent Green's function second-order perturbation theory. *J. Chem. Phys.* **2014**, *140*, 241101.
(119) Phillips, J. J.; Kananenka, A. A.; Zgid, D. Fractional Charge and Spin Errors in Self-Consistent Green's Function Theory. *J. Chem. Phys.* **2015**, *142*, 194108.
(120) Rusakov, A. A.; Phillips, J. J.; Zgid, D. Local Hamiltonians for Quantitative Green's Function Embedding Methods. *J. Chem. Phys.* **2014**, *141*, 194105.
(121) Rusakov, A. A.; Zgid, D. Self-Consistent Second-Order Green's Function Perturbation Theory for Periodic Systems. *J. Chem. Phys.* **2016**, *144*, 054106.
(122) Hirata, S.; Hermes, M. R.; Simons, J.; Ortiz, J. V. General-Order Many-Body Green's Function Method. *J. Chem. Theory Comput.* **2015**, *11*, 1595−1606.
(123) Hirata, S.; Doran, A. E.; Knowles, P. J.; Ortiz, J. V. One-Particle Many-Body Green's Function Theory: Algebraic Recursive Definitions, Linked-Diagram Theorem, Irreducible-Diagram Theorem, and General-Order Algorithms. *J. Chem. Phys.* **2017**, *147*, 044108.
(124) Backhouse, O. J.; Santana-Bonilla, A.; Booth, G. H. Scalable and Predictive Spectra of Correlated Molecules with Moment Truncated Iterated Perturbation Theory. *J. Phys. Chem. Lett.* **2021**, *12*, 7650−7658.
(125) Backhouse, O. J.; Booth, G. H. Efficient Excitations and Spectra within a Perturbative Renormalization Approach. *J. Chem. Theory Comput.* **2020**, *16*, 6294−6304.
(126) Backhouse, O. J.; Nusspickel, M.; Booth, G. H. Wave Function Perspective and Efficient Truncation of Renormalized Second-Order Perturbation Theory. *J. Chem. Theory Comput.* **2020**, *16*, 1090−1104.
(127) Pokhilko, P.; Zgid, D. Interpretation of multiple solutions in fully iterative GF2 and GW schemes using local analysis of two-particle density matrices. *J. Chem. Phys.* **2021**, *155*, 024101.
(128) Pokhilko, P.; Iskakov, S.; Yeh, C.-N.; Zgid, D. Evaluation of two-particle properties within finite-temperature self-consistent one-particle Green's function methods: Theory and application to GW and GF2. *J. Chem. Phys.* **2021**, *155*, 024119.
(129) Pokhilko, P.; Yeh, C.-N.; Zgid, D. Iterative subspace algorithms for finite-temperature solution of Dyson equation. *J. Chem. Phys.* **2022**, *156*, 094101.
(130) Liebsch, A. Ni d-band self-energy beyond the low-density limit. *Phys. Rev. B: Condens. Matter Mater. Phys.* **1981**, *23*, 5203−5212.
(131) Bickers, N. E.; Scalapino, D. J.; White, S. R. Conserving Approximations for Strongly Correlated Electron Systems: Bethe-Salpeter Equation and Dynamics for the Two-Dimensional Hubbard Model. *Phys. Rev. Lett.* **1989**, *62*, 961−964.
(132) Bickers, N. E.; White, S. R. Conserving approximations for strongly fluctuating electron systems. II. Numerical results and parquet extension. *Phys. Rev. B: Condens. Matter Mater. Phys.* **1991**, *43*, 8044−8064.
(133) Katsnelson, M. I.; Lichtenstein, A. I. LDA++ approach to the electronic structure of magnets: correlation effects in iron. *J. Phys.: Condens. Matter* **1999**, *11*, 1037−1048.
(134) Katsnelson, M.; Lichtenstein, A. Electronic structure and magnetic properties of correlated metals. *Eur. Phys. J. B* **2002**, *30*, 9−15.
(135) Zhukov, V. P.; Chulkov, E. V.; Echenique, P. M. GW + T Theory of Excited Electron Lifetimes in Metals. *Phys. Rev. B: Condens. Matter Mater. Phys.* **2005**, *72*, 155109.
(136) Puig von Friesen, M.; Verdozzi, C.; Almbladh, C.-O. Kadanoff-Baym dynamics of Hubbard clusters: Performance of many-body schemes, correlation-induced damping and multiple steady and quasi-steady states. *Phys. Rev. B: Condens. Matter Mater. Phys.* **2010**, *82*, 155108.
(137) Romaniello, P.; Bechstedt, F.; Reining, L. Beyond the G W Approximation: Combining Correlation Channels. *Phys. Rev. B: Condens. Matter Mater. Phys.* **2012**, *85*, 155131.
(138) Gukelberger, J.; Huang, L.; Werner, P. On the dangers of partial diagrammatic summations: Benchmarks for the two-dimensional Hubbard model in the weak-coupling regime. *Phys. Rev. B: Condens. Matter Mater. Phys.* **2015**, *91*, 235114.
(139) Müller, M. C. T. D.; Blügel, S.; Friedrich, C. Electron-magnon scattering in elementary ferromagnets from first principles: Lifetime broadening and band anomalies. *Phys. Rev. B* **2019**, *100*, 045130.
(140) Friedrich, C. Tetrahedron integration method for strongly varying functions: Application to the GT self-energy. *Phys. Rev. B* **2019**, *100*, 075142.
(141) Biswas, T.; Singh, A. Excitonic effects in absorption spectra of carbon dioxide reduction photocatalysts. *npj Comput. Mater.* **2021**, *7*, 189.
(142) Zhang, D.; Su, N. Q.; Yang, W. Accurate Quasiparticle Spectra from the T-Matrix Self-Energy and the Particle−Particle Random Phase Approximation. *J. Phys. Chem. Lett.* **2017**, *8*, 3223−3227.
(143) Li, J.; Chen, Z.; Yang, W. Renormalized Singles Green's Function in the T-Matrix Approximation for Accurate Quasiparticle Energy Calculation. *J. Phys. Chem. Lett.* **2021**, *12*, 6203−6210.
(144) Li, J.; Yu, J.; Chen, Z.; Yang, W. Linear Scaling Calculations of Excitation Energies with Active-Space Particle−Particle Random-Phase Approximation. *J. Phys. Chem. A* **2023**, *127*, 7811−7822.

https://doi.org/10.1021/acs.jctc.4c00216
J. Chem. Theory Comput. 2024, 20, 4751−4777

(145) Loos, P.-F.; Romaniello, P. Static and dynamic Bethe−Salpeter equations in the T-matrix approximation. *J. Chem. Phys.* **2022**, *156*, 164101.
(146) Orlando, R.; Romaniello, P.; Loos, P.-F. *Advances in Quantum Chemistry*; Elsevier, 2023; pp 183−211.
(147) Orlando, R.; Romaniello, P.; Loos, P.-F. The three channels of many-body perturbation theory: GW, particle−particle, and electron−hole T-matrix self-energies. *J. Chem. Phys.* **2023**, *159*, 184113.
(148) Lewis, A. M.; Berkelbach, T. C. Vertex Corrections to the Polarizability Do Not Improve the GW Approximation for the Ionization Potential of Molecules. *J. Chem. Theory Comput.* **2019**, *15*, 2925−2932.
(149) Bruneval, F.; Dattani, N.; van Setten, M. J. The GW Miracle in Many-Body Perturbation Theory for the Ionization Potential of Molecules. *Front. Chem.* **2021**, *9*, 749779.
(150) Monino, E.; Loos, P.-F. Connections and performances of Green's function methods for charged and neutral excitations. *J. Chem. Phys.* **2023**, *159*, 034105.
(151) Baym, G.; Kadanoff, L. P. Conservation Laws and Correlation Functions. *Phys. Rev.* **1961**, *124*, 287−299.
(152) Baym, G. Self-Consistent Approximations in Many-Body Systems. *Phys. Rev.* **1962**, *127*, 1391−1401.
(153) De Dominicis, C.; Martin, P. C. Stationary Entropy Principle and Renormalization in Normal and Superfluid Systems. I. Algebraic Formulation. *J. Math. Phys.* **1964**, *5*, 14−30.
(154) De Dominicis, C.; Martin, P. C. Stationary Entropy Principle and Renormalization in Normal and Superfluid Systems. II. Diagrammatic Formulation. *J. Math. Phys.* **1964**, *5*, 31−59.
(155) Bickers, N.; Scalapino, D. Conserving approximations for strongly fluctuating electron systems. I. Formalism and calculational approach. *Ann. Phys.* **1989**, *193*, 206−251.
(156) Hedin, L. On correlation effects in electron spectroscopies and the GW approximation. *J. Phys.: Condens. Matter* **1999**, *11*, R489−R528.
(157) Bickers, N. E. In *Theoretical Methods for Strongly Correlated Electrons*; Sénéchal, D., Tremblay, A.-M., Bourbonnais, C., Eds.; Springer New York: New York, NY, 2004; pp 237−296.
(158) Shirley, E. L. Self-consistent GW and higher-order calculations of electron states in metals. *Phys. Rev. B: Condens. Matter Mater. Phys.* **1996**, *54*, 7758−7764.
(159) Del Sole, R.; Reining, L.; Godby, R. W. GWΓ approximation for electron self-energies in semiconductors and insulators. *Phys. Rev. B: Condens. Matter Mater. Phys.* **1994**, *49*, 8024−8028.
(160) Schindlmayr, A.; Godby, R. W. Systematic Vertex Corrections through Iterative Solution of Hedin's Equations Beyond the $ \mathit{GW}$ Approximation. *Phys. Rev. Lett.* **1998**, *80*, 1702−1705.
(161) Morris, A. J.; Stankovski, M.; Delaney, K. T.; Rinke, P.; García-González, P.; Godby, R. W. Vertex corrections in localized and extended systems. *Phys. Rev. B: Condens. Matter Mater. Phys.* **2007**, *76*, 155106.
(162) Shishkin, M.; Marsman, M.; Kresse, G. Accurate Quasiparticle Spectra from Self-Consistent GW Calculations with Vertex Corrections. *Phys. Rev. Lett.* **2007**, *99*, 246403.
(163) Romaniello, P.; Guyot, S.; Reining, L. The Self-Energy beyond GW: Local and Nonlocal Vertex Corrections. *J. Chem. Phys.* **2009**, *131*, 154111.
(164) Grüneis, A.; Kresse, G.; Hinuma, Y.; Oba, F. Ionization Potentials of Solids: The Importance of Vertex Corrections. *Phys. Rev. Lett.* **2014**, *112*, 096401.
(165) Hung, L.; Bruneval, F.; Baishya, K.; Öğüt, S. Benchmarking the GW Approximation and Bethe−Salpeter Equation for Groups IB and IIB Atoms and Monoxides. *J. Chem. Theory Comput.* **2017**, *13*, 2135−2146.
(166) Maggio, E.; Kresse, G. GW Vertex Corrected Calculations for Molecular Systems. *J. Chem. Theory Comput.* **2017**, *13*, 4765−4778.
(167) Mejuto-Zaera, C.; Vlček, V. Self-consistency in GWΓ formalism leading to quasiparticle-quasiparticle couplings. *Phys. Rev. B* **2022**, *106*, 165129.
(168) Wen, M.; Abraham, V.; Harsha, G.; Shee, A.; Whaley, B.; Zgid, D. Comparing Self-Consistent GW and Vertex-Corrected G_0W_0 ($G_0W_0\Gamma$) Accuracy for Molecular Ionization Potentials. *J. Chem. Theory Comput.* **2024**. in press
(169) Schirmer, J.; Cederbaum, L. S.; Domcke, W.; von Niessen, W. Strong Correlation Effects in Inner Valence Ionization of N2 AND CO. *Chem. Phys.* **1977**, *26*, 149−153.
(170) Cederbaum, L. S.; Schirmer, J.; Domcke, W.; Niessen, W. v. Complete Breakdown of the Quasiparticle Picture for Inner Valence Electrons. *J. Phys. B: At. Mol. Phys.* **1977**, *10*, L549−L553.
(171) Schirmer, J.; Cederbaum, L. S. The Two-Particle-Hole Tamm-Dancoff Approximation (2ph-TDA) Equations for Closed-Shell Atoms and Molecules. *J. Phys. B: At. Mol. Phys.* **1978**, *11*, 1889−1900.
(172) Schirmer, J.; Domcke, W.; Cederbaum, L. S.; Niessen, W. v. Break-down of the Molecular-Orbital Picture of Ionization: CS, PN and P2. *J. Phys. B: At. Mol. Phys.* **1978**, *11*, 1901−1915.
(173) Schirmer, J.; Cederbaum, L. S.; Domcke, W.; Von Niessen, W. Complete Breakdown of the Quasiparticle Picture for Inner-Valence Electrons: Hydrogen Cyanide and Formic Acid. *Chem. Phys. Lett.* **1978**, *57*, 582−587.
(174) Domcke, W.; Cederbaum, L. S.; Schirmer, J.; von Niessen, W.; Maier, J. P. Breakdown of the Molecular Orbital Picture of Ionization for Inner Valence Electrons: Experimental and Theoretical Study of H2S and PH3. *J. Electron Spectrosc. Relat. Phenom.* **1978**, *14*, 59−72.
(175) Cederbaum, L. S.; Schirmer, J.; Domcke, W.; Von Niessen, W. On the Adequacy of the Molecular-Orbital Picture for Describing Ionization Processes. *Int. J. Quantum Chem.* **1978**, *14*, 593−601.
(176) Cederbaum, L. S.; Domcke, W.; Schirmer, J.; Niessen, W. v. Many-Body Effects in Valence and Core Photoionization of Molecules. *Phys. Scr.* **1980**, *21*, 481−491.
(177) von Niessen, W.; Bieri, G.; Åsbrink, L. 30.4-Nm He (II) Photoelectron Spectra of Organic Molecules: Part III. Oxo-compounds (C, H, O). *J. Electron Spectrosc. Relat. Phenom.* **1980**, *21*, 175−191.
(178) Von Niessen, W.; Cederbaum, L. S.; Domcke, W.; Diercksen, G. H. F. Green's Function Calculations on the Complete Valence Ionization Spectra of HF, HCl, HBr AND HI. *Chem. Phys.* **1981**, *56*, 43−52.
(179) Walter, O.; Schirmer, J. The Two-Particle-Hole Tamm-Dancoff Approximation (2ph-TDA) for Atoms. *J. Phys. B: At. Mol. Phys.* **1981**, *14*, 3805−3826.
(180) Schirmer, J.; Walter, O. Complete Valence-Shell Ionization Spectra of N2 and CO: Application of the Extended Two-Particle-Hole Tamm-Dancoff Approximation (2ph-TDA). *Chem. Phys.* **1983**, *78*, 201−211.
(181) Cederbaum, L. S.; Domcke, W.; Schirmer, J.; Niessen, W. V. Correlation Effects in the Ionization of Molecules: Breakdown of the Molecular Orbital Picture. *Adv. Chem. Phys.* **1986**, *65*, 115−159.
(182) Bagus, P. S.; Viinikka, E.-K. Origin of Satellite Structure in the Valence X-Ray Photoelectron Spectrum of CO: A Theoretical Study. *Phys. Rev. A* **1977**, *15*, 1486−1496.
(183) Kosugi, N.; Kuroda, H.; Iwata, S. Breakdown of Koopmans' Theorem and Strong Shake-up Bands in the Valence Shell Region of N2 Photoelectron Spectra. *Chem. Phys.* **1979**, *39*, 337−349.
(184) Kosugi, N.; Kuroda, H.; Iwata, S. Double Breakdown of Koopmans' Theorem and Strong Correlation Satellites in the He II Photoelectron Spectrum of O3. *Chem. Phys.* **1981**, *58*, 267−273.
(185) Honjou, N.; Sasajima, T.; Sasaki, F. Theoretical Study of the Satellite Bands in the Valence Shell XPS Spectra of N2, CO, O2 and NO Molecules. *Chem. Phys.* **1981**, *57*, 475−485.
(186) Nakatsuji, H.; Yonezawa, T. Cluster Expansion of the Wavefunction. Satellite Peaks of the Inner-Valence Ionization of H2O Studied by the SAC and SAC CI Theories. *Chem. Phys. Lett.* **1982**, *87*, 426−431.
(187) Arneberg, R.; Müller, J.; Manne, R. Configuration Interaction Calculations of Satellite Structure in Photoelectron Spectra of H2O. *Chem. Phys.* **1982**, *64*, 249−258.
(188) Roy, P.; Nenner, I.; Millie, P.; Morin, P.; Roy, D. Experimental and Theoretical Study of Configuration Interaction States of CO+2. *J. Chem. Phys.* **1986**, *84*, 2050−2061.

https://doi.org/10.1021/acs.jctc.4c00216
J. Chem. Theory Comput. 2024, 20, 4751−4777

(189) Bawagan, A. O.; Müller-Fiedler, R.; Brion, C. E.; Davidson, E. R.; Boyle, C. The Valence Orbitals of NH3 by Electron Momentum Spectroscopy: Quantitative Comparisons Using Hartree-Fock Limit and Correlated Wavefunctions. *Chem. Phys.* **1988**, *120*, 335−357.
(190) Bawagan, A. O.; Brion, C. E.; Davidson, E. R.; Boyle, C.; Frey, R. F. The Valence Orbital Momentum Distributions and Binding Energy Spectra of H2CO: A Comparison of Electron Momentum Spectroscopy and Quantum Chemical Calculations Using near-Hartree-Fock Quality and Correlated Wavefunctions. *Chem. Phys.* **1988**, *128*, 439−455.
(191) Clark, S. A. C.; Brion, C. E.; Davidson, E. R.; Boyle, C. The Momentum Distributions and Binding Energies of the Valence Orbitals of Phosphine by Electron Momentum Spectroscopy: Quantitative Comparisons Using near Hartree-Fock Limit and Correlated Wavefunctions. *Chem. Phys.* **1989**, *136*, 55−66.
(192) Clark, S. A. C.; Reddish, T. J.; Brion, C. E.; Davidson, E. R.; Frey, R. F. The Valence Orbital Momentum Distributions and Binding Energy Spectra of Methane by Electron Momentum Spectroscopy: Quantitative Comparisons Using near Hartree-Fock Limit and Correlated Wavefunctions. *Chem. Phys.* **1990**, *143*, 1−10.
(193) Lisini, A.; Decleva, P.; Fronzoni, G. Theoretical Study of the Satellite Structure in the Valence Photoelectron Spectra of the Second and Third Row Hydrides. *J. Mol. Struct.: THEOCHEM* **1991**, *228*, 97−116.
(194) Nakatsuji, H. Cluster Expansion of the Wavefunction, Valence and Rydberg Excitations, Ionizations, and Inner-Valence Ionizations of CO2 and N2O Studied by the Sac and Sac CI Theories. *Chem. Phys.* **1983**, *75*, 425−441.
(195) Wasada, H.; Hirao, K. Computational Studies of Satellite Peaks of the Inner-Valence Ionization of C2H4, C2H2 and H2S Using the SAC CI Method. *Chem. Phys.* **1989**, *138*, 277−290.
(196) Nakatsuji, H. Description of Two- and Many-Electron Processes by the SAC-CI Method. *Chem. Phys. Lett.* **1991**, *177*, 331−337.
(197) Ehara, M.; Nakatsuji, H. Outer- and inner-valence ionization spectra of N2 and CO: *Chem. Phys. Lett.* **1998**, *282*, 347−354.
(198) Ehara, M.; Nakatsuji, H. Ionization Spectrum of CO2 Studied by the SAC-CI General-R Method. *Spectrochim. Acta, Part A* **1999**, *55*, 487−493.
(199) Ehara, M.; Tomasello, P.; Hasegawa, J.; Nakatsuji, H. SAC-CI General-R Study of the Ionization Spectrum of HCl. *Theor. Chem. Acc.* **1999**, *102*, 161−164.
(200) Ehara, M.; Ishida, M.; Nakatsuji, H. Theoretical study on the outer- and inner-valence ionization spectra of H2O, H2S and H2Se using the SAC-CI general-R method. *J. Chem. Phys.* **2001**, *114*, 8990−8999.
(201) Ishida, M.; Ehara, M.; Nakatsuji, H. Outer- and inner-valence ionization spectra of NH3, PH3, and AsH3: symmetry-adapted cluster configuration interaction general-R study. *J. Chem. Phys.* **2002**, *116*, 1934−1943.
(202) Ehara, M.; Yasuda, S.; Nakatsuji, H. Fine Theoretical Spectroscopy Using SAC-CI General-R Method: Outer- and Inner-Valence Ionization Spectra of N2O and HN3. *Z. Phys. Chem.* **2003**, *217*, 161−176.
(203) Ohtsuka, Y.; Nakatsuji, H. Inner-Shell Ionizations and Satellites Studied by the Open-Shell Reference Symmetry-Adapted Cluster/Symmetry-Adapted Cluster Configuration-Interaction Method. *J. Chem. Phys.* **2006**, *124*, 054110.
(204) Ning, C. G.; Hajgató, B.; Huang, Y. R.; Zhang, S. F.; Liu, K.; Luo, Z. H.; Knippenberg, S.; Deng, J. K.; Deleuze, M. S. High Resolution Electron Momentum Spectroscopy of the Valence Orbitals of Water. *Chem. Phys.* **2008**, *343*, 19−30.
(205) Tian, Q.; Yang, J.; Shi, Y.; Shan, X.; Chen, X. Outer- and Inner-Valence Satellites of Carbon Dioxide: Electron Momentum Spectroscopy Compared with Symmetry-Adapted-Cluster Configuration Interaction General-R Calculations. *J. Chem. Phys.* **2012**, *136*, 094306.
(206) Aryasetiawan, F.; Hedin, L.; Karlsson, K. Multiple Plasmon Satellites in Na and Al Spectral Functions from Ab Initio Cumulant Expansion. *Phys. Rev. Lett.* **1996**, *77*, 2268−2271.
(207) Vos, M.; Kheifets, A. S.; Weigold, E.; Aryasetiawan, F. Electron Correlation Effects in the Spectral Momentum Density of Graphite. *Phys. Rev. B: Condens. Matter Mater. Phys.* **2001**, *63*, 033108.
(208) Vos, M.; Kheifets, A.; Sashin, V.; Weigold, E.; Usuda, M.; Aryasetiawan, F. Quantitative Measurement of the Spectral Function of Aluminum and Lithium by Electron Momentum Spectroscopy. *Phys. Rev. B: Condens. Matter Mater. Phys.* **2002**, *66*, 155414.
(209) Kheifets, A. S.; Sashin, V. A.; Vos, M.; Weigold, E.; Aryasetiawan, F. Spectral Properties of Quasiparticles in Silicon: A Test of Many-Body Theory. *Phys. Rev. B: Condens. Matter Mater. Phys.* **2003**, *68*, 233205.
(210) Guzzo, M.; Lani, G.; Sottile, F.; Romaniello, P.; Gatti, M.; Kas, J. J.; Rehr, J. J.; Silly, M. G.; Sirotti, F.; Reining, L. Valence Electron Photoemission Spectrum of Semiconductors: Ab Initio Description of Multiple Satellites. *Phys. Rev. Lett.* **2011**, *107*, 166401.
(211) Guzzo, M.; Kas, J. J.; Sponza, L.; Giorgetti, C.; Sottile, F.; Pierucci, D.; Silly, M. G.; Sirotti, F.; Rehr, J. J.; Reining, L. Multiple Satellites in Materials with Complex Plasmon Spectra: From Graphite to Graphene. *Phys. Rev. B: Condens. Matter Mater. Phys.* **2014**, *89*, 085425.
(212) Lischner, J.; Vigil-Fowler, D.; Louie, S. G. Physical Origin of Satellites in Photoemission of Doped Graphene: An Ab Initio G W Plus Cumulant Study. *Phys. Rev. Lett.* **2013**, *110*, 146801.
(213) Zhou, J. S.; Kas, J. J.; Sponza, L.; Reshetnyak, I.; Guzzo, M.; Giorgetti, C.; Gatti, M.; Sottile, F.; Rehr, J. J.; Reining, L. Dynamical Effects in Electron Spectroscopy. *J. Chem. Phys.* **2015**, *143*, 184109.
(214) Vigil-Fowler, D.; Louie, S. G.; Lischner, J. Dispersion and Line Shape of Plasmon Satellites in One, Two, and Three Dimensions. *Phys. Rev. B* **2016**, *93*, 235446.
(215) Vlček, V.; Rabani, E.; Neuhauser, D. Quasiparticle Spectra from Molecules to Bulk. *Phys. Rev. Mater.* **2018**, *2*, 030801.
(216) Holm, B.; Aryasetiawan, F. Self-Consistent Cumulant Expansion for the Electron Gas. *Phys. Rev. B: Condens. Matter Mater. Phys.* **1997**, *56*, 12825−12831.
(217) Holm, B.; Aryasetiawan, F. Total Energy from the Galitskii-Migdal Formula Using Realistic Spectral Functions. *Phys. Rev. B: Condens. Matter Mater. Phys.* **2000**, *62*, 4858−4865.
(218) Lischner, J.; Vigil-Fowler, D.; Louie, S. G. Satellite Structures in the Spectral Functions of the Two-Dimensional Electron Gas in Semiconductor Quantum Wells: A G W plus Cumulant Study. *Phys. Rev. B: Condens. Matter Mater. Phys.* **2014**, *89*, 125430.
(219) Kas, J. J.; Rehr, J. J.; Reining, L. Cumulant Expansion of the Retarded One-Electron Green Function. *Phys. Rev. B: Condens. Matter Mater. Phys.* **2014**, *90*, 085112.
(220) McClain, J.; Lischner, J.; Watson, T.; Matthews, D. A.; Ronca, E.; Louie, S. G.; Berkelbach, T. C.; Chan, G. K.-L. Spectral Functions of the Uniform Electron Gas via Coupled-Cluster Theory and Comparison to the G W and Related Approximations. *Phys. Rev. B* **2016**, *93*, 235139.
(221) Kas, J. J.; Vila, F. D.; Tan, T. S.; Rehr, J. J. Green's Function Methods for Excited States and x-Ray Spectra of Functional Materials. *Electron. Struct.* **2022**, *4*, 033001.
(222) Mayers, M. Z.; Hybertsen, M. S.; Reichman, D. R. Description of Quasiparticle and Satellite Properties via Cumulant Expansions of the Retarded One-Particle Green's Function. *Phys. Rev. B* **2016**, *94*, 081109.
(223) Zhou, J. S.; Gatti, M.; Kas, J. J.; Rehr, J. J.; Reining, L. Cumulant Green's Function Calculations of Plasmon Satellites in Bulk Sodium: Influence of Screening and the Crystal Environment. *Phys. Rev. B* **2018**, *97*, 035137.
(224) Tzavala, M.; Kas, J. J.; Reining, L.; Rehr, J. J. Nonlinear Response in the Cumulant Expansion for Core-Level Photoemission. *Phys. Rev. Res.* **2020**, *2*, 033147.
(225) Lundqvist, B. I. Characteristic Structure in Core Electron Spectra of Metals Due to the Electron-Plasmon Coupling. *Phys. kondens Materie* **1969**, *9*, 236−248.
(226) Langreth, D. C. Singularities in the X-Ray Spectra of Metals. *Phys. Rev. B: Solid State* **1970**, *1*, 471−477.

https://doi.org/10.1021/acs.jctc.4c00216
J. Chem. Theory Comput. 2024, 20, 4751−4777

(227) Hedin, L. Effects of Recoil on Shake-Up Spectra in Metals. *Phys. Scr.* **1980**, *21*, 477−480.
(228) Garniron, Y.; Scemama, A.; Giner, E.; Caffarel, M.; Loos, P. F. Selected Configuration Interaction Dressed by Perturbation. *J. Chem. Phys.* **2018**, *149*, 064103.
(229) Chien, A. D.; Holmes, A. A.; Otten, M.; Umrigar, C. J.; Sharma, S.; Zimmerman, P. M. Excited States of Methylene, Polyenes, and Ozone from Heat-Bath Configuration Interaction. *J. Phys. Chem. A* **2018**, *122*, 2714−2722.
(230) Loos, P. F.; Scemama, A.; Blondel, A.; Garniron, Y.; Caffarel, M.; Jacquemin, D. A Mountaineering Strategy to Excited States: Highly-Accurate Reference Energies and Benchmarks. *J. Chem. Theory Comput.* **2018**, *14*, 4360−4379.
(231) Loos, P. F.; Lipparini, F.; Boggio-Pasqua, M.; Scemama, A.; Jacquemin, D. A Mountaineering Strategy to Excited States: Highly-Accurate Energies and Benchmarks for Medium Sized Molecules. *J. Chem. Theory Comput.* **2020**, *16*, 1711−1741.
(232) Holmes, A. A.; Tubman, N. M.; Umrigar, C. J. Heat-Bath Configuration Interaction: An Efficient Selected Configuration Interaction Algorithm Inspired by Heat-Bath Sampling. *J. Chem. Theory Comput.* **2016**, *12*, 3674−3680.
(233) Sharma, S.; Holmes, A. A.; Jeanmairet, G.; Alavi, A.; Umrigar, C. J. Semistochastic Heat-Bath Configuration Interaction Method: Selected Configuration Interaction with Semistochastic Perturbation Theory. *J. Chem. Theory Comput.* **2017**, *13*, 1595−1604.
(234) Chatterjee, K.; Sokolov, A. Y. Second-Order Multireference Algebraic Diagrammatic Construction Theory for Photoelectron Spectra of Strongly Correlated Systems. *J. Chem. Theory Comput.* **2019**, *15*, 5908−5924.
(235) Chatterjee, K.; Sokolov, A. Y. Extended Second-Order Multireference Algebraic Diagrammatic Construction Theory for Charged Excitations. *J. Chem. Theory Comput.* **2020**, *16*, 6343−6357.
(236) Loos, P.-F.; Scemama, A.; Boggio-Pasqua, M.; Jacquemin, D. Mountaineering Strategy to Excited States: Highly Accurate Energies and Benchmarks for Exotic Molecules and Radicals. *J. Chem. Theory Comput.* **2020**, *16*, 3720−3736.
(237) Véril, M.; Scemama, A.; Caffarel, M.; Lipparini, F.; Boggio-Pasqua, M.; Jacquemin, D.; Loos, P.-F. QUESTDB: A database of highly accurate excitation energies for the electronic structure community. *Wiley Interdiscip. Rev.: Comput. Mol. Sci.* **2021**, *11*, No. e1517.
(238) Loos, P.-F.; Comin, M.; Blase, X.; Jacquemin, D. Reference Energies for Intramolecular Charge-Transfer Excitations. *J. Chem. Theory Comput.* **2021**, *17*, 3666−3686.
(239) Loos, P.-F.; Lipparini, F.; Matthews, D. A.; Blondel, A.; Jacquemin, D. A Mountaineering Strategy to Excited States: Revising Reference Values with EOM-CC4. *J. Chem. Theory Comput.* **2022**, *18*, 4418−4427.
(240) Jacquemin, D.; Kossoski, F.; Gam, F.; Boggio-Pasqua, M.; Loos, P.-F. Reference Vertical Excitation Energies for Transition Metal Compounds. *J. Chem. Theory Comput.* **2023**, *19*, 8782−8800.
(241) Loos, P.-F.; Lipparini, F.; Jacquemin, D. Heptazine, Cyclazine, and Related Compounds: Chemically-Accurate Estimates of the Inverted Singlet−Triplet Gap. *J. Phys. Chem. Lett.* **2023**, *14*, 11069−11075.
(242) Loos, P.-F.; Jacquemin, D. A Mountaineering Strategy to Excited States: Accurate Vertical Transition Energies and Benchmarks for Substituted Benzenes. **2024**, arXiv preprint arXiv:2401.13809.
(243) Matthews, D. A.; Cheng, L.; Harding, M. E.; Lipparini, F.; Stopkowicz, S.; Jagau, T.-C.; Szalay, P. G.; Gauss, J.; Stanton, J. F. Coupled-Cluster Techniques for Computational Chemistry: The CFOUR Program Package. *J. Chem. Phys.* **2020**, *152*, 214108.
(244) Christiansen, O.; Koch, H.; Jo/rgensen, P. Response Functions in the CC3 Iterative Triple Excitation Model. *J. Chem. Phys.* **1995**, *103*, 7429−7441.
(245) Koch, H.; Christiansen, O.; Jo/rgensen, P.; Sanchez de Merás, A. M.; Helgaker, T. The CC3Model: An Iterative Coupled Cluster Approach Including Connected Triples. *J. Chem. Phys.* **1997**, *106*, 1808−1818.
(246) Gordon, M. S.; Binkley, J. S.; Pople, J. A.; Pietro, W. J.; Hehre, W. J. Self-Consistent Molecular-Orbital Methods. 22. Small Split-Valence Basis Sets for Second-Row Elements. *J. Am. Chem. Soc.* **1982**, *104*, 2797−2803.
(247) Francl, M. M.; Pietro, W. J.; Hehre, W. J.; Binkley, J. S.; Gordon, M. S.; DeFrees, D. J.; Pople, J. A. Self-consistent Molecular Orbital Methods. XXIII. A Polarization-type Basis Set for Second-row Elements. *J. Chem. Phys.* **1982**, *77*, 3654−3665.
(248) Clark, T.; Chandrasekhar, J.; Spitznagel, G. W.; Schleyer, P. V. R. Efficient Diffuse Function-Augmented Basis Sets for Anion Calculations. III. The 3-21+G Basis Set for First-Row Elements, Li−F. *J. Comput. Chem.* **1983**, *4*, 294−301.
(249) Ditchfield, R.; Hehre, W. J.; Pople, J. A. Self-Consistent Molecular-Orbital Methods. IX. An Extended Gaussian-Type Basis for Molecular-Orbital Studies of Organic Molecules. *J. Chem. Phys.* **1971**, *54*, 724−728.
(250) Hehre, W. J.; Ditchfield, R.; Pople, J. A. Self—Consistent Molecular Orbital Methods. XII. Further Extensions of Gaussian—Type Basis Sets for Use in Molecular Orbital Studies of Organic Molecules. *J. Chem. Phys.* **1972**, *56*, 2257−2261.
(251) Dill, J. D.; Pople, J. A. Self-consistent Molecular Orbital Methods. XV. Extended Gaussian-type Basis Sets for Lithium, Beryllium, and Boron. *J. Chem. Phys.* **1975**, *62*, 2921−2923.
(252) Binkley, J. S.; Pople, J. A. Self-consistent Molecular Orbital Methods. XIX. Split-valence Gaussian-type Basis Sets for Beryllium. *J. Chem. Phys.* **1977**, *66*, 879−880.
(253) Dunning, T. H. Gaussian basis sets for use in correlated molecular calculations. I. The atoms boron through neon and hydrogen. *J. Chem. Phys.* **1989**, *90*, 1007−1023.
(254) Kendall, R. A.; Dunning, T. H.; Harrison, R. J. Electron Affinities of the First-row Atoms Revisited. Systematic Basis Sets and Wave Functions. *J. Chem. Phys.* **1992**, *96*, 6796−6806.
(255) Prascher, B. P.; Woon, D. E.; Peterson, K. A.; Dunning, T. H.; Wilson, A. K. Gaussian Basis Sets for Use in Correlated Molecular Calculations. VII. Valence, Core-Valence, and Scalar Relativistic Basis Sets for Li, Be, Na, and Mg. *Theor. Chem. Acc.* **2011**, *128*, 69−82.
(256) Woon, D. E.; Dunning, T. H. Gaussian Basis Sets for Use in Correlated Molecular Calculations. III. The Atoms Aluminum through Argon. *J. Chem. Phys.* **1993**, *98*, 1358−1371.
(257) Giner, E.; Scemama, A.; Caffarel, M. Using perturbatively selected configuration interaction in quantum Monte Carlo calculations. *Can. J. Chem.* **2013**, *91*, 879−885.
(258) Giner, E.; Scemama, A.; Caffarel, M. Fixed-node diffusion Monte Carlo potential energy curve of the fluorine molecule F2 using selected configuration interaction trial wavefunctions. *J. Chem. Phys.* **2015**, *142*, 044115.
(259) Caffarel, M.; Applencourt, T.; Giner, E.; Scemama, A. *Recent Progress in Quantum Monte Carlo*; American Chemical Society, 2016; Chapter 2, pp 15−46.
(260) Garniron, Y.; Scemama, A.; Loos, P.-F.; Caffarel, M. Hybrid Stochastic-Deterministic Calculation of the Second-Order Perturbative Contribution of Multireference Perturbation Theory. *J. Chem. Phys.* **2017**, *147*, 034101.
(261) Garniron, Y.; Applencourt, T.; Gasperich, K.; Benali, A.; Ferté, A.; Paquier, J.; Pradines, B.; Assaraf, R.; Reinhardt, P.; Toulouse, J.; et al. Quantum Package 2.0: An Open-Source Determinant-Driven Suite of Programs. *J. Chem. Theory Comput.* **2019**, *15*, 3591−3609.
(262) Scemama, A.; Caffarel, M.; Benali, A.; Jacquemin, D.; Loos, P. F. Influence of Pseudopotentials on Excitation Energies from Selected Configuration Interaction and Diffusion Monte Carlo. *Res. Chem.* **2019**, *1*, 100002.
(263) Frisch, M. J.; et al. *Gaussian 16*, Revision C.01; Gaussian Inc.: Wallingford CT, 2016.
(264) Damour, Y.; Quintero-Monsebaiz, R.; Caffarel, M.; Jacquemin, D.; Kossoski, F.; Scemama, A.; Loos, P.-F. Ground- and Excited-State Dipole Moments and Oscillator Strengths of Full Configuration Interaction Quality. *J. Chem. Theory Comput.* **2023**, *19*, 221−234.

https://doi.org/10.1021/acs.jctc.4c00216
J. Chem. Theory Comput. 2024, 20, 4751−4777

(265) Burton, H. G. A.; Loos, P.-F. Rationale for the Extrapolation Procedure in Selected Configuration Interaction. *J. Chem. Phys.* **2024**, *160*, 104102.
(266) Inc., W. R. *Mathematica*, Version 13.3: Champaign, IL, 2023. https://www.wolfram.com/mathematicweba.
(267) Alvertis, A. M.; Williams-Young, D. B.; Bruneval, F.; Neaton, J. B. Capturing Electronic Correlations in Electron-Phonon Interactions in Molecular Systems with the GW Approximation. **2024**, arXiv preprint arXiv:2403.08240.
(268) Scuseria, G. E.; Scheiner, A. C.; Lee, T. J.; Rice, J. E.; Schaefer, H. F. The closed-shell coupled cluster single and double excitation (CCSD) model for the description of electron correlation. A comparison with configuration interaction (CISD) results. *J. Chem. Phys.* **1987**, *86*, 2881−2890.
(269) Koch, H.; Jensen, H. J. A.; Jo/rgensen, P.; Helgaker, T. Excitation Energies from the Coupled Cluster Singles and Doubles Linear Response Function (CCSDLR). Applications to Be, CH^+, CO, and H_2O. *J. Chem. Phys.* **1990**, *93*, 3345−3350.
(270) Koch, H.; Jo/rgensen, P. Coupled cluster response functions. *J. Chem. Phys.* **1990**, *93*, 3333−3344.
(271) Stanton, J. F. Many-body methods for excited state potential energy surfaces. I. General theory of energy gradients for the equation-of-motion coupled-cluster method. *J. Chem. Phys.* **1993**, *99*, 8840−8847.
(272) Noga, J.; Bartlett, R. J. The Full CCSDT Model for Molecular Electronic Structure. *J. Chem. Phys.* **1987**, *86*, 7041−7050.
(273) Scuseria, G. E.; Schaefer, H. F. A new implementation of the full CCSDT model for molecular electronic structure. *Chem. Phys. Lett.* **1988**, *152*, 382−386.
(274) Kucharski, S. A.; Włoch, M.; Musiał, M.; Bartlett, R. J. Coupled-cluster theory for excited electronic states: The full equation-of-motion coupled-cluster single, double, and triple excitation method. *J. Chem. Phys.* **2001**, *115*, 8263−8266.
(275) Kucharski, S. A.; Bartlett, R. J. Recursive Intermediate Factorization and Complete Computational Linearization of the Coupled-Cluster Single, Double, Triple, and Quadruple Excitation Equations. *Theor. Chim. Acta* **1991**, *80*, 387−405.
(276) Kállay, M.; Surján, P. R. Higher excitations in coupled-cluster theory. *J. Chem. Phys.* **2001**, *115*, 2945−2954.
(277) Hirata, S. Higher-Order Equation-of-Motion Coupled-Cluster Methods. *J. Chem. Phys.* **2004**, *121*, 51−59.
(278) Kállay, M.; Gauss, J.; Szalay, P. G. Analytic first derivatives for general coupled-cluster and configuration interaction models. *J. Chem. Phys.* **2003**, *119*, 2991−3004.
(279) Kállay, M.; Gauss, J. Analytic second derivatives for general coupled-cluster and configuration-interaction models. *J. Chem. Phys.* **2004**, *120*, 6841−6848.
(280) Nooijen, M.; Bartlett, R. J. Equation of motion coupled cluster method for electron attachment. *J. Chem. Phys.* **1995**, *102*, 3629−3647.
(281) Rishi, V.; Perera, A.; Bartlett, R. J. A route to improving RPA excitation energies through its connection to equation-of-motion coupled cluster theory. *J. Chem. Phys.* **2020**, *153*, 234101.
(282) Quintero-Monsebaiz, R.; Monino, E.; Marie, A.; Loos, P.-F. Connections between many-body perturbation and coupled-cluster theories. *J. Chem. Phys.* **2022**, *157*, 231102.
(283) Tölle, J.; Kin-Lic Chan, G. Exact Relationships between the GW Approximation and Equation-of-Motion Coupled-Cluster Theories through the Quasi-Boson Formalism. *J. Chem. Phys.* **2023**, *158*, 124123.
(284) Christiansen, O.; Koch, H.; Jørgensen, P. The Second-Order Approximate Coupled Cluster Singles and Doubles Model CC2. *Chem. Phys. Lett.* **1995**, *243*, 409−418.
(285) Hättig, C.; Weigend, F. CC2 Excitation Energy Calculations on Large Molecules Using the Resolution of the Identity Approximation. *J. Chem. Phys.* **2000**, *113*, 5154−5161.
(286) Koch, H.; Christiansen, O.; Jørgensen, P.; Olsen, J. Excitation Energies of BH, CH2 and Ne in Full Configuration Interaction and the Hierarchy CCS, CC2, CCSD and CC3 of Coupled Cluster Models. *Chem. Phys. Lett.* **1995**, *244*, 75−82.
(287) Hald, K.; Jørgensen, P.; Olsen, J.; Jaszuński, M. An analysis and implementation of a general coupled cluster approach to excitation energies with application to the B2 molecule. *J. Chem. Phys.* **2001**, *115*, 671−679.
(288) Paul, A. C.; Myhre, R. H.; Koch, H. New and Efficient Implementation of CC3. *J. Chem. Theory Comput.* **2021**, *17*, 117−126.
(289) Kállay, M.; Gauss, J. Calculation of Excited-State Properties Using General Coupled-Cluster and Configuration-Interaction Models. *J. Chem. Phys.* **2004**, *121*, 9257−9269.
(290) Kállay, M.; Gauss, J. Approximate treatment of higher excitations in coupled-cluster theory. *J. Chem. Phys.* **2005**, *123*, 214105.
(291) Loos, P.-F.; Matthews, D. A.; Lipparini, F.; Jacquemin, D. How accurate are EOM-CC4 vertical excitation energies? *J. Chem. Phys.* **2021**, *154*, 221103.
(292) Rowe, D. J. Equations-of-Motion Method and the Extended Shell Model. *Rev. Mod. Phys.* **1968**, *40*, 153−166.
(293) Emrich, K. An extension of the coupled cluster formalism to excited states (I). *Nucl. Phys. A* **1981**, *351*, 379−396.
(294) Sekino, H.; Bartlett, R. J. A linear response, coupled-cluster theory for excitation energy. *Int. J. Quantum Chem.* **1984**, *26*, 255−265.
(295) Geertsen, J.; Rittby, M.; Bartlett, R. J. The equation-of-motion coupled-cluster method: Excitation energies of Be and CO. *Chem. Phys. Lett.* **1989**, *164*, 57−62.
(296) Comeau, D. C.; Bartlett, R. J. The equation-of-motion coupled-cluster method. Applications to open- and closed-shell reference states. *Chem. Phys. Lett.* **1993**, *207*, 414−423.
(297) Stanton, J. F.; Gauss, J. A. A simple scheme for the direct calculation of ionization potentials with coupled-cluster theory that exploits established excitation energy methods. *J. Chem. Phys.* **1999**, *111*, 8785−8788.
(298) Loos, P. F. QuAcK: a software for emerging quantum electronic structure methods. 2019, https://github.com/pfloos/QuAcK, https://github.com/pfloos/QuAcwebK.
(299) Lange, M. F.; Berkelbach, T. C. On the Relation between Equation-of-Motion Coupled-Cluster Theory and the GW Approximation. *J. Chem. Theory Comput.* **2018**, *14*, 4224−4236.
(300) Werner, H.-J.; Knowles, P. J.; Manby, F. R.; Black, J. A.; Doll, K.; Heßelmann, A.; Kats, D.; Köhn, A.; Korona, T.; Kreplin, D. A.; et al. The Molpro Quantum Chemistry Package. *J. Chem. Phys.* **2020**, *152*, 144107.
(301) Edvardsson, D.; Baltzer, P.; Karlsson, L.; Wannberg, B.; Holland, D. M. P.; Shaw, D. A.; Rennie, E. E. A Photoabsorption, Photodissociation and Photoelectron Spectroscopy Study of NH3 and ND3. *J. Phys. B: At. Mol. Phys.* **1999**, *32*, 2583−2609.
(302) Göthe, M. C.; Wannberg, B.; Karlsson, L.; Svensson, S.; Baltzer, P.; Chau, F. T.; Adam, M.-Y. X-ray, Ultraviolet, and Synchrotron Radiation Excited Inner-valence Photoelectron Spectra of CH4. *J. Chem. Phys.* **1991**, *94*, 2536−2542.
(303) Bieri, G.; Schmelzer, A.; Åsbrink, L.; Jonsson, M. Fluorine and the Fluoroderivatives of Acetylene and Diacetylene Studied by 30.4 Nm He(II) Photoelectron Spectroscopy. *Chem. Phys.* **1980**, *49*, 213−224.
(304) Svensson, S.; Eriksson, B.; Mårtensson, N.; Wendin, G.; Gelius, U. Electron Shake-up and Correlation Satellites and Continuum Shake-off Distributions in X-Ray Photoelectron Spectra of the Rare Gas Atoms. *J. Electron Spectrosc. Relat. Phenom.* **1988**, *47*, 327−384.
(305) Joshi, S.; Barth, S.; Marburger, S.; Ulrich, V.; Hergenhahn, U. $2p$ Correlation Satellites in Neon Clusters Investigated by Photoemission. *Phys. Rev. B: Condens. Matter Mater. Phys.* **2006**, *73*, 235404.
(306) Cambi, R.; Ciullo, G.; Sgamellotti, A.; Brion, C. E.; Cook, J. P. D.; McCarthy, I. E.; Weigold, E. Experimental and Theoretical Binding Energy Spectra and Momentum Distributions for the Valence Orbitals of H2O. *Chem. Phys.* **1984**, *91*, 373−381.
(307) Banna, M. S.; McQuaide, B. H.; Malutzki, R.; Schmidt, V. The Photoelectron Spectrum of Water in the 30 to 140 eV Photon Energy Range. *J. Chem. Phys.* **1986**, *84*, 4739−4744.
(308) Moitra, T.; Paul, A. C.; Decleva, P.; Koch, H.; Coriani, S. Multi-Electron Excitation Contributions towards Primary and Satellite States in the Photoelectron Spectrum. *Phys. Chem. Chem. Phys.* **2022**, *24*, 8329−8343.

https://doi.org/10.1021/acs.jctc.4c00216
J. Chem. Theory Comput. 2024, 20, 4751−4777

(309) Banna, M. S.; Shirley, D. A. Molecular Photoelectron Spectroscopy at 132.3 eV. Methane, the Fluorinated Methanes and Hydrogen Fluoride. *Chem. Phys. Lett.* **1975**, *33*, 441−446.
(310) Banna, M. S.; Shirley, D. A. Molecular Photoelectron Spectroscopy at 132.3 eV. The Second-row Hydrides. *J. Chem. Phys.* **1975**, *63*, 4759−4766.
(311) Yencha, A. J.; Lopes, M. C. A.; MacDonald, M. A.; King, G. C. Threshold Photoelectron Spectroscopy of HF in the Inner Valence Ionization Region. *Chem. Phys. Lett.* **1999**, *310*, 433−438.
(312) Bintrim, S. J.; Berkelbach, T. C. Full-frequency GW without frequency. *J. Chem. Phys.* **2021**, *154*, 041101.
(313) Monino, E.; Loos, P.-F. Spin-Conserved and Spin-Flip Optical Excitations from the Bethe−Salpeter Equation Formalism. *J. Chem. Theory Comput.* **2021**, *17*, 2852−2867.
(314) Monino, E.; Loos, P.-F. Unphysical discontinuities, intruder states and regularization in GW methods. *J. Chem. Phys.* **2022**, *156*, 231101.
(315) Tölle, J.; Chan, G. K.-L. AB-G_0W_0: A practical G0W0 method without frequency integration based on an auxiliary boson expansion. **2023**, arXiv preprint arXiv:2311.18304
(316) Scott, C. J. C.; Backhouse, O. J.; Booth, G. H. A "moment-conserving" reformulation of GW theory. *J. Chem. Phys.* **2023**, *158*, 124102.
(317) Ring, P.; Schuck, P. *The Nuclear Many-Body Problem*; Springer, 2004.
(318) Scuseria, G. E.; Henderson, T. M.; Bulik, I. W. Particle-particle and quasiparticle random phase approximations: Connections to coupled cluster theory. *J. Chem. Phys.* **2013**, *139*, 104113.
(319) Peng, D.; Steinmann, S. N.; van Aggelen, H.; Yang, W. Equivalence of Particle-Particle Random Phase Approximation Correlation Energy and Ladder-Coupled-Cluster Doubles. *J. Chem. Phys.* **2013**, *139*, 104112.
(320) Berkelbach, T. C. Communication: Random-phase approximation excitation energies from approximate equation-of-motion coupled-cluster doubles. *J. Chem. Phys.* **2018**, *149*, 041103.
(321) Trofimov, A. B.; Schirmer, J. Molecular Ionization Energies and Ground- and Ionic-State Properties Using a Non-Dyson Electron Propagator Approach. *J. Chem. Phys.* **2005**, *123*, 144115.
(322) Banerjee, S.; Sokolov, A. Y. Third-Order Algebraic Diagrammatic Construction Theory for Electron Attachment and Ionization Energies: Conventional and Green's Function Implementation. *J. Chem. Phys.* **2019**, *151*, 224112.
(323) Schirmer, J.; Cederbaum, L. S.; Walter, O. New Approach to the One-Particle Green's Function for Finite Fermi Systems. *Phys. Rev. A* **1983**, *28*, 1237−1259.
(324) Sokolov, A. Y. Multi-Reference Algebraic Diagrammatic Construction Theory for Excited States: General Formulation and First-Order Implementation. *J. Chem. Phys.* **2018**, *149*, 204113.
(325) Hildebrand, D. First Ionization Potentials of the Molecules BF, SiO and GeO. *Int. J. Mass Spectrom. Ion Phys.* **1971**, *7*, 255−260.
(326) Svensson, S.; Carlsson-Göthe, M.; Karlsson, L.; Nilsson, A.; Mårtensson, N.; Gelius, U. Inner Valence Satellite Structure in High Resolution X-ray Excited Photoelectron Spectra of N2 and CO. *Phys. Scr.* **1991**, *44*, 184−190.
(327) Baltzer, P.; Larsson, M.; Karlsson, L.; Wannberg, B.; Carlsson Göthe, M. Inner-Valence States of ${\mathrm{\bvphantom}} \evphantomN}}_{2}^{+}$ Studied by Uv Photoelectron Spectroscopy and Configuration-Interaction Calculations. *Phys. Rev. A* **1992**, *46*, 5545−5553.
(328) Potts, A. W.; Williams, T. A. The Observation of "Forbidden" Transitions in He II Photoelectron Spectra. *J. Electron Spectrosc. Relat. Phenom.* **1974**, *3*, 3−17.
(329) Åsbrink, L.; Fridh, C. The C State of N2+, Studied by Photoelectron Spectroscopy. *Phys. Scr.* **1974**, *9*, 338−340.
(330) Åsbrink, L.; Fridh, C.; Lindholm, E.; Codling, K. Photoelectron Spectrum and Rydberg Transitions of CO. *Phys. Scr.* **1974**, *10*, 183−185.
(331) Banna, M. S.; Shirley, D. A. Molecular Photoelectron Spectroscopy at 132.3 eV: N2, CO, C2H4 and O2. *J. Electron Spectrosc. Relat. Phenom.* **1976**, *8*, 255−270.
(332) Norton, P. R.; Tapping, R. L.; Broida, H. P.; Gadzuk, J. W.; Waclawski, B. J. High Resolution Photoemission Study of Condensed Layers of Nitrogen and Carbon Monoxide. *Chem. Phys. Lett.* **1978**, *53*, 465−470.
(333) Langhoff, S. R.; Bauschlicher, C. W. Theoretical Study of the First and Second Negative Systems of N+2. *J. Chem. Phys.* **1988**, *88*, 329−336.
(334) Morrison, R. C.; Liu, G. Extended Koopmans' Theorem: Approximate Ionization Energies from MCSCF Wave Functions. *J. Comput. Chem.* **1992**, *13*, 1004−1010.
(335) Dutta, A. K.; Vaval, N.; Pal, S. EOMIP-CCSD(2)*: An Efficient Method for the Calculation of Ionization Potentials. *J. Chem. Theory Comput.* **2015**, *11*, 2461−2472.
(336) Berkowitz, J.; Batson, C. H.; Goodman, G. L. PES of Higher Temperature Vapors: Lithium Halide Monomers and Dimers. *J. Chem. Phys.* **1979**, *71*, 2624−2636.
(337) Bauschlicher, C. W.; Langhoff, S. R.; Langhoff, S. R. Ab initio calculations on C2, Si2, and SiC. *J. Chem. Phys.* **1987**, *87*, 2919−2924.
(338) Abrams, M. L.; Sherrill, C. D. Full configuration interaction potential energy curves for the X1g+,B1g, and B1g+ states of C2: A challenge for approximate methods. *J. Chem. Phys.* **2004**, *121*, 9211−9219.
(339) Sherrill, C. D.; Piecuch, P. The Xg+1, Bg1, and Bg+1 states of C2: A comparison of renormalized coupled-cluster and multireference methods with full configuration interaction benchmarks. *J. Chem. Phys.* **2005**, *122*, 124104.
(340) Li, X.; Paldus, J. Singlet−triplet separation in BN and C2: Simple yet exceptional systems for advanced correlated methods. *Chem. Phys. Lett.* **2006**, *431*, 179−184.
(341) Booth, G. H.; Cleland, D.; Thom, A. J. W.; Alavi, A. Breaking the Carbon Dimer: The Challenges of Multiple Bond Dissociation with Full Configuration Interaction Quantum Monte Carlo Methods. *J. Chem. Phys.* **2011**, *135*, 084104.
(342) Evangelista, F. A. Alternative single-reference coupled cluster approaches for multireference problems: The simpler, the better. *J. Chem. Phys.* **2011**, *134*, 224102.
(343) Gulania, S.; Jagau, T.-C.; Krylov, A. I. EOM-CC guide to Fock-space travel: the C2 edition. *Faraday Discuss.* **2019**, *217*, 514−532.
(344) Ammar, A.; Marie, A.; Rodríguez-Mayorga, M.; Burton, H. G. A.; Loos, P.-F. Can. GW Handle Multireference Systems? *J. Chem. Phys.* **2024**, *160*, 114101.
(345) Hamrin, K.; Johansson, G.; Gelius, U.; Nordling, C.; Siegbahn, K. Valence Bands and Core Levels of the Isoelectronic Series LiF, BeO, BN, and Graphite Studied by ESCA. *Phys. Scr.* **1970**, *1*, 277−280.
(346) Patanen, M.; Børve, K.; Kettunen, J. A.; Urpelainen, S.; Huttula, M.; Aksela, H.; Aksela, S. Valence Photoionization and Photoelectron−Photoion Coincidence (PEPICO) Study of Molecular LiCl and Li2Cl2. *J. Electron Spectrosc. Relat. Phenom.* **2012**, *185*, 285−293.
(347) Zheng, Y.; Brion, C. E.; Brunger, M. J.; Zhao, K.; Grisogono, A. M.; Braidwood, S.; Weigold, E.; Chakravorty, S. J.; Davidson, E. R.; Sgamellotti, A.; von Niessen, W. Orbital Momentum Profiles and Binding Energy Spectra for the Complete Valence Shell of Molecular Fluorine. *Chem. Phys.* **1996**, *212*, 269−300.
(348) Frost, D. C.; Lee, S. T.; McDowell, C. A. The High Resolution Photoelectron Spectrum of CS. *Chem. Phys. Lett.* **1972**, *17*, 153−156.
(349) Jonathan, N.; Morris, A.; Okuda, M.; Ross, K. J.; Smith, D. J. Photoelectron Spectroscopy of Transient Species. The CS Molecule. *Faraday Discuss. Chem. Soc.* **1972**, *54*, 48−55.
(350) Potts, A. W.; Lee, E. P. F. Photoelectron Spectra and Electronic Structure of Lithium Halide Monomers and Dimers. *Faraday Discuss. Chem. Soc.* **1979**, *75*, 941−951.
(351) Tomasello, P.; von Niessen, W. Electronic Structure of Lithium Halide Monomers and Dimers: Ionization Energies and Electron Affinities. *Mol. Phys.* **1990**, *69*, 1043−1058.
(352) French, C. L.; Brion, C. E.; Davidson, E. R. A Study of the Valence Orbitals of H2S by Electron Momentum Spectroscopy:

https://doi.org/10.1021/acs.jctc.4c00216
J. Chem. Theory Comput. 2024, 20, 4751−4777

Quantitative Comparisons Using Hartree-Fock Limit and Correlated Wavefunctions. *Chem. Phys.* **1988**, *122*, 247−269.
(353) Cook, J. P. D.; Brion, C. E.; Hamnett, A. On the Ionization and Momentum Distributions of the Valence Electrons of H2S. *Chem. Phys.* **1980**, *45*, 1−13.
(354) Adam, M. Y.; Cauletti, C.; Piancastelli, M. N. Final State Multiple Structures in Photoionization of the Inner Valence Shell of H2S: Angular Distribution in the 40−70 e V Photon Energy Range. *J. Electron Spectrosc. Relat. Phenom.* **1987**, *42*, 1−10.
(355) Chipman, D. M. Assignment of States in the Valence Photoelectron Spectrum of H2S. *J. Electron Spectrosc. Relat. Phenom.* **1978**, *14*, 323−329.
(356) Yencha, A. J.; Cormack, A. J.; Donovan, R. J.; Hopkirk, A.; King, G. C. Threshold Photoelectron Spectroscopy of HCl and DCl. *Chem. Phys.* **1998**, *238*, 109−131.
(357) Adam, M. Y. Highly Resolved Photoelectron Spectra of the HCl Inner Valence Shell. *Chem. Phys. Lett.* **1986**, *128*, 280−286.
(358) Svensson, S.; Karlsson, L.; Baltzer, P.; Wannberg, B.; Gelius, U.; Adam, M. Y. The Photoelectron Spectrum of HCl and DCl Studied with Ultraviolet Excitation, High Resolution X-ray Excitation, and Synchrotron Radiation Excitation: Isotope Effects on Line Profiles. *J. Chem. Phys.* **1988**, *89*, 7193−7200.
(359) Edvardsson, D.; Baltzer, P.; Karlsson, L.; Lundqvist, M.; Wannberg, B. Rotational Fine Structure in the UV Photoelectron Spectra of HF and HCl. *J. Electron Spectrosc. Relat. Phenom.* **1995**, *73*, 105−124.
(360) Kikas, A.; Osborne, S. J.; Ausmees, A.; Svensson, S.; Sairanen, O. P.; Aksela, S. High-Resolution Study of the Correlation Satellites in Photoelectron Spectra of the Rare Gases. *J. Electron Spectrosc. Relat. Phenom.* **1996**, *77*, 241−266.
(361) Guyon, P.-M.; Spohr, R.; Chupka, W. A.; Berkowitz, J. Threshold Photoelectron Spectra of HF, DF, and F2. *J. Chem. Phys.* **1976**, *65*, 1650−1658.
(362) Domcke, W.; Cederbaum, L. S.; Schirmer, J.; von Niessen, W.; Brion, C. E.; Tan, K. H. Experimental and Theoretical Investigation of the Complete Valence Shell Ionization Spectra of CO2and N2O. *Chem. Phys.* **1979**, *40*, 171−183.
(363) Hochlaf, M.; Eland, J. H. D. Single and Double Photo-ionizations of Methanal (Formaldehyde). *J. Chem. Phys.* **2005**, *123*, 164314.
(364) Fehlner, T. P.; Koski, W. S. Direct Detection of the Borane Molecule and the Boryl Radical by Mass Spectrometry. *J. Am. Chem. Soc.* **1964**, *86*, 2733−2734.
(365) Wilson, J. H.; McGee, H. A. Mass-Spectrometric Studies of the Synthesis, Energetics, and Cryogenic Stability of the Lower Boron Hydrides. *J. Chem. Phys.* **1967**, *46*, 1444−1453.
(366) Tian, S. X. Ab Initio and Electron Propagator Theory Study of Boron Hydrides. *J. Phys. Chem. A* **2005**, *109*, 5471−5480.
(367) Wälz, G.; Usvyat, D.; Korona, T.; Schütz, M. A. Hierarchy of Local Coupled Cluster Singles and Doubles Response Methods for Ionization Potentials. *J. Chem. Phys.* **2016**, *144*, 084117.
(368) Dutta, A. K.; Vaval, N.; Pal, S. Lower Scaling Approximation to EOM-CCSD: A Critical Assessment of the Ionization Problem. *Int. J. Quantum Chem.* **2018**, *118*, No. e25594.
(369) Paran, G. P.; Utku, C.; Jagau, T.-C. On the Performance of Second-Order Approximate Coupled-Cluster Singles and Doubles Methods for Non-Valence Anions. *Phys. Chem. Chem. Phys.* **2024**, *26*, 1809−1818.
(370) Kánnár, D.; Tajti, A.; Szalay, P. G. Accuracy of Coupled Cluster Excitation Energies in Diffuse Basis Sets. *J. Chem. Theory Comput.* **2017**, *13*, 202−209.
(371) Kozma, B.; Tajti, A.; Demoulin, B.; Izsák, R.; Nooijen, M.; Szalay, P. G. A New Benchmark Set for Excitation Energy of Charge Transfer States: Systematic Investigation of Coupled Cluster Type Methods. *J. Chem. Theory Comput.* **2020**, *16*, 4213−4225.
(372) Patanen, M.; Abid, A. R.; Pratt, S. T.; Kivimäki, A.; Trofimov, A. B.; Skitnevskaya, A. D.; Grigoricheva, E. K.; Gromov, E. V.; Powis, I.; Holland, D. M. P. Valence Shell Photoelectron Angular Distributions and Vibrationally Resolved Spectra of Imidazole: A Combined Experimental−Theoretical Study. *J. Chem. Phys.* **2021**, *155*, 054304.
(373) Hättig, C. In *Response Theory and Molecular Properties (A Tribute to Jan Linderberg and Poul Jørgensen)*; Jensen, H. A., Ed.; Advances in Quantum Chemistry; Academic Press, 2005; Vol. *50*, pp 37−60.
(374) Govoni, M.; Galli, G. GW100: Comparison of Methods and Accuracy of Results Obtained with the WEST Code. *J. Chem. Theory Comput.* **2018**, *14*, 1895−1909.
(375) Clark, S. A. C.; Weigold, E.; Brion, C. E.; Davidson, E. R.; Frey, R. F.; Boyle, C. M.; von Niessen, W.; Schirmer, J. The Valence Orbital Momentum Distributions and Binding Energy Spectra of Silane by Electron Momentum Spectroscopy: Quantitative Comparisons Using Hartree-Fock Limit and Correlated Wavefunctions. *Chem. Phys.* **1989**, *134*, 229−239.
(376) Riva, G.; Audinet, T.; Vladaj, M.; Romaniello, P.; Berger, A. Photoemission spectral functions from the three-body Green's function. *SciPost Phys.* **2022**, *12*, 093.
(377) Riva, G.; Romaniello, P.; Berger, J. A. Multichannel Dyson Equation: Coupling Many-Body Green's Functions. *Phys. Rev. Lett.* **2023**, *131*, 216401.
(378) Loos, P.-F.; Marie, A.; Ammar, A. Cumulant Green's Function Methods for Molecules. *Faraday Discuss.* **2024**. in press
(379) Ferté, A.; Palaudoux, J.; Penent, F.; Iwayama, H.; Shigemasa, E.; Hikosaka, Y.; Soejima, K.; Ito, K.; Lablanquie, P.; Taïeb, R.; Carniato, S. Advanced Computation Method for Double Core Hole Spectra: Insight into the Nature of Intense Shake-up Satellites. *J. Phys. Chem. Lett.* **2020**, *11*, 4359−4366.
(380) Ferté, A.; Penent, F.; Palaudoux, J.; Iwayama, H.; Shigemasa, E.; Hikosaka, Y.; Soejima, K.; Lablanquie, P.; Taïeb, R.; Carniato, S. Specific Chemical Bond Relaxation Unraveled by Analysis of Shake-up Satellites in the Oxygen Single Site Double Core Hole Spectrum of CO 2. *Phys. Chem. Chem. Phys.* **2022**, *24*, 1131−1146.

https://doi.org/10.1021/acs.jctc.4c00216
J. Chem. Theory Comput. 2024, 20, 4751−4777